The Role of Citrullination on Defensin-Lipid Binding and its Function in Innate Defence and Cancer

Submitted by

MINURI SUHARA RATNAYAKE, Bachelor of Biological Sciences

The thesis submitted in total fulfilment of the requirements

for the degree of Master of Science

Department of Biochemistry and Genetics

School of Molecular Sciences

College of Science, Health and Engineering

La Trobe University

Victoria, Australia

December 2020

Table of Contents

Table of Contents ..... **ii**

List of Figures ..... **vi**

List of Tables ..... **ix**

Abbreviations ..... **x**

Abstract ..... **xiii**

Statement of Authorship ..... **xiv**

Acknowledgments ..... **xv**

Chapter 1:Introduction **1**

1.1 Innate immunity and cancer 2

1.2 Antimicrobial peptides 3

1.2.1 Overview of Cationic antimicrobial peptides 3

1.2.2 Plant defensins 6

1.2.3 Mammalian defensins 8

1.3 Membrane phospholipids and their importance in CAP antimicrobial activity 9

1.3.1 CAP mediated membrane targeting 9

1.3.4 Binding of defensins to other lipids 13

1.4 Citrullination 14

1.4.1 Overview of citrullination and biological function in innate defence 14

1.4.1.1Peptidylarginine deaminase structure and function 15

1.4.1.2 Physiological role of citrullination 17

1.4.2 Role of citrullination in diseases 19

1.4.2.1 Sepsis 19

1.4.2.2 Periodontal diseases 20

1.4.2.3 Rheumatoid Arthritis 21
1.4.3 Citrullination and NETosis 22
1.4.4 Role of PAD in tumour progression 24
1.5 Nature and scope of study 26
Chapter 2:Materials and Methods 27
2.1 Recombinant protein expression and purification 28
2.1.1 Recombinant protein expression in P. pastoris 28
2.1.2 Recombinant protein purification by cation exchange column chromatography ……29
2.2 Protein quality control 29
2.2.1 Sodium dodecyl sulphate polyacrylamide gel electrophoresis (SDS-PAGE) .. 29
2.2.2 Immunoblot analysis 30
2.2.3 Circular dichroism (CD) spectroscopy 31
2.3 Citrullination of NaD1, HBD-2, HBD-3 and LL-37 32
2.3.1 Citrullination by human PAD2 32
2.3.2 Immunoblot analysis 32
2.3.3 Mass spectrometry analysis 32
2.4 Investigating citrullinated NaD1 interactions with cellular lipids 33
2.4.1 Protein-lipid overlay assay 33
2.4.2 Transmission electron microscopy (TEM) 33
2.4.3 Protein crosslinking assay……34
2.4.4 Liposome pulldown assay……34
2.5 Functional analysis 35
2.5.1 Candida albicans growth inhibition assay 35
2.5.2 C. albicans propidium iodide (PI) uptake assay 36

2.5.3 Human histiocytic lymphoma (U937) PI uptake assay 36
2.5.4 Cell culture and cell viability assay 37
2.5.5 Confocal laser scanning microscopy (CLSM) 39
Chapter 3:NaD1, HBD-2 and HBD-3 protein expression and quality control 40
3.1 Interaction of NaD1, HBD-2 and HBD-3 with $PI(4,5)P_2$ 41
3.2 Recombinant protein expression and characterisation 43
3.3 Functional analysis of NaD1, HBD-2 and HBD-3 47
Chapter 4:Citrullination and functional analysis of NaD1 49
4.1 Introduction 50
4.2 Citrullination of NaD1 and LL-37 51
4.3 Interaction of citrullinated NaD1 with cellular lipids 54
4.3.1 Protein-lipid overlay assay 54
4.3.2 Interaction of NaD1 and citrullinated NaD1 with PIP_2 56
4.3.3 Detection of citrullinated NaD1:PIP_2 oligomer formation using chemical crosslinking 57
4.3.4 Detection of native and citrullinated NaD1:PIP_2 fibril formation using TEM . 59
4.4 Functional analysis of citrullinated NaD1 61
4.4.1 Effect of citrullinated NaD1 on fungal growth inhibition 61
4.4.2 Effect of citrullinated NaD1 on fungal membrane permeabilisation 62
4.4.3 The effect of citrullinated NaD1 on C. albicans (ATCC90028) growth and membrane permeabilisation 66
4.4.4 Effect of citrullinated NaD1 on mammalian tumour cell viability 68
4.4.5 Effect of citrullinated NaD1 on membrane permeabilisation of U937 72
4.5 Recombinant expression and citrullination of NaD1 R40E and NaD1 R39A mutants 76
Chapter 5:Citrullination and functional analysis of HBD-3 78

5.1 Introduction 79
5.2 Citrullination of HBD-2 and HBD-3 80
5.3 Functional analysis of citrullinated HBD-3 83
5.3.1 Effect of citrullinated HBD-3 on fungal growth inhibition 83
5.3.2 Effect of citrullinated HBD-3 on membrane permeabilisation 85
5.3.3 Effect of citrullinated HBD-3 on U937 tumour cell permeabilisation 87
5.3.4 Effect of citrullinated HBD-3 on cell viability 92
Chapter 6:Discussion 94
6.1 Introduction 95
6.2 Interactions of NaD1, HBD-2 and HBD-3 $PI(4,5)P_2$ 96
6.3 Recombinant defensin expression and characterisation 96
6.4 Functional analysis of purified recombinant NaD1, HBD-2 and HBD-3 98
6.5 Citrullination of NaD1, HBD-2, HBD-3 and LL-37 99
6.6 Interaction of citrullinated NaD1 with cellular lipids.....101
6.7 Functional analysis of citrullinated NaD1 105
6.8 Recombinant expression and citrullination of NaD1 R40E and NaD1 R39A mutants 109
6.9 Functional analysis of citrullinated HBD-3 109
Concluding remarks 113
Appendix 114
List of References.....120

List of Figures

Figure 1. Examples of the six classes of CAPs**.** 4

Figure 2. β-strand arrangement of the cis- and trans- defensins superfamilies. 5

Figure 3. The two classes of plant defensins. 7

Figure 4. Structures of the three classes of mammalian defensins. 8

Figure 5. Models of CAP mediated membrane targeting. 10

Figure 6. Structures involved in NaD1 membrane permeabilisation. 12

Figure 7. The process of citrullination. 14

Figure 8. Mature defensin sequence and structures of NaD1, HBD-2 and HBD-3. 42

Figure 9. Characterisation of purified NaD1, HBD-2 and HBD-3 44

Figure 10. CD spectrum and secondary structure composition of NaD1, HBD-2 and HBD-3 46

Figure 11. The effect of NaD1, HBD-2 and HBD-3 on growth, PI uptake and viability of *C. albicans* and HeLa cells. 48

Figure 12. Characterisation of citrullinated NaD1 and LL-37. 52

Figure 13. ESI-Q-Tof mass spectrometry analysis of untreated and citrullinated LL-37 and NaD1**.** 53

Figure 14. Interaction of native and citrullinated NaD1 with membrane phospholipids. 55

Figure 15. Binding of native and citrullinated NaD1 to $PI(4,5)P_2$. 56

Figure 16. Formation of oligomers by NaD1 and citrullinated NaD1 with PIP_2 and PA. 58

Figure 17. TEM analysis of the interaction between native or citrullinated NaD1 with PIP_2 60

Figure 18. Effect of citrullinated and native NaD1 on the growth *C. albicans.* 61

Figure 19. Effect of citrullinated and native NaD1 on the PI uptake of *C. albicans* (ATCC 10231). 62

Figure 20. Confocal imaging of *C.albicans* (ATCC10231). 64

Figure 21. Confocal time course imaging of *C.albicans* (ATCC10231) cells. 65

Figure 22. Effect of citrullinated and native NaD1 on the growth of *C. albicans* (ATCC90028). 67

Figure 23. Effect of citrullinated and native NaD1 on the PI uptake of *C. albicans* (ATCC90028). 68

Figure 24. Effect of native and citrullinated NaD1 on HeLa and PC3 cell viability. 69

Figure 25. The effect of native and citrullinated NaD1 on U937 and THP1 cell viability. ... 71

Figure 26. Effect of citrullinated and native NaD1 on the PI uptake of U937 tumour cells.. 72

Figure 27. CLSM endpoint imaging of U937 cells. 74

Figure 28. CLSM time course imaging of U937 cells. 75

Figure 29. Characterisation of purified NaD1 R40E and NaD1 R39A. 77

Figure 30. Characterisation of citrullinated HBD-2, HBD-3 and LL-37. 80

Figure 31. ESI-Q-Tof mass spectrometry analysis of untreated and citrullinated HBD-2 and HBD-3. 82

Figure 32. Effect of citrullinated and native HBD-3 on the growth of *C. albicans* (ATCC100231). 84

Figure 33. Effect of citrullinated and native HBD-3 on the growth of *C. albicans* (ATCC90028). 85

Figure 34. Effect of Citrullinated and native HBD-3 on the PI uptake of *C. albicans* (ATCC10231). 86

Figure 35. Effect of Citrullinated and native HBD-3 on the PI uptake of *C. albicans* (ATCC90028). 87

Figure 36. Effect of native and citrullinated HBD-3 on the PI uptake of U937 tumour cells. 88

Figure 37. Confocal imaging of U937. 90

Figure 38. Confocal time course imaging of U937 cells. 91

Figure 39. Effect of native and citrullinated HBD-3 on HeLa and PC3 cell viability 93

List of Tables

Table 1. The 5 PAD isozymes and their known substrate targets 16

Table 2. Characteristics of NaD1, HBD-2 and HBD-3 in terms of the number of amino acids in each defensin and Arg/Lys residues known to be involved in PIP_2 binding 42

Abbreviations

ACPA	Anticitrullinated peptide antibodies
ADI	Arginine deiminases
AD	Alzheimer's disease
AMP	Antimicrobial peptides
AR	Androgen receptor
BMG	Buffered minimal glycerol
BMM	Buffered minimal methanol
CAPS	Cationic antimicrobial peptides
CD	Circular dichroism
CLSM	Confocal laser scanning microscopy
CSα/β	Cysteine stabilised αβ motif
CTTP	C terminal propeptide
DmAMP1	*Dahlia merckii* antimicrobial peptide 1
ER	Endoplasmic reticulum
FACS	Fuorescence-activated cell sorting
GRIP1	Glutamate receptor-interacting protein 1
HBD-2	Human β-defensin 2
HBD-3	Human β-defensin 3
HDAC2	Histone deacetylases 2
HNP	Human neutrophil defensin
LPS	Lipopolysaccharides
LP9	Lysoyme degraded peptide 9

LTH	Leukotoxic hypercitrullination
MPO	Myeloperoxidase
MtDef4	*Medicago sativa* defensin 1
MTT	3-(4,5-dimethylthiazol-2-yl)-2,5-diphenyltetrazolium bromide
NaD1	*Nicotiana alata* defensin 1
NADPH	Nicotinamide adenine dinucleotide phosphate
NE	Neutrophil elastase
NETs	Neutrophil extracellular traps
=NH	Ketimine
NsD7	*Nicotiana suaveolens* defensin 7
=O	Ketone group
PA	Phosphatidic acid
PAD	Peptidylarginine deaminase
PC3	Prostate cancer cell
PDB	Potato dextrose broth
PI	Phosphatidylinositol
PIP	Phosphatidylinositol phosphate
PI(3)P	Phosphatidylinositol 3-phosphate
PI(4)P	Phosphatidylinositol 4-phosphate
PI(5)P	Phosphatidylinositol 5-phosphate
$PI(3,4)P_2$	Phosphatidylinositol *3*,*4*-bisphosphate
$PI(3,5)P_2$	Phosphatidylinositol 3,5-bisphosphate
$PI(4,5)P_2$	Phosphatidylinositol 4,5-bisphosphate

$PI(3,4,5)P_2$	Phosphatidylinositol *3*,*4*,*5*-trisphosphate
PMA	Phorbol myristate acetate
PPAD	*P. gingivalis* peptidylarginine deiminase
PUMA	p53 upregulated modulator of apoptosis
PVDF	Polyvinylidene difluoride
RA	Rheumatoid arthritis
RGP	Arginine specific ginipians
RNAP2	RNA polymerase II
ROS	Reactive oxygen species
RsAFP2	*Raphanus sativus* antifungal protein 2
SEM	Standard error of the mean
ST	Synovial tissue
TEM	Transmission electron microscopy
THP1	Monocytic leukemia
TLR	Toll like receptors
TPP3	Tomato pistil predominant 3
U937	Monocytic lymphoma
YNB	Yeast nitrogen base
YPD	Yeast peptone dextrose

Abstract

Defensins, a subclass of small, cysteine-rich cationic antimicrobial peptides, play a significant role in eukaryotic immune defence and are emerging as promising therapeutic agents. Defensins from various species including plants (NaD1) and humans (HBD-2 and HBD-3) exhibit membrane permeabilisation activity against pathogenic microbes and cancer cells. This activity is attributed to the binding of defensins to membrane phospholipids such as phosphoinositides (PIPs), an interaction mediated by key arginine residues such as arginine 40 for NaD1 and arginine 22 for HBD-2. Citrullination is an important post-translational modification process in humans, particularly at sites of inflammation and the tumour microenvironment, where arginine residues are modified to neutral citrulline that can modulate protein function. In addition, to counteract the host defences, microbes have also been shown to use citrullination to render inactive arginine-dependent peptides in innate immunity. For example, the citrullination of human cathelicidin LL37 has been shown to inactivate its antimicrobial activity. However, the regulatory function of defensin citrullination remains to be investigated. In this thesis, the citrullination of NaD1, HBD-2 and HBD-3, were examined, where for the first time NaD1 and HBD-3 were demonstrated to be citrullinated. Liposome pulldown and biochemical crosslinking assays revealed that citrullinated NaD1 does not interact with $PI(4,5)P_2$. Citrullinated NaD1 and HBD-3 had substantial reduction in activity against human fungal pathogen *Candida albicans* as well as tumourigenic cervical (HeLa), prostate (PC3) and human histiocytic lymphoma (U937) cancer cell lines when compared to native NaD1 and HBD-3. This study provides new insights into the citrullination of defensins and its potential regulatory effects on defensin-mediated lipid binding and membranolytic ability, as well as raising potential issues in the use of defensins as therapeutic agents.

Statement of Authorship

Except where reference is made in the text of the thesis, this thesis contains no material published elsewhere or extracted in whole or in part from a thesis accepted for the award of any other degree or diploma.

No other person's work has been used without due acknowledgment in the main text of the thesis.

This thesis has not been submitted for the award of any degree or diploma in any other tertiary institution.

Minuri Suhara Ratnayake

29 December 2020

Acknowledgments

First and foremost, I would like to express my sincerest gratitude and admiration for my supervisor, Professor Mark Hulett, for his tremendous expertise, advice, guidance and continuous support throughout my Masters studies. Despite his busy schedule, he was always willing to listen to me patiently, spend time discussing the project progression and results and helping me to solve my experimental issues.

I would like to thank Professor Ivan Poon for his continuous academic guidance and giving constructive feedback whenever I had experimental issues. I thank Dr Fung Lay for his guidance, technical and academic support throughout this year,

A very big thank you to Guneet Bindra for her academic and non-academic support. I appreciate all the moral support throughout the past 2 year and being an incredible friend especially during the times when I needed it the most. I would also like to thank all member of the Hulett and Poon labs for all the help I received and for making this experience absolutely enjoyable. Being able to work alongside surrounded by so many talented people was such an inspiration.

For my parents, I don't think saying 'thank you' will be able to express my gratitude and unconditional love for your continuous support at every step of the way for my career in science

I would also like to thank Pierre Faou and Shane Gorden from Comprehensive Proteomic Platform, La Trobe University, for their assistance with mass spectrometry. As well as Julian Ratcliffe for his assistance with transmission electron microscopy. Thanks also to Peter Lock for his assistance with microscopy.

The research procedures reported in this thesis was approved by the relevant safety committee and authorised officers

This work was supported by a La Trobe University Full Fee Research Scholarship.

Due to the COVID-19 pandemic, all research was stopped and resulted in a ‘lock-out of the laboratories at LIMS for a duration of 3 months (March-May). From June onwards only shift based access was granted to conduct research resulting in a limited period to complete the said research

Chapter 1

Introduction

1.1 Innate immunity and cancer

Innate immunity is an ancient evolutionary component of host defence that is present in all classes of plants and animals where it serves as the first line of defence against invading pathogens in a rapid, non-specific and antigen-independent manner (Turvey & Broide, 2010). In addition to playing a critical role in the host defence, the innate immune system is also an important regulator of human disease including autoimmune diseases and cancer (Bachmann & Kopf, 2001; Turvey & Broide, 2010).

Cancer is one of the leading causes of mortality and morbidity worldwide accounting for approximately 9.6 million deaths in 2018 (World Health Organisation, 2019). Cancer has been proposed to arise in a multistage manner whereby a 'normal' cell transitions to a tumour cell by acquiring the ability to proliferate in an uncontrolled manner together with a number of other 'hallmarks' of cancer (inducing angiogenesis, evading growth suppressors) (Hanahan & Weinberg, 2011). A key characteristic feature of malignant cancer is the ability to circulate from a primary site to a secondary site, known as metastasis which is responsible for most recorded mortality (Hanahan & Weinberg, 2011). While chemotherapy, surgery and radiotherapy are the most commonly used conventional cancer treatments, these methods are often met with numerous side effects such as multi-drug resistance, cardiotoxicity and various adverse health effects (Baxter et al., 2017; Devlin et al., 2017). Therefore, there is an urgent need for new therapeutics that have a high efficacy while being less toxic to normal cells. A class of antimicrobial peptides (AMPs) called defensins represent a promising source of novel therapeutics against cancer and inflammatory diseases.

1.2 Antimicrobial peptides

1.2.1 Overview of Cationic antimicrobial peptides

One of the major subclasses of AMPs, known as cationic antimicrobial peptides (CAPs), form an important component innate immune defence and are present in all organisms, including plants, animals, bacteria and fungi (Peschel & Sahl, 2006). CAPs are small (10-50 amino acids), positively charged peptides (owing to arginine and lysine), that are constitutively expressed or induced during an immune response (Hancock & Sahl, 2006). Based on their tertiary structure, CAPs can be broadly classified into six groups; α-helical, β-sheet, β-hairpin, mix of α- helical and β-sheet, extended and cyclic (Figure 1) (Hancock & Diamond, 2000; Baxter et al., 2017). Despite variances in structure, the amphipathic nature of CAPs allows them to interact with membrane phospholipids to target and permeabilise the plasma membrane by forming pores or destabilising the membrane (Hancock & Diamond, 2000; Hancock & Sahl, 2006). In addition to antimicrobial activity, CAPs have demonstrated the ability to preferentially lyse tumourigenic cells owing to the increased anionicity of such cells when compared to healthy cells, making CAPs attractive candidates for novel anti-cancer therapeutics (Riedl et al., 2011).

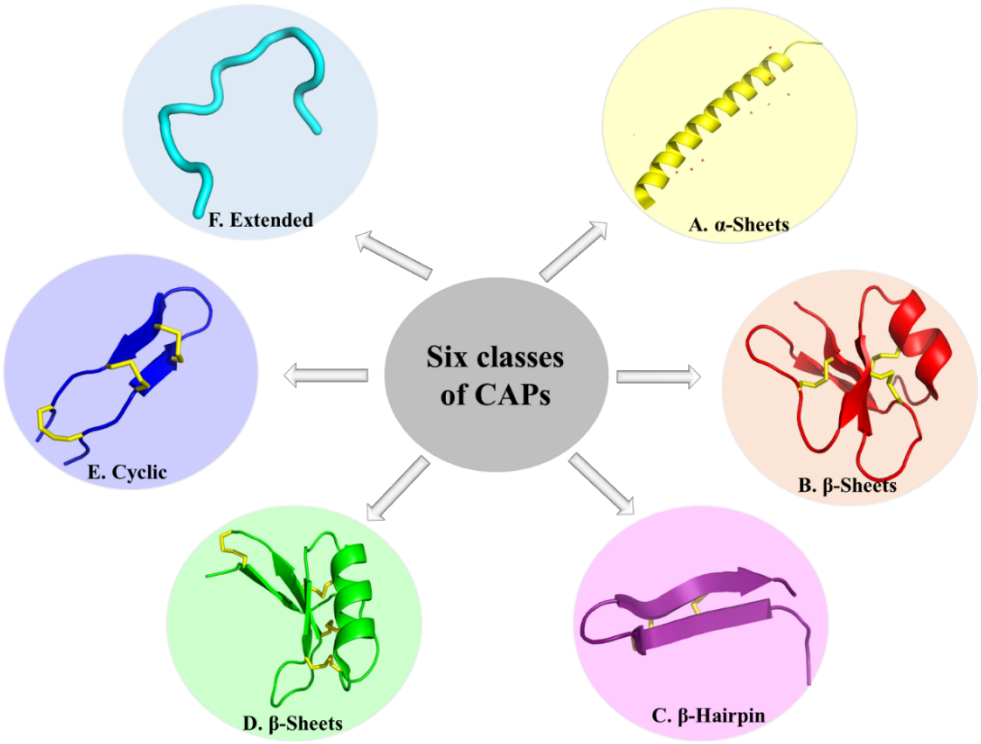

Figure 1. Examples of the six classes of CAPs

(A) α-Helical: human cathelicidin LL-37 (PDB code: 5NMN). (**B**) β-sheet: Human beta defensin-2 (PDB code: 6CS9). (**C**) β-Hairpin: porcine protegrin-1 (PDB code: 1PG1). (**D**) Mixed: plant defensin NaD1 (PDB code: 1MR4). (**E**) Cyclic: rhesus macaque θ-defensin RTD-1 (PDB code: 1HVZ). (**F)** Extended bovine indolicidin (PDB code: 1QXQ). Figures drawn using PyMOL.

Defensins, a family of CAPs, are small (<10 kDa) positively charged, cysteine-rich peptides with a conserved β-sheet fold (Shafee et al., 2016; Shafee et al., 2017). The cysteine residues are involved in the formation of disulphide bonds which provide stability to the peptide. Despite variations in the amino acid sequence, defensins share a similar tertiary structure which consist of a double- or triple-stranded β-sheets (typically with an α-helix) held together by intramolecular disulphide bridges (Shafee et al., 2017). Recent studies indicate that defensins did not originate from the same ancestral protein and instead consist of two superfamilies, *cis* and *trans,* that have arisen by convergent evolution (Shafee et al., 2016; Shafee et al., 2017).

In *cis*-defensins, found in plants, fungi and most invertebrates, the final β-strand is joined to an α-helix through disulphide bonds, whereas, in the *trans*-defensins found in vertebrates, disulphide binds to different secondary structure within the protein (Figure 2) (Shafee et al., 2016). Defensins are known to exhibit various mechanisms of action including the modulation of immune responses and demonstrate antimicrobial activity mainly via direct permeabilisation of the membrane (Baxter et al., 2017). Plant and mammalian defensins have also been demonstrated to possess toxicity towards tumour cells (Baxter et al., 2015; Phan et al., 2016).

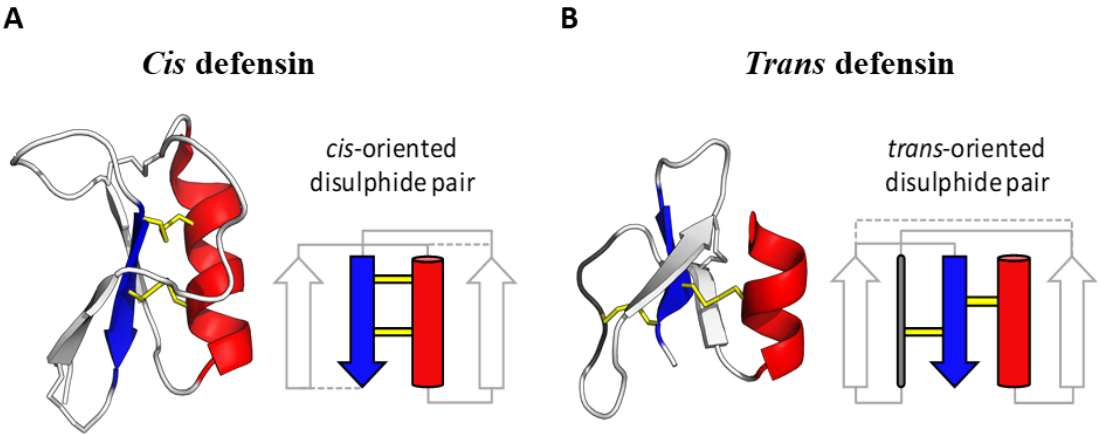

Figure 2. β-strand arrangement of the cis- and trans- defensins superfamilies

(A) In cis-defensins the two disulphide bonds from the final β-strand bind to the same structure. (**B)** Trans-defensins form two disulphide bonds from the final β-strand which binds to different structural elements within protein. Figure adapted from Shafee et al. (2016).

1.2.2 Plant defensins

Plant defensins, formerly known as γ-thionins, comprise a family of proteins (~ 5kDa) that contain a characteristic feature of eight highly conserved cysteine residues (Lay & Anderson, 2005). These residues participate in the formation of four disulphide bonds that stabilise one α-helix and triple-stranded antiparallel β-sheet into a cysteine stabilised αβ motif (CSα/β) providing structural and thermostability (Lay et al., 2003; Lay & Anderson, 2005).

Plant defensins can be classified into two classes based on the precursor sequence and structure: class I and class II defensins (Lay & Anderson, 2005). Class I defensins are expressed with a N-terminal endoplasmic reticulum (ER) signal sequence and mature defensin domain and are secreted into the secretory pathway (Figure 3) (Lay & Anderson, 2005). In contrast the class II defensins (only found in solanaceous plants) have an additional C terminal propeptide (CTPP) domain (33 amino acids) following the defensin domain which directs storage in vacuoles (Figure 3) (Lay & Anderson, 2005; Lay et al., 2014).

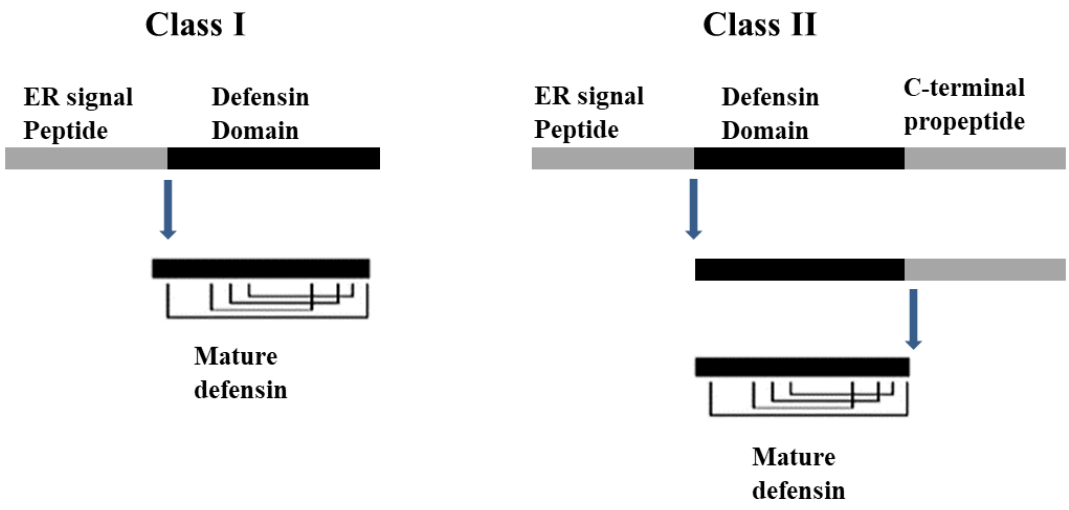

Figure 3. The two classes of plant defensins

Class I plant defensins are expressed with an ER sequence preceding the defensin domain that is cleaved to produce a mature defensin. Class II solanaceous plant defensins contain a C terminal propeptide (CTPP) domain following the defensin domain which is cleaved to produce the mature defensin. Figure adapted from Lay & Anderson, 2005.

The large variation in the primary amino acids sequence of plant defensins may help to explain the broad range of biological activities including antimicrobial, antifungal, insecticidal, membrane disruption and induction of signal pathways (Lacerda et al., 2014). More recently class II defensins, NaD1 (Poon et al., 2014), TPP3 (Baxter et al., 2015), and NsD7 (Kvansakul et al., 2017) were shown to effectively induce fungal and/or tumour cell lysis by binding specific phospholipids in cell membranes (see Section 1.3).

1.2.3 Mammalian defensins

Mammalian defensins can be classified into three structural subfamilies; α, β and θ defensins (Yang et al., 2002; Selsted & Ouellette, 2005). The mature peptides contain six cysteine residues that are involved in three intramolecular disulphide bonds and a turn-linked β-strand dominated tertiary structure (Selsted & Ouellette, 2005). Regardless of the primary sequence, α- and β- defensins consist of triple-stranded β-sheet-rich folds, whereas θ-defensins form structurally distinct cyclic peptides (Figure 4) (Tang et al., 1999; Selsted & Ouellette, 2005). Primarily, α- defensins are found in leukocytes, neutrophils and Paneth cells of the small intestine in many primate and rodent species. β-defensins are expressed in epithelial cells and gastrointestinal tract of all vertebrates, whereas θ-defensins are only found in Old World primates and Rhesus monkeys (Tang et al., 1999; Selsted & Ouellette, 2005).

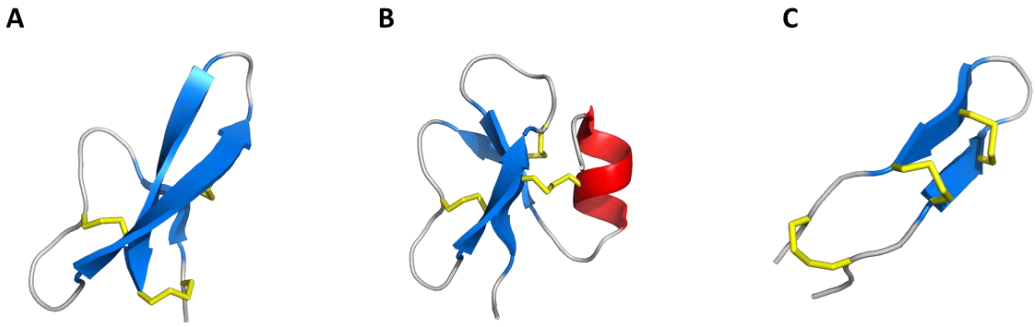

Figure 4. Structures of the three classes of mammalian defensins

(A) α-defensin: Human α- defensin (PDB code: 1FD3). **(B)** β-defensin: Human beta defensin-2 (PDB code: 6CS9). **(C)** θ-defensin: rhesus macaque RTD-1 (PDB code: 1HVZ). Figures drawn using PyMOL.

Mammalian defensins can be expressed constitutively or induced in response to pathogens and/or inflammatory cytokines (Yang et al., 2002). Defensins posses the ability to act as direct effectors of immunity as they have been shown to inactivate bacteria, fungi and certain viruses, such as adenovirus (Bastian & Schäfer, 2001; Yang et al., 2002). Defensins are also known to regulate innate immunity, for example the human neutrophil defensins (HNPs) are α-defensins that have been reported to increase the expression of tumour necrosis factor and other cytokines, regulate complement activation and promote degranulation of mast cells (Yang et al., 2002). This suggest that defensins play a vital role in linking innate immunity and adaptive immunity.

1.3 Membrane phospholipids and their importance in CAP antimicrobial activity

1.3.1 CAP mediated membrane targeting

The net positive charge of CAPs allows electrostatic interaction with the negatively charged cell membrane components (glycoproteins or phospholipids) which can lead to membrane permeabilisation (Yin et al., 2012; Baxter et al., 2017). The mechanism of how membrane permeabilisation after the initial contact occurs by CAPs, including defensins, remains to be determined, however, several models of membrane permeabilisation have been proposed (Figure 5) (Brogden, 2005). CAPs can oligomerise and be vertically inserted into bilayer resulting in membrane rupture, known as the 'barrel stave model' (Brogden, 2005). CAPs can aggregate on the membrane and once a threshold concentration is reached, similar to detergents, form micelles leading to membrane permeabilisation, defined as the 'carpet model' (Brogden, 2005). Alternatively, in the 'toroidal pore model', the polar heads of CAPs associate with the polar heads of the membrane lipids which induces the lipid bilayer to bend forming a pore (Brogden, 2005). In addition, defensins have also demonstrated antimicrobial activity via

alternative mechanism such as perturbing intracellular pathways and activation of caspases (Mader et al., 2011; Baxter et al., 2017).

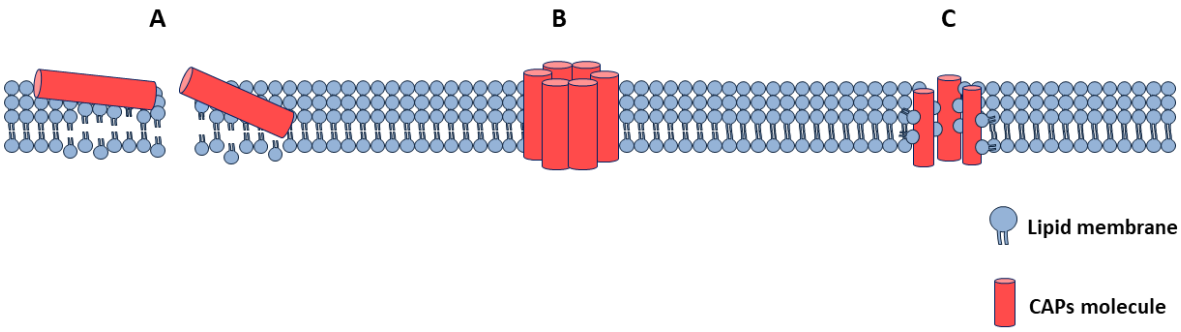

Figure 5. Models of CAP mediated membrane targeting

(A) Carpet model: CAPs aggregate on the surface of the membrane leading to membrane permeabilisation. **(B)** Barrel stave model: CAPs oligomerise into pores and are inserted vertically into the membrane. **(C)** Toroidal pore: Electrostatic interactions between the CAPs and lipid membrane result in the membrane to bend allowing membrane permeabilisation.

1.3.2 Phosphatidylinositol phosphates (PIPs)

PIP molecules are produced by phosphorylation of phosphatidylinositol (PI). The phosphorylation of the inositol ring of PI in position 3, 4 and 5 give rise to seven diverse mono-, bis- and tris- PIP molecules: monophosphates (PI(3)P, PI(4)P and PI(5)P), bisphosphates ($PI(3,4)P_2$), $PI(3,5)P_2$ and $PI(4,5)P_2$) and trisphosphates ($PI(3,4,5)P_3$) (Lupyan et al., 2010, Phan et al., 2019). The seven phosphorylated products are then transported to subcellular organelle membranes to contribute to diverse cellular processes (Di Paolo & De Camilli, 2006). $PI(4,5)P_2$ and $PI(3,4,5)P_3$ are predominantly enriched at the inner leaflet of plasma membrane, while PI(4)P is located at the plasma membrane as well as Golgi-endosomal trafficking and exocytic vesicles (Di Paolo & De Camilli, 2006; Phan et al., 2019). PI(3)P,

$PI(3,4)P_2$ and PI(3,5) are associated with early endosomes, non-clathrin endocytic vesicles and late endo-lysosomal membranes respectively (Di Paolo & De Camilli, 2006; Phan et al., 2019). Recently, interest has been directed towards $PI(4,5)P_2$ or PIP_2 as it is a key player involved in defensin-induced cell death.

1.3.3 PIP_2 in membrane targeting

PIP_2, a minor component of the plasma membrane, is involved in various cellular mechanisms such as cell migration, signal transduction and its sequestration or enzyme modification result in membrane permeabilisation (Di Paolo & De Camilli, 2006). While the membranolytic action of defensins is known, the mechanism of membrane interaction is poorly understood. However, novel studies on plant defensin NaD1 and TTP3, human defensins human β-defensin 2 (HBD-2) and human β-defensin 3 (HBD-3) have revealed the importance of phosphatidylinositol 4,5-bisphosphate (PIP_2) in defensin binding to the membrane (Poon et al., 2014; Baxter et al., 2015; Phan et al., 2016; Järvå et al., 2018b). Upon entry of the cell (which is poorly understood), plant defensin NaD1 and TTP3 dimerise and the conserved β2-β3 loops, (SKILRR and **S**KLQRK respectively), form a cationic grip which interacts with the negatively charged head of PIP_2 molecules on the cytosolic side of the membrane (Poon et al., 2014; Baxter et al., 2015). This binding allows oligomerisation of defensins and eventually results in the permeabilisation of the membrane suggesting a conserved PIP_2-mediated mechanism of membrane disruption for the class II plant defensins (Figure 6) (Poon et al., 2014; Baxter et al., 2015). Interestingly, HBD-3 also contains a homologous β2-β3 loop (STRGRK**)** and NMR revealed HBD-3 dimerises and may bind to PIP_2 via a cationic grip similar to the plant defensins (Schibli et al., 2002). Similarly, X-ray crystallography and site-directed mutagenesis revealed NaD1, TPP3 and HBD-3 mediate tumour cell cytotoxicity

by targeting PIP_2 (Poon et al., 2014; Baxter et al., 2015; Phan et al., 2016). The structure of a HBD-2:PIP_2 complex has also been solved and is structurally different to the NaD1:PIP_2 complex, as HBD-2 binds PIP_2 through two distinct binding sites which are crucial for membrane disruption of fungal cells (*Candida albicans*) (Järvå et al., 2018b). This suggests that despite differences in defensin-lipid structures, recognition of lipid binding by defensins is conserved across species and could potentially be exploited as a potent antimicrobial and anticancer therapeutic.

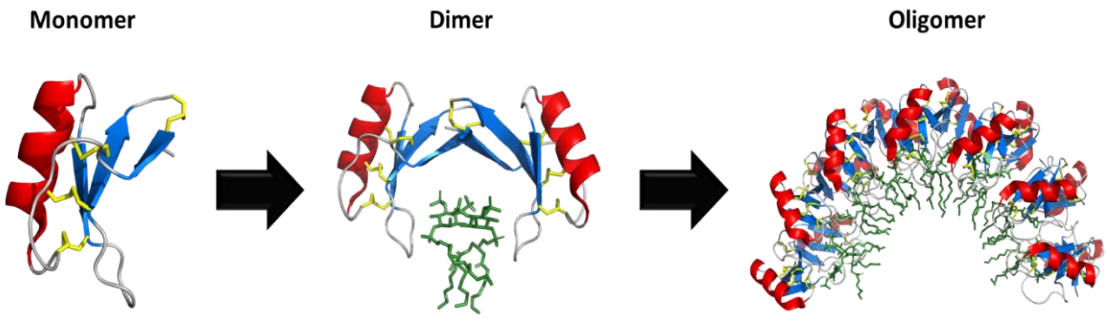

Figure 6. Structures involved in NaD1 membrane permeabilisation

NaD1 monomers enter a cell and dimerises to form a cationic grip between the β2-β3 cationic loops. This allows the dimer to bind to two PIP_2 molecules (green). Dimers oligomerize to a NaD1-PIP2 complex (PDB code: 4CQK) forming an arch shape configuration, which can result in membrane permeabilisation. Figures drawn using PyMOL.

1.3.4 Binding of defensins to other lipids

While PIP binding is the most common target for the defensins, other lipids have also been reported to bind defensins. The plant defensin *Nicotiana suaveolens* defensin 7 (NsD7) targets the phospholipid phosphatidic acid (PA) forming a coiled oligomer, mediated by lysine 36 and lysine 39, that permeabilise the cell membrane (Kvansakul et al., 2016). Intriguingly, X-ray crystallography revealed, that the structure of NsD7:PA oligomer complex is different when compared to NaD1:PIP_2 oligomer which is believed to be due to different linking of the dimers to PIP_2 or PA (Kvansakul et al., 2016). In addition NaD1 is known to interact with PA mediated by arginine 39 that was found to be crucial for PA binding, oligomerisation and for killing *Candida albicans* (Järvå et al., 2018a). Similarly the interaction of PA with plant defensin MtDef4 (from *M. truncatula*) is important for the internalisation and toxicity of fungal cells (Sagaram et al., 2013). Plant defensin DmAMP1 and RsAFP2 (from *Raphanus sativus*) which interact with sphingolipids including glycosylceramides are associated with fungal toxicity, however, whether binding of these defensins leads to the formation of defensin-lipid complexes has yet to be confirmed. These findings suggest that different lipids can be recognised and targeted by defensins for defensin based immunity.

1.4 Citrullination

1.4.1 Overview of citrullination and biological function in innate defence

As proteins are encoded by a limited number of genes, posttranslational modifications are critical to increase structural and functional diversity of the proteome (Gyorgy et al., 2006). One such modification which has been demonstrated to have a role in innate immunity and several diseases is identified as citrullination. However, it is important to note that this citrullination process is distinct from the formation of free amino acid citrulline, produced as a part of the urea cycle, catalysed by arginine deiminases (ADIs) (Majsnerowska et al., 2018). As first described in 1958, citrullination or deamination involves the conversion of a peptidyl-arginine to peptidyl-citrulline, a non-genetically coded amino acid, which converts the primary ketimine group (=NH) to a ketone group (=O) and results in an increase of 1Da in mass (Figure 7) (Gyorgy et al., 2006; Witalison et al., 2015; Brentville et al., 2020). Replacement of the postively charged arginine to a neutral citrulline residue increases the hydrophobicity which may the affect structure of protein, protein-protein interactions and function of the protein (Gyorgy et al., 2006; Witalison et al., 2015). This enzymatic reaction is catalysed by peptidylarginine deaminase (PAD).

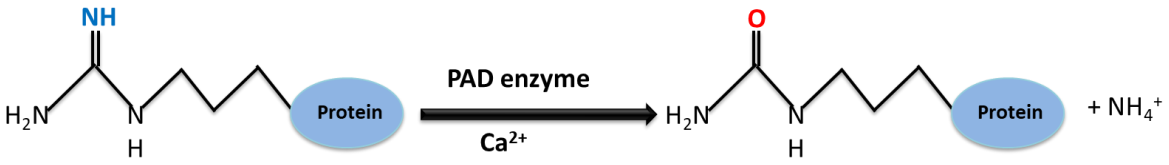

Figure 7. The process of citrullination

The conversion of peptidyl-arginine to peptidyl-citrulline by peptidylarginine deaminase (PAD) and the release of a free ammonium ion.

1.4.1.1Peptidylarginine deaminase structure and function

PAD enzymes are a group of cysteine hydrolases and five isozymes of PAD are found in humans (PAD1-4 and PAD6), which share a 70-95% amino acid homology (Rogers et al., 1977; Vossenaar et al., 2003; Witalison et al., 2015). The PAD genes are localized in one cluster at 1p36.13 and are expressed in distinct mammalian tissues. PAD1 and 3 are both expressed in the epidermis and hair follicles while PAD1 is additionally expressed in uterus (Gyorgy et al., 2006; Chang et al., 2009; Witalison et al., 2015). PAD2 and PAD4 have a wider distribution with PAD2 expressed in the brain, skeletal muscles, secretory muscles and leukocytes while PAD4 is expressed in macrophages, neutrophils granulocytes and specific tumours (Gyorgy et al., 2006; Chang et al., 2009; Witalison et al., 2015). The catalytically inactive PAD6 is only expressed in ovaries and early embryos (Chang et al., 2009; Gyorgy et al., 2006; Witalison et al., 2015). In addition to the cytoplasmic localisation, PAD2 and PAD4 are known to localise to the nucleus for citrullination of histones. PAD4 contains a nuclear localisation signal that allows it to be localised to the nucleus and it is believed that PAD2 contains the ability to localise to the nucleus despite not containing a localisation signal (Witalison et al., 2015; Zheng et al., 2019). Despite containing various sites of expression, PADs have specific substrate targets (Table 1) (Senshu et al., 1995; Tanikawa et al., 2012; Hsu et al., 2014; Witalison et al., 2015).

Table 1. The 5 PAD isozymes and their known substrate targets

PAD Isozyme	Substrate target
PAD1	Keratin, filaggrin
PAD2	Histones, vimentin, myelin protein, actin
PAD3	Filaggrin, vimentin, apoptosis inducing factor, trichohyalin
PAD4	Histones, nucleophosmin, nuclear lamin C, p21
PAD6	No known targets

The crystal structure of PAD4 has provided further understanding of the structure and function of PAD enzymes and it was demonstrated that they are calcium dependent enzymes (Arita et al., 2006; Witalison et al., 2015). The enzymes have two immunoglobulin-like subdomains in the N-terminus, with PAD4 containing a nuclear localisation signal, and an α/β propeller structure conserved C-terminus that contains the catalytical active site (Arita et al., 2006). There are five calcium binding sites in PAD4 with two located in the C-terminus and three located in the N-terminus, and in the absence of calcium, the active site-containing nucleophile region Cys645 faces away from the active site (Arita et al., 2006). However, binding of calcium results in a series of conformational shifts that allow Cys645 and other key residues to position themselves in the active site for catalysis and allow for protein-protein interaction in the N-terminus (Arita et al., 2006; Bicker & Thompson, 2013). Under physiological conditions, calcium concentrations are maintained at low levels (10^{-8} to 10^{-6} M), therefore PADs are inactive and only become activated during processes such as apoptosis and epidermal differentiation when the calcium concentrations have increased (Gyorgy et al., 2006). Intriguingly PADs have been implicated in gene regulation and other processes at

physiological conditions, suggesting additional regulatory mechanisms (not identified) independent to calcium may exist which allows them to function (Witalison et al., 2015).

Interestingly, all arginine residues in a protein will not be citrullinated. Proteins which are mainly disordered, contain β-helices, or arginine residues next to aspartic acid, are highly susceptible to citrullination, while arginine residues next to glutamic acid, flanked by proline residues and near the N-terminus are less susceptible to citrullination. (Tarcsa et al., 1996; Knuckley et al., 2010; Gyorgy et al., 2006; Witalison et al., 2015). All these factors play a key role in maintaining citrullination in physiological cellular processes.

1.4.1.2 Physiological role of citrullination

Citrullination is involved in early stages of apoptosis; calcium is a signalling molecule in apoptosis and is needed in high concentrations which activates PAD enzymes resulting in citrullination of secondary and tertiary protein structures. Vimentin, an intermediate filament, contains a β-turn head domain that gets citrullinated which results in the polymer disassembly, monomers not able to re-join, and finally collapse of structural support leading to apoptosis (Inagaki et al., 1989; Gyorgy et al., 2006). Likewise, histone and nucleophosmin citrullination are targets of PAD4 for initiating apoptosis. The oligomerisation of the nucleophosmin is essential for nucleolus localisation and prevent apoptosis by inhibiting p53 localisation into the mitochondria (Dhar & St. Clair, 2009). However, citrullination of the nucleophosmin results in p53 linked apoptosis and additionally upregulation of PAD4 is associated with mitochondrial associated apoptosis (Witalison et al., 2015). The nuclear lamina plays an important role for the mechanical support of the nucleus and it was found that citrullination of a 70 kDa nuclear protein in the lamina contributes to the disintegration of the lamina during the initial stages of apoptosis (Mizoguchi et al., 1998).

In addition to apoptosis, PAD enzymes are involved in terminal epidermal differentiation as differentiation occurs during high calcium concentrations that activate the enzymes. Upon terminal epidermal differentiation PAD enzymes can citrullinate keratin, filaggrin and vimentin, making them undergo unfolding to be more susceptible to degradation and formation of the keratin matrix (Senshu et al., 1996; Gyorgy et al., 2006).

PAD enzymes can regulate gene expression in cells that do not undergo apoptosis. As PAD4 contains a nuclear localisation signal, it allows gene regulation and contributes to citrullination of histones (Witalison et al., 2015). Most research has been performed on the PAD4 mediated regulation of the p53 pathway. PAD4 is recruited to gene promoters and is involved in citrullination of histone H4 and H3 which results in gene repression (Li et al., 2010; Christophorou et al., 2014). For example, PAD4 interacts with the regulatory domain of p53 and with the citrullinated p21 promoter region which results in the repression of p21 transcription as p53 is unable to bind to p21 (Li et al., 2008). PAD4 also found to function as a corepressor to regulate expression of p53 targets. Increased levels of PAD4 and histone levels were detected on the promoter of p53 target including p21, PUMA and CIP1 before DNA damage, and after DNA damage levels of citrullinations have been found to decrease (Li et al., 2008; Li et al., 2010). Similarly, PAD4 and histone deacetylase 2 (HDAC2) were found to interact with p53 target gene promoters (such as p21 and PUMA) before DNA damage and dissociate from the target promoters after DNA damage allowing for their activation (Li et al., 2010). PAD4 was also found to be a transcriptional coactivator. PAD4 citrullinates the Glutamate receptor-interacting protein 1 (GRIPI) binding domain of p300 which leads to an enhanced interaction to GRIPI and increased ER-mediated transcription (Lee et al., 2005; Gyorgy et al., 2006). In addition, PAD4 also acts as a transcriptional regulator of key genes

involved in pluripotency. PAD4 upregulates pluripotent markers and downregulates differential markers (Christophorou et al., 2014; Slade et al., 2014). During early embryonic development, citrullination of histones regulates the initiation of pluripotency and stem cell reprogramming (Christophorou et al., 2014; Slade et al., 2014). PAD enzymes play a role in maintaining cellular processes, and dysregulation and/or elevated levels of citrullination has been associated with several inflammatory and autoimmune diseases such as sepsis, rheumatoid arthritis (RA), periodontal disease and Alzheimer's disease (AD) and several cancers.

1.4.2 Role of citrullination in diseases

1.4.2.1 Sepsis

Sepsis is an inflammatory syndrome that is caused by a dysregulated response by the host immune response to an infection. Human cathelicidin LL-37 has been found to play a role in sepsis (Koziel et al., 2014; Denning et al., 2019). LL-37, the only cathelicidin-derived antimicrobial peptide found in humans, is an amphipathic helical peptide that is expressed in the epitheilal cells of broad range of tissues (Dürr et al., 2006). It is also expresed in different immune cells such as monocytes, neutrophils, T cells, B cells and natural killer cells (Dürr et al., 2006). In addition to its antimicrobial acitivy, it plays a role in cytoxicity, promoting epitheilal cell re-activation, wound repair, as a chemoattract of adaptive immune cells to infection sites and regulating the inflammatory response (Dürr et al., 2006). LL-37 also regulates innate immunity through its ability to bind negatively charged lipopolysaccharides (LPS). By preventing LPS from binding to CD14+ cells, LL-37 reduces LPS-induced cytokine production, thereby diminishing the harmful effects of sepsis and endotoxemia (Cirioni et al., 2006; Koziel et al., 2014). Koziel et al (2014) discovered that citrullinated LL-37 leads to

aggravated sepsis in mouse models as a result of the inability of LL-37 to neutralize LPS and an enhanced inflammatory response when compared to its native form.

1.4.2.2 Periodontal diseases

Periodontitis is a disease that is associated with the chronic inflammation of tissues and imbalance of the oral microbiome that is commonly found as biofilms in the periodontal pocket (Hajishengallis, 2014). This results in the infiltration by immune cells, mainly neutrophils, that play a vital role in maintaining the health of the periodontal area by various bactericidal mechanisms (Hajishengallis, 2014; Stobernack et al., 2018). However, *Porphyromonas gingivalis (P. gingivalis)*, the main etiological agent of periodontal disease, has evolved into adapting mechanisms to produce and secretes *P. gingivalis* peptidylarginine deiminase (PPAD) (McGraw et al., 1999; Stobernack et al., 2018). Unlike human PAD enzymes, PPAD is calcium-independent, requires high pH and is able to citrullinate both bacterial and host proteins (Mangat et al., 2010; Goulas et al., 2015). *P. gingivalis* expresses several virulence factors and arginine specific gingipains (RGPs) which allows the bacteria to manipulate the host innate defence (Potempa & Potempa, 2012). The RGPs cleave proteins followed by citrullination by PPAD, making *P. gingivalis* resistant to complement pathways and degrade anti-microbial peptides that allow *P. gingivalis* and other pathogenic bacteria to persevere in gingiva (Potempa & Potempa, 2012; Quirke et al., 2014). PPAD citrullinates epidermal growth factor (EGF) inhibiting its functions including wound healing, stimulating epidermal cell proliferation and EGF signalling pathways allowing the disease to persist (Pyrc et al., 2013). Recently it was found that PPAD diminishes the immune defence via impeding binding and internalisation by neutrophils, hindering bacterial phagocytosis and citrullinating lysozyme degraded peptide (LP9) to neutralise its antimicrobial activity (Stobernack et al., 2018).

1.4.2.3 Rheumatoid Arthritis

Rheumatoid arthritis (RA) is a chronic inflammatory joint disease and occurs in response to different environmental and genetic factors. It is characterised by the production of anticitrullinated peptide antibodies (ACPAs) which are significant markers in the diagnosis of the disease (Alghamdi et al., 2019). Synovial tissue (ST) studies of RA patients revealed an increase in citrullinated proteins both intra- and extracellularly, with intracellular proteins related to PAD2 and extracellular protein linked to PAD4 (Chang et al., 2005; de Rycke et al., 2005). Synovial fluid of RA patients contain a unique type of citrullination, that include a range of proteins, known as hypercitrullination and proteomic analysis have identified more than 100 intra and extra cellular substrates which together comprises the RA citrullinome (Romero et al., 2013; Tilvawala et al., 2018). As calcium concentration increases, PAD enzymes can citrullinate cellular proteins such as antithrombin, fibrinogen, vimentin and enolases and seep out of the cell to citrullinate extracellular proteins (Masson-Bessière et al., 2001; Blachère et al., 2017). This initiates the immune response to generate ACPAs, forming immune complexes and attracting immune cells through direct or complement activation which leads to the progression of the disease (Trouw et al., 2009). Several mechanisms of cell death, particularly NETosis (see section 1.4.3), have been implicated in the generation of citrullinated antigens which leads to triggering of ACPAs in RA (Khandpur et al., 2013; Wang et al., 2016). Dysregulated and enhanced NETosis is found in RA patients resulting in an increase in autoantibodies to citrullinated antigens (ACPA) (Khandpur et al., 2013; Wang et al., 2016). This corresponds to elevated levels of ACPA found in ST of RA patients which may explain inflammatory response correlated with RA (Khandpur et al., 2013).

1.4.3 Citrullination and NETosis

Neutrophils constitute approximately 70% of leucocytes and serve as a first line of defence against invading pathogens. The mechanisms of actions include phagocytosis, degranulation which involves in the release of cytotoxic molecules from granules, and nicotinamide adenine dinucleotide phosphate (NADPH) oxidative burst (Mesa & Vasquez, 2013; de Bont et al., 2018). However, Brinkmann et al (2004), discovered a new antibacterial strategy known as NETosis, which involves extrusion of neutrophilic chromatin together with antimicrobial proteins resulting in the formation of neutrophil extracellular traps (NETs). NETs are composed of DNA and histone backbones that are studded with different globular proteins such as primary granules (Cathepsin, Neutrophil elastase (NE), myeloperoxidase (MPO)), secondary granules (Lactoferrin and pentraxin), tertiary granules (gelatinase) and various cytoplasmic components (Brinkmann, 2004). While the function of NETs appear to be trapping and direct microbial activity, the exact biochemical events leading to its formation remains elusive. Upon induction of NETosis through toll like receptors (TLRs), interleukin 8 or LPS, the nicotinamide adenine dinucleotide phosphate (NADPH) oxidase complex is activated leading to the production of hydrogen peroxide (ROS molecule) (Brinkmann, 2004). This leads to NE being released from the granules in an MPO dependent process, migrating to the nucleus, and with the help of MPO leads to chromatin decondensation (Papayannopoulos et al., 2010; Metzler et al., 2011). Once the nuclear membrane disintegrates, the chromatin mixes with the cytosolic and granular proteins and forms a network once the cell membrane disrupts (Brinkmann, 2004; Papayannopoulos et al., 2010; Metzler et al., 2011). This form of NETosis is known as “suicidal” NETosis. However, additionally a second form that is still not understood termed “vital” NETosis has been described which is largely induced by bacterial

stimulations that are independent of NADPH or ROS production and does not involve membrane lysis of neutrophils (Pilsczek et al., 2010).

An important step is the increase in intracellular calcium in the neutrophils which leads to citrullination of histones by PAD4, further assisting in chromatin decondensation (Wang et al., 2009). However, there are still controversies about the role PAD4 plays in NET release and recently it is believed that various stimuli can produce different NETs with different roles in citrullination. For example, neutrophils stimulated by phorbol myristate acetate (PMA), fungi (*C. albicans*) and bacteria (*Klebsiella pneumoniae*) has been described to induced NETosis in a NADPH-dependent and PAD4-independent manner (Neeli & Radic, 2013; Konig & Andrade, 2016; Claushuis et al., 2018). Moreover, Phorbol myristate acetate (PMA) was found to inhibit PAD4 activation and considering the requirement of reducing environment for PAD function, the oxidation condition via ROS may inactivate PAD which suggest that PAD4 may not be required for the formation of all NETs (Neeli & Radic, 2013; Claushuis et al., 2018). In contrast, when calcium ionophores and other pore forming bacteria are used, NET are formed that are completely dependent on calcium influx and are characterized by hypercitrullination which results in the activation of PAD4 (Heather et al., 2012; Lewis et al., 2015). This form has been described as leukotoxic hypercitrullination (LTH) as it is independent of NADPH oxidase activity which is a hallmark of NETosis (Heather et al., 2012; Lewis et al., 2015; Konig & Andrade, 2016). Although the mechanism by which histones kill bacteria is not understood, it has been established that histones possess antimicrobial activity owing to the high content of positively charged residues, such as lysine and arginine, which are thought to bind and disrupt the membrane (Cutrona et al., 2015). Therefore, the decrease of arginine residues during histone citrullination may reduce the antimicrobial properties. This may account for the

inhibition of PAD4 that occurs during NETosis whereby avoiding citrullination mediated inactivation of key antimicrobial elements (Cutrona et al., 2015). This suggest LTH may be used by pathogens as an evasive mechanism that targets neutrophils which results in the deleterious effects of its antimicrobial function (Konig & Andrade, 2016). Different NET-inducing stimuli may engage in PAD enzymes in various ways and further understanding of the role of PAD enzymes in NETosis may help to determine relevant immunopathogenic mechanism.

1.4.4 Role of PAD in tumour progression

In addition to playing a role in several disease, PADs, particularly PAD2 and PAD4, seem to play a vital role in tumour progression of several cancers. Citrullination correlates with an increase in PAD enzymes and it was found that PAD enzyme expression is higher in malignant tumours when compared to benign tumours and healthy tissues (Yuzhalin, 2019; Brentville et al., 2020). PAD4 overexpression was found in various malignant tumours including ovarian, breast, colorectal, renal esophageal and as well as other malignant tumours (Chang & Han, 2006; Chang et al., 2009; Lange et al., 2017). Healthy tissues and benign tissues did not express PAD4, however, metastastatic cancer (liver) expressed higher levels of PAD4 compared to the primary cell tumour (Yuzhalin et al., 2018). This implies a role of PAD enzymes in the progression a benign tumour to an invasive metastatic tumour. Similarly, PAD2 expression was observed in invasive breast carcinomas, skin neoplasia, lung and prostate cancers (McElwee et al., 2012; McElwee et al., 2014; Wang et al., 2017). Interestingly, downregulation of PAD2 was detected in ealry onset of colorectal cancers possibly suggesting a mulifactorial role for PAD enzymes which depends on the tumour type (Cantarino et al., 2016; Lange et al., 2017).

Citrullination and PAD enzymes are also involved in gene regulation (see section 1.4.1.3) and transcriptional regulation, which is of high importance to cancer, a process dependent on certain signalling pathways. PAD4 was found to bind and citrullinate the nuclear sequence region of inhibitor of growth 4 (IGN4) preventing p53 binding to IGN4, leading to suppression of p53 activity and inhibition of downstream p21 expression (Guo & Fast, 2011). PAD4 was also found to inhibit *OKL38,* a p53 target gene, thereby influencing apoptosis and inhibition of PAD4 resulting in OKL38 gene expression and mitochondrial dependent apoptosis in osteosarcoma and breast cells (Hongjie et al., 2008). Similarly, HDAC2 and PAD4 interact together and bind to p53 and simultaneously associate with p21 to regulate gene expression (Li et al., 2010). Inhibition of PAD4 and/or HDA2 resulted in the decrease in growth of osteosarcoma cancer cells in a p53 dependent manner (Li et al., 2010). PAD2 was also found to play a role in cell signalling pathways. RNA polymerase II (RNAP2) directs gene expression and citrullination of RNAP2 in breast cancer cell lines was found to activate transcription of many genes and maintain cell proliferation (Sharma et al., 2019). However, the inhibition of PAD2 or PAD2 gene silencing resulted in reduced cell proliferation by arresting cell cycle at G1 phase (Sharma et al., 2019). As mentioned above, PAD2 expression is linked to survival and progression of prostate cancer cells and the androgen receptor (AR) signal pathway contributes to progression of prostate cancer (Crona et al., 2015). PAD driven citrullination protects AR from degradation and activates AR pathway by citrullination of histone H3 after nuclear localisation leading to proliferation of prostate cancer (Crona et al., 2015). Inhibition of PAD2 or PAD2 knockdowns demonstrated a delayed progression of prostate cancer (Crona et al., 2015). Collectively these studies demonstrates the versatile interaction of PAD enzymes

in citrullination of histones or transcription factors and cell signalling pathways that can contribute to cancer progression.

1.5 Nature and scope of study

Defensins are an important component of innate immunity to combat invading pathogens. Research on defensins is critical to understand their mechanism of action that could potentially be exploited to develop novel antimicrobial and anticancer therapeutic agents. Recent studies have identified that the membranolytic action of certain defensins is through binding to a membrane component known as PIP_2 (Poon et al., 2014; Baxter et al., 2015; Phan et al., 2016). The binding of PIP_2 by defensins is primarily dependent on interaction with positively charged residues such as arginine (e.g. R40 in NaD1, R22 in HBD-2). Citrullination of antimicrobial peptides has been found to be important for the propagation of several diseases. However, the role of citrullination in regulating plant and mammalian defensin function has not been investigated. It was hypothesised that citrullination of arginine residues in human and plant defensins regulates their ability to bind lipid and target cell membranes. Hence, this study aims to (i) define the citrullination of mammalian and plant defensins (ii) compare the lipid binding ability of citrullinated and non-citrullinated defensins, (iii) determine the effects of citrullination on the anti-fungal and anti-cancer activity of defensins.

Chapter 2

Materials and Methods

2.1 Recombinant protein expression and purification

2.1.1 Recombinant protein expression in P. pastoris

P. pastoris transformed with defensin expression constructs (native NaD1, HBD-2 and HBD-3 or NaD1 mutants R40E and R39A) were inoculated in YPD medium (1% yeast extract, 2% peptone, 2% dextrose) and cultured at 30° C and 160 rpm for 24 h. The cultures were transferred to Buffered Minimal Glycerol (BMG) medium (100 mM potassium phosphate, pH 6.0, 1.34% (v/v) yeast nitrogen base (YNB) with ammonium sulphate without amino acid, 0.2% biotin (v/v), 1% glycerol (v/v)) at 30°C and 160 rpm. The following day cultures were transferred to Buffered Minimal Methanol (BMM) medium (similar to BMG, however 1% glycerol was replaced with 1% methanol) and cultured at 30°C and 160 rpm for 24 h. After cultures were initially transferred to BMM, cells were supplemented with 10 ml of methanol, containing 1.5625% (v/v) ammonia for the next 3 days. 72 h post induction, yeast cultures were centrifuged at 6000 *g* for 45 min at 4°C to obtain defensin-containing supernatant. Prior to filtration using Whatman membrane filters (Sigma-Aldrich), potassium hydroxide (10 M) was added to the supernatant to obtain a pH of 6.0.

2.1.2 Recombinant protein purification by cation exchange column chromatography

Cation exchange column chromatography using HiPrep SP FF 16/10 (GE Healthcare, Chicago, LL, USA) was used to purify recombinant proteins from culture supernatants. The columns were equilibrated with 50 mM HEPES buffer, pH 6.0 using an Äkta Start pump system (GE Healthcare) prior to passing of supernatant through columns. Following the washing of columns with 50 mM HEPES buffer, pH 6.0, bound proteins were eluted with 50 mM HEPES pH 6.0 containing 1M NaCl.

The eluted protein fractions were concentrated using Amicon ultra 15 (3000MWCO) centrifugal filters (Merck) and desalted using milliQ water using the same units. The protein concentration was determined using a Pierce™ Bicinchoninic Acid (BCA) protein assay kit (Thermo Fisher Scientific, Waltham, MA, USA).

2.2 Protein quality control

2.2.1 Sodium dodecyl sulphate polyacrylamide gel electrophoresis (SDS-PAGE)

Protein samples (2 µg and 4 µg) were prepared with 1x NuPAGE LDS sample buffer (Thermo Fisher Scientific) and 100 mM Dithiotheitol (DTT). Samples were heated at 70°C for 10 minutes before being loaded onto NuPAGE 4-12% Bis-Tris gel (Thermo Fisher Scientific) and run for 33 min at 200 V with 1x NuPAGE MES SDS running buffer (50 mM MES, 50 mM Tris base, 0.1% SDS, 1 mM EDTA, pH 7.3, Thermo Fisher Scientific), in a Xcell SureLock Mini-cell gel tank (Thermo Fisher Scientific). Protein samples were visualised using Coomassie Blue (0.4% (w/v) Coomassie Brilliant Blue R-250, 7% (v/v) acetic acid, 20% (v/v) ethanol) for several hours and destained in 20% (v/v) ethanol with 7% (v/v) acetic acid. The gel was imaged using a G:BOX chemi XL1.4 system and analysed using GeneSys software (v1.2.8.0;GeneSys, Cambridge, UK).

2.2.2 Immunoblot analysis

Following SDS-PAGE, protein samples of NaD1, HBD-2 and HBD-3, NaD1 R40E and NaD1 R39A (2 µg and 4 µg) were electrotransferred onto a 0.22-µM nitrocellulose membrane with 1x NUPAGE Transfer Buffer (25 mM bicine, 25 mM Bis-Tris, 1.0 mM EDTA, 0.05 mM chlorobutanol, 10% (v/v) methanol, pH 7.2, Thermo Fisher Scientific) at 35 V for 75 min. Following electrotransfection, membranes were blocked with 5% skim milk in 1x phosphate buffered saline (PBS; 137 mM NaCl, 2.7 mM potassium dihydrogen phosphate, pH 7.4) with 0.1% (v/v) tween-20 (PBST) (Sigma-Aldrich) for 1 h at room temperature (RT). Membranes were then washed with PBST for 30 min at RT and incubated overnight at 4°C with several primary antibodies (rabbit anti-NaD1, goat anti-HBD-2 or rabbit anti-HBD-3) diluted in 3% Bovine Serum Albumin (BSA). Following overnight incubation, membranes were then washed with PBST for 30 min and incubated with secondary antibody (donkey anti-rabbit or swine anti-goat) conjugated to horseradish peroxidase (1:5000 dilution) in 5% skim milk. Proteins were detected using Amersham ECL primer Western Blotting Detection Reagent (GE Healthcare) and imaged using a G:BOX Chemi XL1.4 system and GeneSys software (v1.2.8.0).

2.2.3 Circular dichroism (CD) spectroscopy

NaD1, HBD-2 and HBD-3 were diluted to 150 µg/mL in milliQ water and transferred to a 1 mm Quartz SUPRASIL® cuvette (Hellma Analytics, Müllheim, Germany). Samples were analysed on an Aviv Biomedical Circular Dichroism Spectrometer (Aviv Biomedical Inc., Lakewood, NJ, USA), with data reading at every 1 nm increment (ranging from 190–250 nm) with an averaging time of 5 s at 25°C. A buffer control sample (containing milliQ water) was analysed using the same parameters as the protein samples.

The CD spectroscopy data was analysed using CDPro software package (Sreerama & Woody, 2000) as implemented by the CDGo software package (Shane Gordon, La Trobe Institute for Molecular Science; available at https://github.com/sgordon/CDGo). The data was interpreted by comparing the results against the SP29, SP22X, SP37, SP43 and SP27A databases using the CONTINLL and CDSSTR algorithms. The database which provided the lowest random mean standard deviation (rmsd) value (SP43) was used to determine the secondary structure content of NaD1, HBD-2 or HBD-3.

2.3 Citrullination of NaD1, HBD-2, HBD-3 and LL-37

2.3.1 Citrullination by human PAD2

Defensins (native NaD1, HBD-2 and HBD-3), or LL-37 were diluted to 1 mg/mL in PAD assay buffer (10 mM $CaCl_2$, 100 mM Tris HCl, 5 mM DTT (pH 7.6)) and incubated with human recombinant peptidylarginine deaminase (PAD2) (Sigma-Aldrich, St. Louis, Missouri, United States) at 37°C for 2 h at a concentration of 23 U/mg peptide. The reaction was terminated via addition of RPMI 1640 with 10% FCS or placing on ice and storing at 4°C (Koziel et al., 2014).

2.3.2 Immunoblot analysis

Protein samples (10 µg) were electrotransferred onto a 0.22-µM polyvinylidene difluoride (PVDF) (GE Healthcare) membrane which was activated using 10% methanol and blocked using the same method as section 2.2.2, The membrane was incubated overnight with anti-citrulline (1:1000) (rabbit polyclonal) (Abcam) primary antibody diluted in 3% BSA. Membranes were then incubated with secondary antibody (donkey-anti-rabbit) conjugated to horseradish peroxidase (1:1000 dilution) in 5% skim milk and detected as described in section 2.2.1.

2.3.3 Mass spectrometry analysis

Citrullinated defensins (NaD1, HBD-2 and HBD-3), or LL-37 were prepared at 1mg/mL and submitted to Comprehensive Proteomics Platform (La Trobe institute for Molecular Science, La Trobe University, Melbourne, Australia) for electrospray ionisation-quadrupole-time of flight mass spectrometry (ESI-Q-TOF MS) analysis using a MicroToF-Q mass spectrometer (Bruker Daltonics, Melbourne, VIC, Australia).

2.4 Investigating citrullinated NaD1 interactions with cellular lipids

2.4.1 Protein-lipid overlay assay

Citrullinated NaD1-lipid binding and NaD1-lipid binding assays were performed using commercially available PIP™ strips (Echelon Biosciences, Salt Lake City, UT, USA). The PIP strips were initially blocked with 1x PBS containing 1% BSA for 1 h at room temperature (RT), before incubating with native NaD1 or citrullinated NaD1 (2µg/mL) diluted in 1x PBS with 1% BSA for 1 h at RT. Following incubation, membranes were washed in PBST for 1 h and incubated overnight with rabbit-anti-NaD1 primary antibody (1:1000 dilution) diluted in 1% BSA containing PBS. The membrane was then washed in PBST for 30 min and incubated with secondary antibody (donkey-anti-rabbit) conjugated to horseradish peroxidase (1:5000 dilution) in 1% BSA containing PBS at RT for 1 h. Lipid-bound NaD1 and citrullinated NaD1 were detected using the same method as in section 2.2.2. The chemiluminescence signal intensity was quantified by densitometry analysis using ImageJ (National institute of Health, Bethesda, MD).

2.4.2 Transmission electron microscopy (TEM)

Native NaD1 (0.9 mg/mL) and citrullinated NaD1 (1mg/mL) were added to 0.23 mM PtdIns(4,5)P2 (Avanti Polar Lipids, Birmingham, AL, USA). Following incubation for 30 min at room temperature, samples (10 µL) were applied to mesh copper grids coated with a thin layer of carbon. Excess material was removed by blotting and samples were negatively stained twice with 10 µL of 2% (w/v) uranyl acetate solution (Electron Microscopy Sciences, Fort Washington, PA, USA). The grids were air-dried and viewed using a FEI Tecnai TF30 transmission electron microscope operated at 300 kV. Coating and TEM viewing were conducted by Dr Julian Ratcliffe.

2.4.3 Protein crosslinking assay

Native NaD1 and citrullinated NaD1 at 1 mg/ml (5 µL) was incubated with 2.3, 1.15, and 0.575 mM PIP_2 or PA (5µl) at room temperature for 30 min. Protein complexes were cross-linked through primary amino groups by the addition of 12.5 mM bis[sulfosuccinimidyl] suberate (BS^3; 10 µL) in a buffer containing 20 mM HEPES, pH 6.0, at room temperature for 30 min. Samples were reduced using 1x NuPAGE LDS sample buffer (Thermo Fisher Scientific) and 100 mM Dithiotheitol (DTT). Samples were heated at 70°C for 10 minutes before subjected to SDS-PAGE and instant blue Coomassie staining (Sigma-Aldrich).

2.4.4 Liposome pulldown assay

Liposomes were generated as described previously using natural $PI(4,5)P_2$ and PC purchased from Avanti Polar lipids (Zhang L et al., 2001) (generated by Scott Williams (Hulett lab)).

To produce liposomes, lipid films were acclimatised to room temperature, before 100 µL of 20 mM HEPES (pH 7.4) was added to each tube. Samples were then incubated in a water bath (60°C) for 2 h, with brief vortexing every 20 min. Following this, samples were freeze-thawed for 3-5 cycles which involved dipping samples in liquid nitrogen until frozen and placing tubes back into the water bath before repeating the process. The liposomes were washed 2-3 times in 250 µL of 20 mM HEPES via repeated centrifugation (12,000 *g* for 10 min). The liposomes were then resuspended in 20 mM HEPES (80-100 µL depending on the size of the pellet) and 10 µL of liposome suspension was added to 1 µg of protein (5 µL NaD1 and citrullinated NaD1) and incubated for 30 min. The bound (pellet) and unbound (supernatant) fractions were separated via centrifugation (12,000 *g* for 10 min) and the pellet was resuspended in 15 µL of 20 mM HEPES. Following SDS-PAGE, samples were visualised via Coomassie blue (see

section *2.2.1*). The chemiluminescence signal intensity was quantified by densitometry analysis using ImageJ (National institute of Health, Bethesda, MD).

2.5 Functional analysis

2.5.1 Candida albicans growth inhibition assay

Candida albicans (*C. albicans*) (ATCC10231 and ATCC90028) cultures were grown overnight in yeast peptone dextrose (YPD) media at 30°C and 160 rpm. The cultures were centrifuged at 2000 *g* for 5 min, upon which the pellet was suspended in 1x PBS and centrifuged for 5 min at 2000 *g*. The pellet was resuspended in half concentration potato dextrose broth (PDB) (1.2% (w/v) Difco™ potato dextrose broth) and the cells were counted with a haemocytometer using a Nikon Eclipse TS100 light microscope. The cells were diluted to a final concentration of 8000 cells/mL and used to seed 4000 cells per well (50 µL) onto a 96-well plate. Dilutions of the native defensins (NaD1, HBD-2 or HBD-3; 0-50 µM), citrullinated defensins (NaD1 and HBD-3) (0-25 µM) and a no defensin control (contains all reagents included in citrullination except for defensins) were prepared in half-strength PDB and 50 µL defensins were added per well. No cells (media only) were included as background control. The plate was sealed using a Breath-Easy® sealing membrane (Merck) and incubated at 30°C. After 24 h, the plate was shaken and read at 600 nm in a 9-well scan setting using a Spectramax M5 microplate reader (Molecular Device, Sunnyvale, CA, USA).

2.5.2 C. albicans propidium iodide (PI) uptake assay

C. albicans (ATCC10231 and ATCC90028) was cultured and resuspended using the same methods as section 2.3.1. However, post cell counting, cells were diluted to $2x10^6$ cells /mL and $5x10^4$ cells were added and treated with dilutions of the three defensins (NaD1, HBD-2 or HBD-3; 0–50 μM), citrullinated defensins (NaD1 and HBD-3) (0-25 μM or 0-50 μM, respectively) or a no defensin control were prepared in half-strength PDB. 10 μM of NaD1 was used as a positive control. Following a 30 min incubation period at 30°C and 300 rpm, 2 μg/mL of propidium-iodide (PI) prepared in PBS was added to each well and placed on ice to terminate the reaction. Samples were analysed using flow cytometry, using FACSCanto™ II HTS cell analyser and BD FACSDiva software v8.0.1 (BD Biosciences, Franklin Lakes, NJ, USA). FlowJo v8.8.10 software (Tree Star, San Carlos, CA, USA). The cells were gated based on the forward scatter (FSC) and side scatter (SSC) to determine the proportion of propidium iodide-positive cells using FlowJo v8.8.10 software (Tree Star, San Carlos, CA, USA).

2.5.3 Human histiocytic lymphoma (U937) PI uptake assay

10 μL of native NaD1, citrullinated NaD1, native HBD-3, citrullinated HBD-3 (0-25 μM or 0-50 μM) or no defensin control were incubated with 40 μL of U937 cells with a density of $1x10^6$ cells/mL (resuspended in serum-free RPMI supplemented with 0.1% bovine serum albumin (Sigma-Aldrich), at 37 °C for 30 min. Following incubation, PI solution was added to the samples to a final concentration of 2 μg/mL prepared in PBS and placed on ice to terminate the reaction. Samples were analysed using flow cytometry, using FACSCanto™ II HTS cell analyser and BD FACSDiva software v8.0.1 (BD Biosciences, Franklin Lakes, NJ, USA). FlowJo v8.8.10 software (Tree Star, San Carlos, CA, USA). The cells were gated based on the

forward scatter (FSC) and side scatter (SSC) to determine the proportion of propidium iodide-positive cells using FlowJo v8.8.10 software (Tree Star, San Carlos, CA, USA).

2.5.4 Cell culture and cell viability assay

Human cervical cancer (HeLa) and Monocytic leukemia (THP1) cells lines were cultured in RPMI 1640 medium (Thermo Fisher Scientific), supplemented 10% fetal calf serum (FCS), 100 U/mL penicillin and 100 µg/mL streptomycin (Thermo Fisher Scientific). U937 and prostate cancer (PC3) cells were cultured in RPMI 1640 medium (Thermo Fisher Scientific), supplemented with 5% fetal calf serum (FCS), 100 U/mL penicillin and 100 µg/mL streptomycin. The cells lines were incubated at 37°C in 5% CO_2.

Adherent HeLa and PC3 cell line were suspended via addition of 0.25% (w/v) trypsin and 0.5 mM EDTA (Thermo Fisher Scientific). Cells were pelleted by centrifugation at 300 *g* for 5 min before being resuspended in respective growth media. Trypan Blue (0.1% (w/v); Sigma-Aldrich) was used to assess the number of cells, before adequate dilutions were prepared, and cells were seeded onto a 96-well plate at $5x10^3$ cells in 50 µL of serum-supplemented media. PBS was added to all wells bordering the samples to avoid evaporation of growth media and a media only control was included. The plate was incubated at 30°C with 5% CO_2 for 24 h.

Serial dilutions of the three defensins (NaD1, HBD-2 or HBD-3; 0–50 µM), citrullinated defensins (NaD1 and HBD-3) (0-25 µM or 0-50 µM respectively) and no defensin controls were prepared in growth media and once treated, cells were incubated at 30°C with 5% CO_2 for 48 h. Following the incubation period, 5mg/mL 3-(4,5-dimethylthiazol-2-yl)-2,5diphenyltetrazolium bromide (MTT) (Merck), prepared in PBS was diluted to 1 mg/mL by addition of serum free growth media and added to all samples. Following 3 h incubation, media

was removed from wells without disturbing purple crystals that could have formed. Dimethyl sulfoxide (DMSO) (Merck) was added to each well and briefly shaken to dissolve crystals. The absorbance of samples was measured at 570 nm using a microplate reader.

Similarly, the suspension cell lines U937 or THP1, were seeded into 96-well plates at predetermined density of $5x10^3$ cells, with 50 µL of serum-supplemented media and incubated at 37°C in 5% CO_2 atmosphere for 24 h. Serial dilutions (0–25 µM) of native NaD1, citrullinated NaD1 and a no defensin control were added to the cells in triplicate. Following 48 h co-incubation, 2 mg/mL 3-(4,5-dimethylthiazol-2-yl)-5-(3-carboxymethoxyphenyl)-2(4-sulfophenyl)-2H-tetrazolium (MTS) (Merck) and 90 µg/mL phenazine methosulfate (PMS), (Merck) in 1x Dulbecco's PBS (DPBS; PBS supplemented with 100 mM $MgCl_2$ and 120 mM $CaCl_2$) was added to the treatment cells. The absorbance was measured at 490 nm after 3 h incubation.

2.5.5 Confocal laser scanning microscopy (CLSM)

Live imaging was performed on U937 ($1x10^6$ cells/mL) cells stained with PKH67 in diluent C at 1:200 dilution and incubated at RT for 5 min, followed by three 1x PBS washes. Cells were then recovered with 10% BSA containing 1x PBS, followed by resuspension of pellet in 1% BSA-supplemented serum-free media. $7.5x10^5$ cells/well were seeded onto 8-well chamber slide, coated with 1% poly-L-lysine. Prior to seeding, cell suspensions were stained with PI at a final concentration of 2µg/mL prepared in RPMI medium containing 0.1% BSA. Native and citrullinated NaD1 were directly added to the imaging chamber via a capillary tube. The cells were imaged using Zeiss LSM 800 confocal microscopy in a 37°C/5% CO_2 atmosphere and analysed using Zen software. Live imaging was performed with the assistance of Guneet Bindra (Hulett Lab).

Similarly, live imaging was performed on *C.albicans* (ACT10231). *C. albicans* was cultured and resuspended using the same methods as section 2.3. Cells were diluted to $1x10^6$ cells/mL and seeded onto 8-well chamber slide, coated with 1% poly-L-lysine. Prior to seeding, the cell suspension was stained with PI prepared in PDB at a final concentration of 2 µg/mL. Native and citrullinated NaD1 (25 µM) were directly added to the imaging chamber via a capillary tube. The cells were imaged using Zeiss LSM 800 confocal microscopy in a 37°C/5% CO_2 atmosphere and analysed using Zen software. Live imaging was performed with the assistance of Guneet Bindra (Hulett Lab).

Chapter 3

NaD1, HBD-2 and HBD-3 protein expression and quality control

3.1 Interaction of NaD1, HBD-2 and HBD-3 with PI(4,5)P_2

The membranolytic activity of some defensins, such as the plant defensin NaD1, and human β-defensins HBD-2 and HBD-3, is mediated by the interaction of positively-charged arginine residues with negatively-charged membrane phospholipids, including phosphatidylinositol 4,5-bisphosphate PI(4,5)P_2 (or PIP_2) (Figure 8B) (Poon et al., 2014; Baxter et al., 2015; Phan et al., 2016). Microbial pathogens have developed mechanisms to counteract host innate defences by post-translational modifications such as citrullination, which converts arginine to neutral citrulline. As defensins are attracting interest for potential application as novel anti-infective molecules, their possible citrullination and therefore functional regulation by this process, warrants investigation. In this thesis, the citrullination of the plant defensin NaD1 and human β-defensins, HBD-2 and HBD-3, has been investigated. The primary amino acid sequences of NaD1, HBD-2 and HBD-3 contain 4, 2 and 5 arginine residues, respectively (Figure 8A). Arginine 40 (Arg40) of NaD1 and arginine 22 (Arg22) of HBD-2, have been shown to play key roles in the interaction with PIP_2. In contrast, lysine 39 (Lys39) of HBD-3 appears to be critical for the binding of PIP_2 (Table 2). However, whether any of the arginine residues of these defensins are citrullinated, and if so, whether that regulates their function(s), has not been previously defined.

Table 2. Characteristics of NaD1, HBD-2 and HBD-3 in terms of the number of amino acids in each defensin and Arg/Lys residues known to be involved in PIP_2 binding

Defensin	Number of amino acids	Key residues involved in PIP_2 binding
NaD1	47	Arg40
HBD-2	41	Arg22
HBD-3	45	Lys39

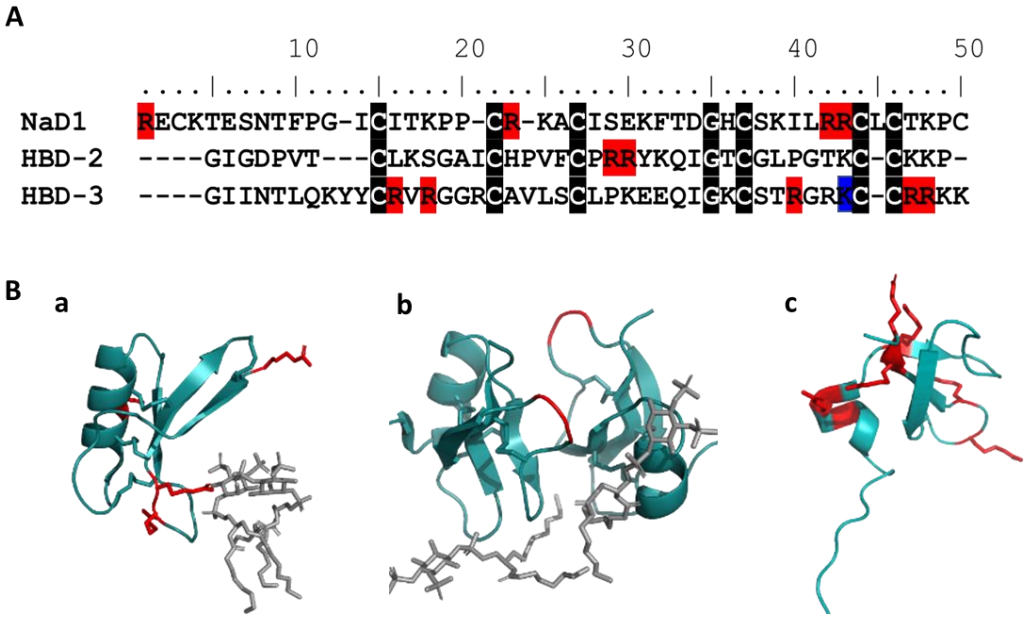

Figure 8. Mature defensin sequence and structures of NaD1, HBD-2 and HBD-3 (A) Amino acid sequence alignment of defensins. The arginine residues (in red) and conserved cysteine residues (highlighted in black) are shown (generated using BioEdit). **(B)** Structures of (a) NaD1 (PDB code: 4CQK), (b) HBD-2 (PDB code: 6CS9) and (c) NMR structure of HBD-3 (PDB code 1KJ6) highlighting the positions of arginine residues (in red), lysine 39 residue (in blue) for HBD-3 and PIP_2 molecule (in grey) for NaD1 and HBD-2. Figures drawn using PyMOL.

3.2 Recombinant protein expression and characterisation

To obtain purified defensin proteins, recombinant expression was performed using the pPIC9 expression system in *Pichia pastoris* with methanol induction. The defensins were purified using cation exchange column chromatography and concentrated. A yield of 2 mg/L, 1.17 mg/L and 0.7 mg/L was obtained for NaD1, HBD-2 and HBD-3 respectively.

The purity and quality of the expressed defensins were initially evaluated using SDS-PAGE and immunoblot analysis. NaD1 and HBD-3 produced single bands at 5-6 kDa, consistent with expected molecular weight of 5.3 kDa and 5.1 kDa for NaD1 and HBD-3, respectively. Interestingly HBD-2 revealed two bands at ~ 4-4.5 kDa suggesting the presence of the expected molecular weight protein of 4.1 kDa and a possible truncated form (Figure 9A). Immunoblot analysis with anti-NaD1, anti-HBD-2 and anti-HBD-3 revealed specific bands of molecular weights similar to that observed by SDS-PAGE, confirming the identity of proteins (Figure 9B).

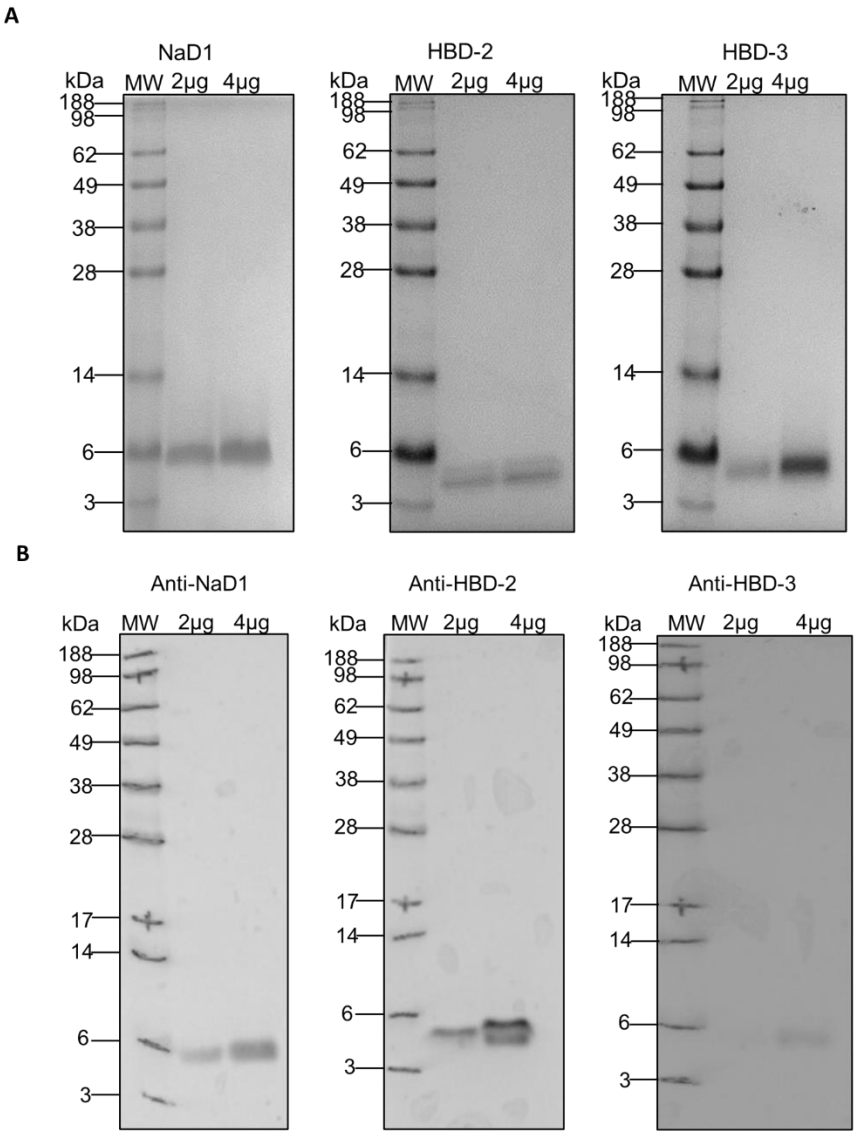

Figure 9. Characterisation of purified NaD1, HBD-2 and HBD-3

(A) SDS-PAGE analysis (2µg and 4 µg protein/lane) and Coomassie stain of purified NaD1, HBD-2 and HBD-3. (**B**) Immunoblot (2µg and 4 µg protein) of rabbit-anti-NaD1, goat-anti-HBD-2 and rabbit-anti-HBD-3, detected with HRP conjugated donkey-anti-rabbit or swine-anti-goat antibodies.

CD spectroscopy was used to determine the secondary structure content of NaD1, HBD-2 and HBD-3. Data was collected and analysed using CONTINLL and CDSSTR algorithms against the soluble protein (SP) datasets which provides lowest rmsd values for NaD1, HBD-2 and HBD-3.

Analysis of data indicate that β-strands (34 %) are most the predominant structures in NaD1, followed by structures comprising unordered (30.6%), turn (19.4%) and α-helical (15.9%) regions (Figure 10A). HBD-2 was revealed to mostly comprise of β-strands (41.7 %) followed by unordered (32.3%), turn (21.1%) regions, with α-helical only comprising of 4.9% (Figure 10B). In contrast, unordered structures (57.4%) were most prevalent in HBD-3, followed by β-strands (24.2%), turn (12.8%) and α-helical (5.4%) regions, respectively (Figure 10C). These data are consistent with that expected and previously reported for each of these defensins (Lay et al., 2012; Poon et al., 2014; Phan et al., 2016; Järvå et al., 2018b).

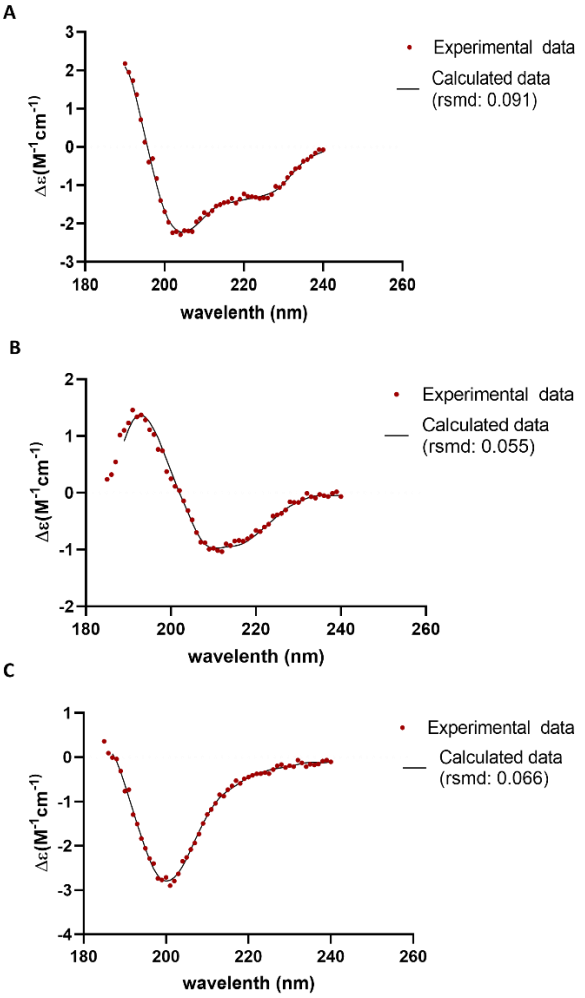

Secondary structures	Percentage of total structures (%)
α-helix	15.9
β-strand	34.0
Turn	19.4
Unordered	30.6

Secondary structures	Percentage of total structures (%)
α-helix	4.9
β-strand	41.7
Turn	21.1
Unordered	32.3

Secondary structures	Percentage of total structures (%)
α-helix	5.4
β-strand	24.4
Turn	12.8
Unordered	57.4

Figure 10. CD spectrum and secondary structure composition of NaD1, HBD-2 and HBD-3

(A) The CD spectrum of NaD1 was generated using the SP43 database and CONTINLL algorithm, which fitted a trend line to the experimental data with a rmsd value of 0.091. Analysis of CD spectrum revealed that β-strands were most prevalent secondary structure within NaD1. **(B)** The spectrum of HBD-2 generated a best fitted trend line to experimental data with a rmsd value of 0.055 and β-strands were found to be most prevalent. **(C)** The spectrum of HBD-3 generated a best fitted trend line to experimental data with a rmsd value of 0.066 and unordered were found to be most prevalent.

3.3 Functional analysis of NaD1, HBD-2 and HBD-3

To confirm the antimicrobial activity of the purified recombinant NaD1, HBD-2 and HBD-3, the antifungal activity against the human fungal pathogen *C. albicans* (strain ATCC10231) was assessed. NaD1, HBD-2 and HBD-3 demonstrated dose dependent inhibition of fungal growth with IC_{50} values of 5.6 µM, 9.37 µM and 6.99 µM, respectively (Figure 11A).

As these defensins exert their activity via membrane permeabilisation, the uptake of the membrane impermeable dye propidium iodide (PI) by *C. albicans* was assessed. NaD1, HBD-2 and HBD-3 were incubated with fungal cells, and the percentage of PI positive cells were quantified by flow cytometry (Figure 11B). At low concentrations (~ 6 µM) of NaD1, PI positivity was 50% and reached 100% at 25 µM. In contrast, fungal cells were relatively unaffected by HBD-2 and HBD-3 at low protein concentrations (<6 µM) with 100% PI positivity observed at 25 µM and 50 µM, respectively.

In addition to antifungal activity, defensins are also known to have oncolytic activity against tumour cells. Tetrazolium dye-based (MTT) cell viability assays were performed to investigate cytotoxic effects of NaD1, HBD-2 and HBD-3 on the human cervical cancer cell line HeLa. MTT assay relies on NAD(P)H-dependent cellular oxidoreductase to reduce MTT dye to an insoluble formazan product which is used to estimate cell viability. The viability of HeLa cells treated for 48 h with defensins (0–50 µM) was assessed. NaD1 was most potent at reducing HeLa cell viability at low concentrations (IC_{50} ~ 3 µM) and approximately 5 times more potent than HBD-3 (IC_{50} = 17.8 µM). Intriguingly, HBD-2 did not reduce HeLa cell viability, and appeared to increase viability at concentrations above 20 µM (Figure 11C).

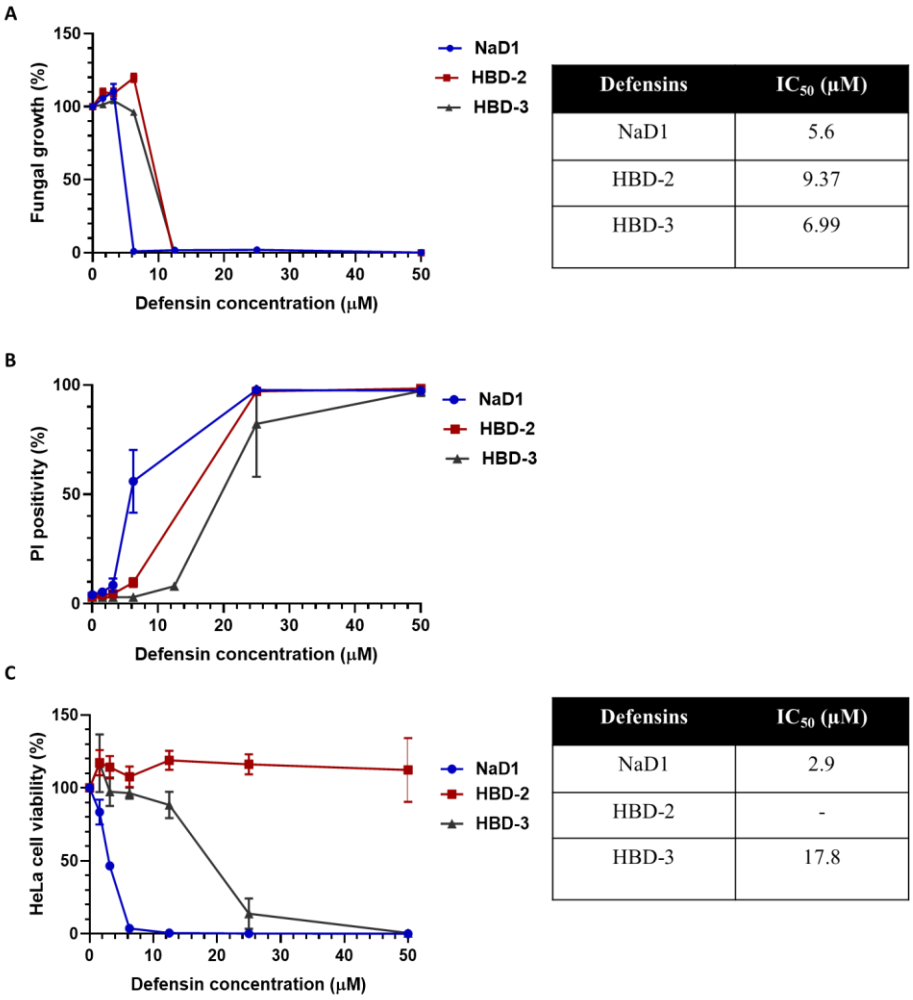

Defensins	IC_{50} (μM)
NaD1	5.6
HBD-2	9.37
HBD-3	6.99

Defensins	IC_{50} (μM)
NaD1	2.9
HBD-2	-
HBD-3	17.8

Figure 11. The effect of NaD1, HBD-2 and HBD-3 on growth, PI uptake and viability of *C. albicans* and HeLa cells

(A) Percentage fungal growth of *C. albicans* were tested against various concentrations of NaD1, HBD-2 and HBD-3 (0–50 μM) after 24 h incubation period. Data were normalised against an untreated control (assigned 100% growth). IC_{50} values (μM) were calculated and displayed in the adjacent table. Data represents mean ± SEM of n=3, performed in triplicate **(B)** Percentage of PI positive cells tested with various NaD1, HBD-2 and HBD-3 concentrations following 30 min incubation. Data represents mean ± SEM of n=3, performed in triplicate. **(C)** HeLa viability treated with various NaD1, HBD-2 and HBD-3 concentrations were assessed using tetrazolium-based spectrometry. Data were normalised against an untreated control (assigned 100% viability). IC_{50} values (μM) were calculated and displayed in the adjacent table. Data represents mean ± SEM of 3 independent experiments (n=3) performed in triplicate.

Chapter 4
Citrullination and functional analysis of NaD1

4.1 Introduction

As previously mentioned, plant defensins such as NaD1 are known to exhibit membranolytic activity by targeting phospholipids, particularly PIP_2. This interaction is mediated by a key arginine residue, R40, and the NaD1-PIP_2 interaction is known to play a vital role in the antifungal and anticancer activity of NaD1 (Poon et al., 2014). Furthermore, as there is an increasing interest in using NaD1 as a novel therapeutic agent (such as the clinical trials currently underway for NaD1-deriviatives by Hexima Ltd for the topical treatment of onychomycosis; https://hexima.com.au/project_tag/onychomycosis/), it is important to identify and characterise any processes that may be able to inactivate the defensin *in vivo*, resulting it in being functionally ineffective. Therefore, this chapter aims to provide novel insight into the citrullination of NaD1and its effect on lipid binding and function of this plant defensin.

4.2 Citrullination of NaD1 and LL-37

To determine whether NaD1 can be citrullinated, it was treated *in vitro* with the PAD2 (peptidylarginine deaminase 2) enzyme. Citrullination was detected using immunoblot analysis with an anti-citrulline antibody which is able to specifically detect citrulline residues. The human cationic antimicrobial peptide LL-37, previously shown as a target for citrullination, was used as a positive control.

A band of ~ 5.5 kDa was observed for citrullinated LL-37 consistent with the expected molecular weight of LL-37, while no band was detected for the non-citrullinated LL-37 (Figure 12A). Interestingly, a band at 98 kDa was also observed for the citrullinated LL-37 sample. Bands consistent with the molecular weight of NaD1 at ~ 6 kDa were observed for citrullinated NaD1 (Figure 12B). A band at 49 kDa was observed for citrullinated NaD1. No bands were observed for non-citrullinated NaD1.

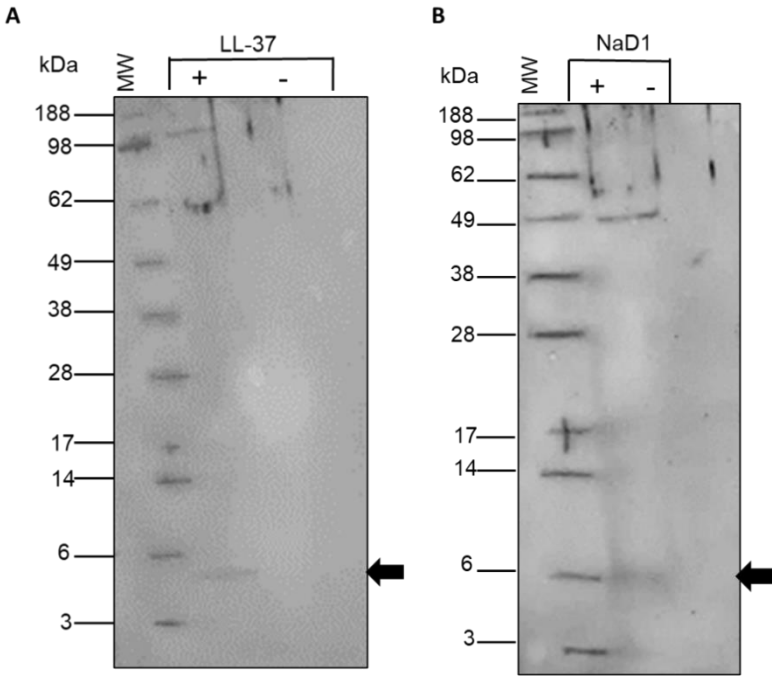

Figure 12. Characterisation of citrullinated NaD1 and LL-37

Immunoblot of (**A**) citrullinated LL-37 (5 µg protein) and (**B**) Citrullinated NaD1 (10 µg protein) probed with anti-citrulline antibody (1:1000 dilution) and detected using HRP conjugated donkey-anti-rabbit antibody. (+ = Citrullinated, - = non-citrullinated). Arrows indicate citrullinated protein bands.

As an increase in 1 Da is observed for every arginine residue that is citrullinated and converted to citrulline, ESI-Q-ToF mass spectrometry was conducted to determine exact mass of citrullinated NaD1 and LL-37, in order to confirm if PAD2 was successfully able to citrullinate defensins (Figure 13).

An increase in 3 Da was observed for citrullinated LL-37 (4493.5) in comparison to native LL-37 (4490.6) (Figure 13A). Similarly, an increase in 3 Da was also observed for citrullinated NaD1 (5374.5) when compared to the untreated NaD1 (5371.6) (Figure 13B). These data suggest that 3 arginine residues in both LL-37 and NaD1 have been converted to citrulline.

Furthermore, the mass spectrometry results were consistent with the immunoblot analysis of citrullinated NaD1 and LL-37 (Figure 12A& B), verifying citrullination of LL-37 and NaD1.

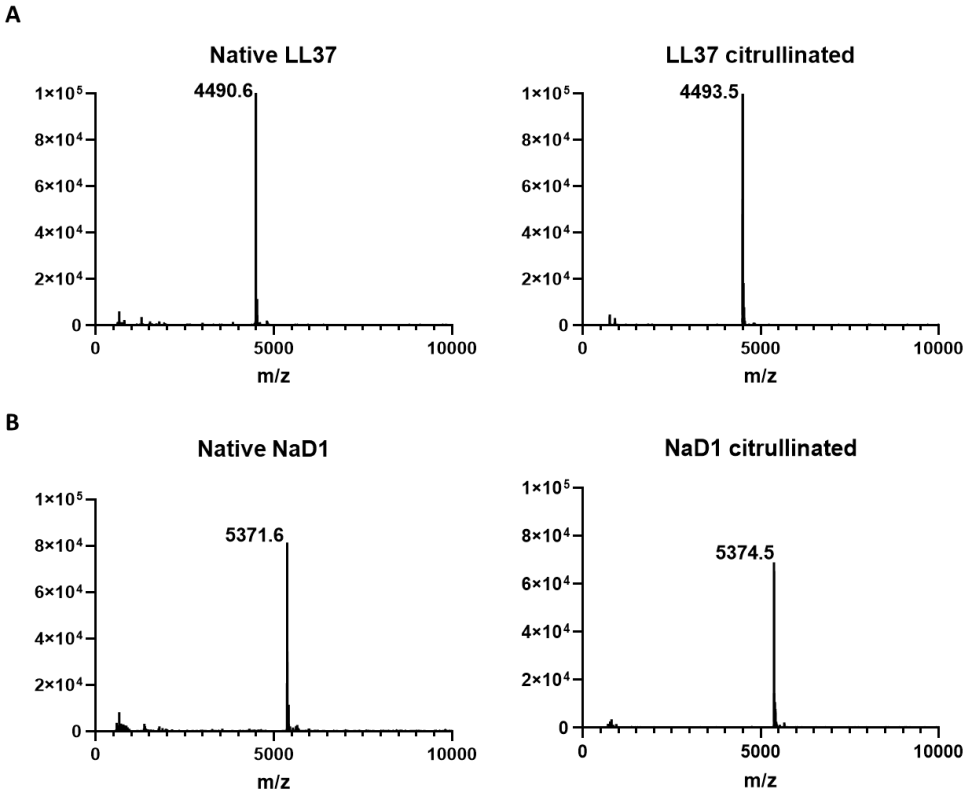

Figure 13. ESI-Q-Tof mass spectrometry analysis of untreated and citrullinated LL-37 and NaD1

(A) Mass spectrum revealed a single peak with an increase in 3 Da for citrullinated LL-37 (4493.5) in comparison to native LL-37 (4490.6). **(B**) Similar results were obtained for citrullinated NaD1 (5374.5) and native NaD1 (5371.6).

4.3 Interaction of citrullinated NaD1 with cellular lipids

4.3.1 Protein-lipid overlay assay

A number of plant and human defensins, including NaD1, have been shown to bind membrane phosphoinositides, resulting in membrane perturbation and cell permeabilisation. Arginine 40 (R40) of NaD1 is critical for the interaction of NaD1 with phospholipids such as PIP_2, and if citrullinated, would expect to lose the ability to bind to PIP_2. Therefore, to investigate whether citrullinated NaD1 can interact with membrane lipids, including PIP_2, protein-lipid overlay assays, using PIP™ strips were performed (Figure 14). Lipid bound native and citrullinated NaD1 were detected with an anti-NaD1 antibody.

As expected, native NaD1 demonstrated greater relative binding intensities to various phospholipids, including several of the mono-/bis-/tris-inositiol phosphates (including PtdIns(4,5)P_2) and phosphatidic acid (PA) (Poon et al., 2014). (Figure 14A). Some interaction with phosphatidylserine (PS) was also observed, however, it was much weaker compared to interaction observed with other phospholipids. Intriguingly, citrullinated NaD1 also bound to the same phospholipids as native NaD1 (Figure 14B), with binding observed to phosphoinositides PtdIns(4)P, PtdIns(3)P, PtdIns(5)P, PtdIns(3,4,5)P_3, PtdIns(4,5)P_2 and PA. Some binding, although much weaker ,were observed to PtdIns(3,5)P2, PtdIns(3,4)P_2 and PS . Consistent with native NaD1, no binding was observed to PE or LPA.

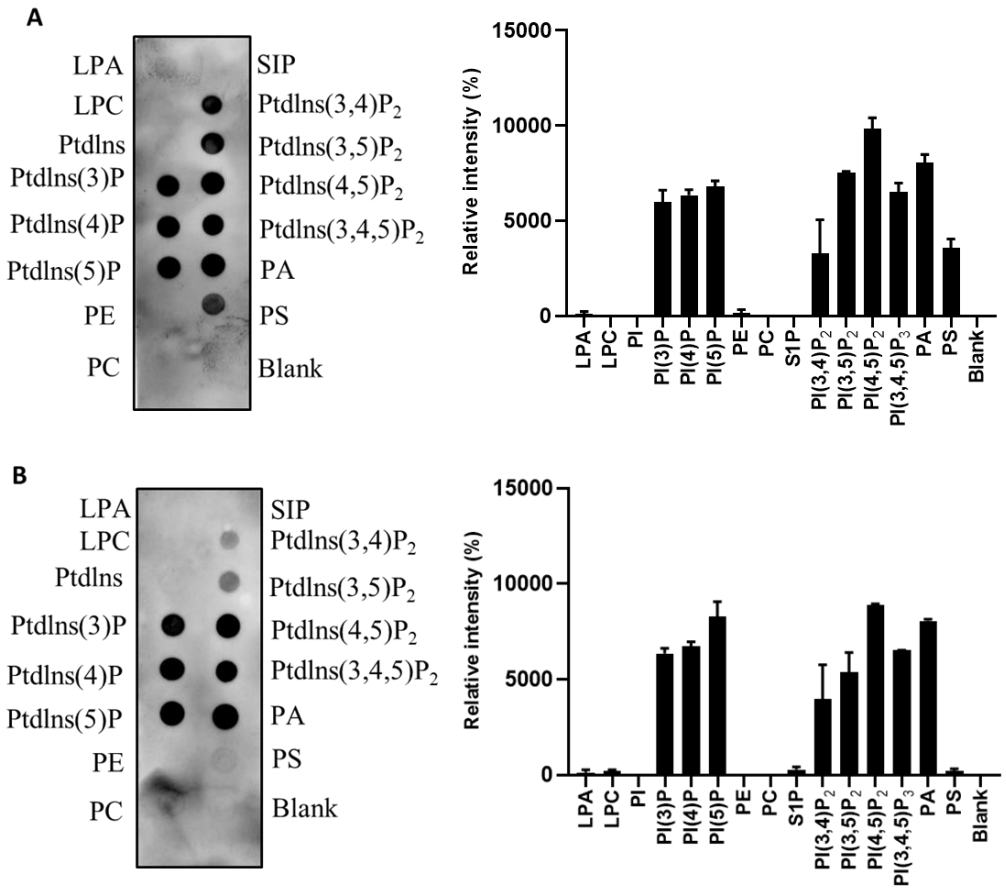

Figure 14. Interaction of native and citrullinated NaD1 with membrane phospholipids **(A)** Binding of native NaD1 (2 µg/mL) and **(B)** citrullinated NaD1 (2 µg/mL) to lipid (100 pmole/spot) PIP™ strips, were immunodetected using rabbit-anti-NaD1 antibody and HRP conjugated donkey-anti-rabbit antibody. The relative binding intensities were determined by densitometry analysis of the chemiluminescence signal. Data represents mean ± SEM of at least two independent experiments.

4.3.2 Interaction of NaD1 and citrullinated NaD1 with PIP_2

As protein lipid overlay assays demonstrated the ability of citrullinated NaD1 to bind to PIP_2 (Figure 14B), liposome pulldown assays were used to confirm if citrullinated NaD1 bound to PIP_2 containing liposomes (Figure 15). Native NaD1 was used as a control.

Native NaD1 bound to liposomes that were enriched in PIP_2 but not to PC-only liposomes. Citrullinated NaD1 did not bind to PIP_2 containing liposomes and were mainly observed in the unbound fraction of PC:PI(4,5)P_2. As with native NaD1, citrullinated did not bind to PC only liposomes.

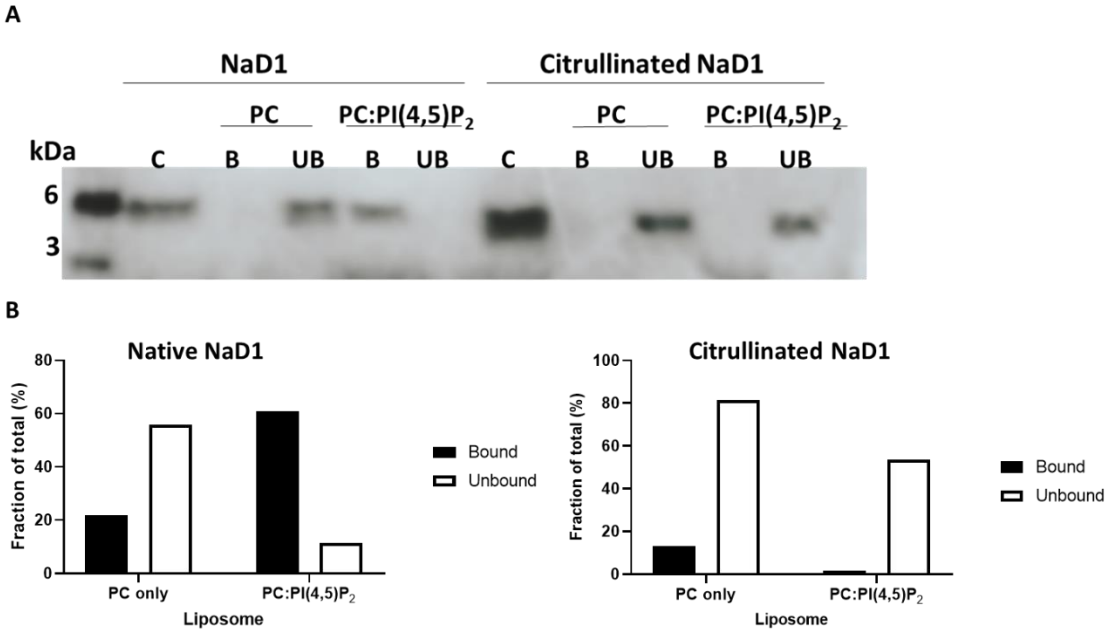

Figure 15. Binding of native and citrullinated NaD1 to PI(4,5)P_2

(A) Liposome pull down assay of liposomes containing PC only or PC:PI(4,5)P_2 were incubated with 1 ug of native and citrullinated NaD1, before centrifugation of bound (pellet) and unbound (supernatant) to separate fractions followed by SDS-PAGE and Coomassie blue staining. **(B)** The protein band intensity was determined and quantified by densitometry using ImageJ software and normalized against HBD-2 loading control. Data is representative of two independent experiments.

4.3.3 Detection of citrullinated NaD1:PIP_2 oligomer formation using chemical crosslinking

As previously mentioned, arginine residues are crucial for interactions of NaD1 with membrane phosphoinositides (R40 for PIP_2) as well as R39 for the binding of PA, to mediate the formation of oligomeric structures which are crucial for membrane permeabilisation activity (Poon et al., 2014). Therefore, to investigate the ability of citrullinated NaD1 to form higher order multimeric structures, biochemical crosslinking assay with BS^3 was used. Native NaD1:PIP_2 (Figure 16A) and native NaD1:PA (Figure 16B) were used as a controls.

In the presence of crosslinker BS^3, higher order multimeric complexes (oligomers) of NaD1 molecules were only seen in the presence of PIP_2 (Figure 16A), whereas NaD1 alone only resulted in the formation of a dimeric structure. No formation of higher order multimeric complexes were seen for citrullinated NaD1:PIP_2, with only dimeric structures observed in the presence or absence of PIP_2. Higher order complexes of NaD1 were seen in the presence of PA at the highest concentration (2300 μM) with only dimeric structures formed for NaD1 alone. In the presence of PA, the formation of multimeric complexes was not observed for citrullinated NaD1 even at the highest concentration of PA (Figure 16B).

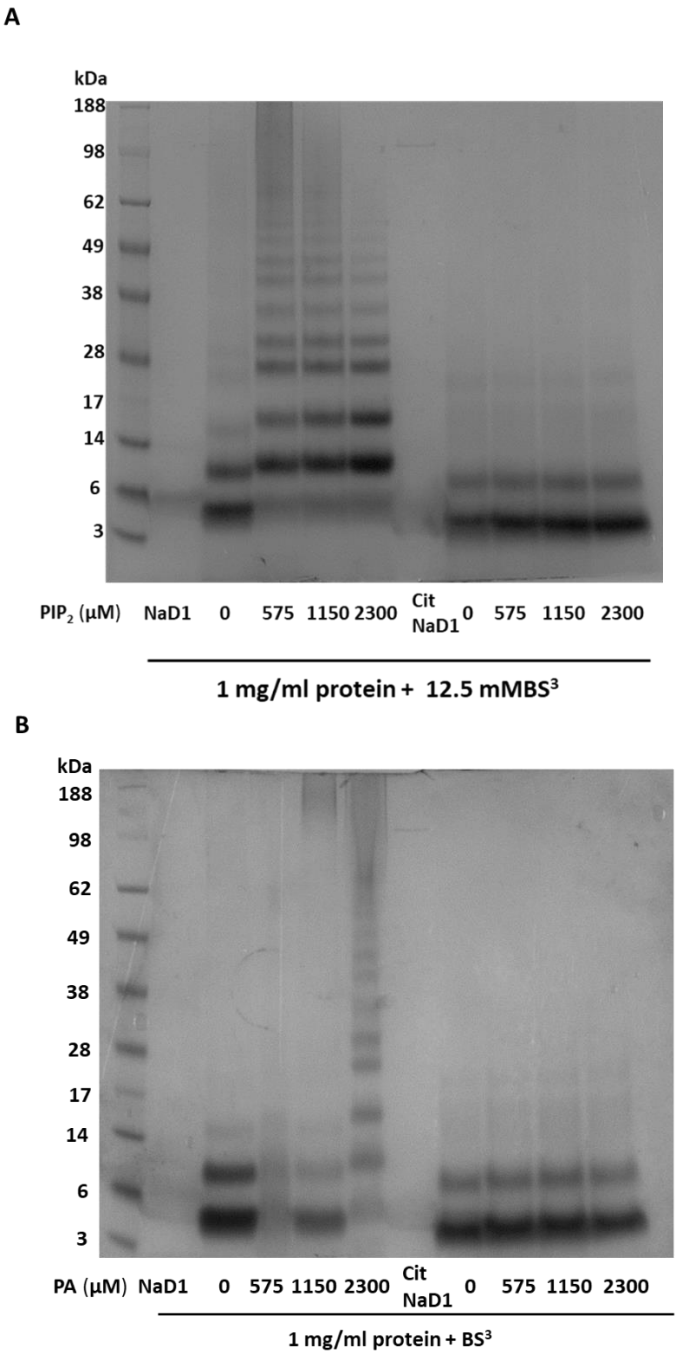

Figure 16. Formation of oligomers by NaD1 and citrullinated NaD1 with PIP_2 and PA

Ability of NaD1 and citrullinated NaD1 (1 mg/ml) to form multimers with **(A)** PIP_2 and **(B)** PA was determined by protein crosslinking with BS^3 (12.5 mM) followed by SDS-PAGE and instant blue staining. Data are representative of 3 independent experiments.

4.3.4 Detection of native and citrullinated NaD1:PIP_2 fibril formation using TEM

Phosphoinositides, are key components of membrane bilayers and binding of NaD1 to these lipids, particularly PIP_2, results in the formation of oligomeric complexes, which can be visualised as long fibril structures by transmission electron microscopy (TEM) (Poon et al., 2014). The PIP_2-mediated oligomerisation of NaD1 has also been linked to membrane permeabilisation. It was therefore of interest to investigate by TEM whether citrullinated NaD1 binding to PIP_2 also results in fibril formation. Native NaD1:PIP_2 was used as a control.

Long string-like fibril structures were observed for native NaD1 in the presence of PIP_2, with no such structures observed for grids containing either the defensin or lipid alone (Figure 17A). Interestingly, citrullinated NaD1 resulted in formation of fibrils structures (Figure 17B). However, in contrast to the string-like fibril structures observed for native NaD1, citrullinated NaD1 formed different structures that were somewhat flatter and elongated. No structures were observed for grids containing either PIP_2 or citrullinated NaD1 alone.

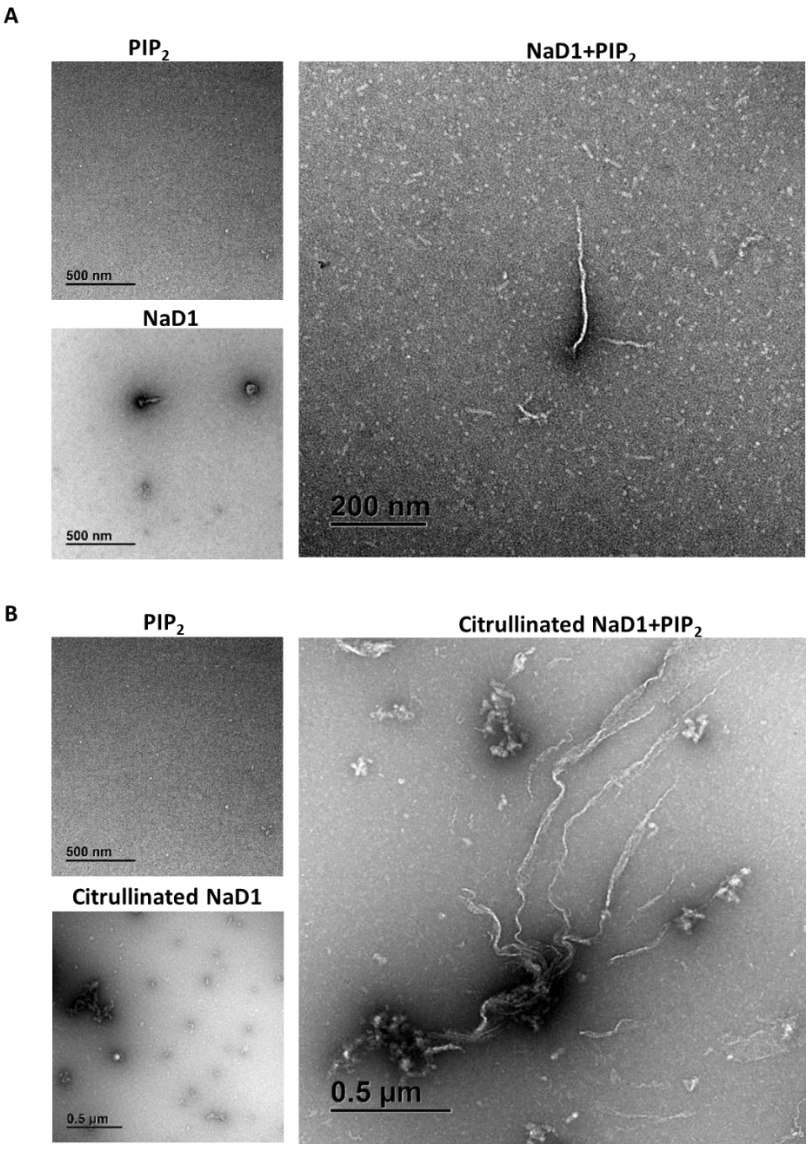

Figure 17. TEM analysis of the interaction between native or citrullinated NaD1 with PIP_2

(A) NaD1 (0.9 mg/mL) and (**B**) citrullinated NaD1 (1 mg/mL) was incubated with 0.23 µM PIP_2 prior to applying on carbon-coated copper grids and viewing by transmission electron microscopy (scale = 0.5 µm -200nm). Data are representative fields of view of one experiment.

4.4 Functional analysis of citrullinated NaD1

4.4.1 Effect of citrullinated NaD1 on fungal growth inhibition

As described in section 3.3, defensins, particularly NaD1, demonstrate anti-fungal activity against the human fungal pathogen *C. albicans*. To investigate whether citrullination decreases the activity of NaD1, the effect of citrullinated NaD1 (0–25 µM) on *C. albicans* following a 24 h incubation period was assessed (Figure 18). Native NaD1 (0–25 µM) was used as a positive control. Additionally, a no defensin control was employed to ensure any effects observed were not due to the reagents present in citrullinated samples.

NaD1 demonstrated a dose-dependent effect on fungal growth with an IC_{50} value of 5.7 µM and growth was completely abolished at 12.5 µM. In contrast, the ability of citrullinated NaD1 to inhibit fungal growth was greatly reduced with an IC_{50} ~ 105 µM. As anticipated, no defensin control exhibited little effect on the fungal growth (Figure 18).

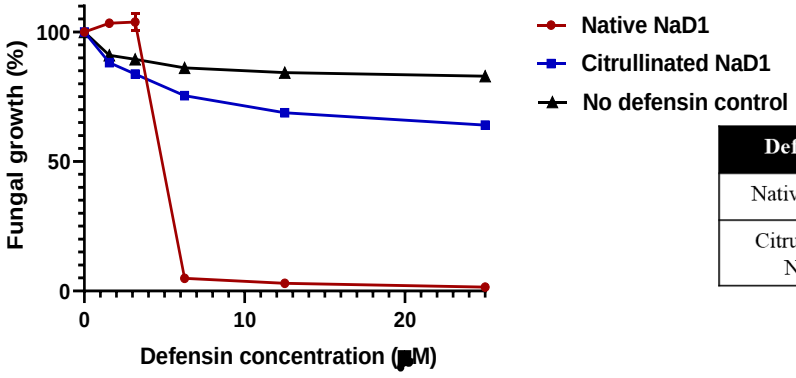

Defensins	IC_{50} (µM)
Native NaD1	5.7
Citrullinated NaD1	105

Figure 18. Effect of citrullinated and native NaD1 on the growth *C. albicans*.

Percentage fungal growth of *C. albicans* (ATCC10231) following incubation with native and citrullinated NaD1 (0–25 µM) after 24 h. A no defensin control was included (in black). Data were normalised against an untreated control (assigned 100% growth). IC_{50} values (µM) were calculated and displayed in the adjacent table. Data represents mean ± SEM of 3 independent experiments (n=3) performed in triplicate.

4.4.2 Effect of citrullinated NaD1 on fungal membrane permeabilisation

To determine whether citrullinated NaD1 maintains membrane permeabilising activity, PI uptake with varying concentrations of citrullinated NaD1 (0–25 µM) on *C. albicans* (ATCC10231) following a 30 min incubation was assessed using flow cytometry (Figure 19). Native NaD1 (0–25 µM) and no defensin samples were used as controls.

As expected at concentrations <6 µM, native NaD1 had no effect on the membrane permeabilisation, however at higher concentrations PI positivity increased to 80% at 12.5 µM and reached ~ 100% at 25 µM. In contrast, *C.albicans* (ATCC10231) was largely unaffected by citrullinated NaD1 even at the highest concentration of 25 µM with almost negligible PI positivity of cells. Likewise, the no defensin control did not have any effect on the PI positivity of cells (Figure 19).

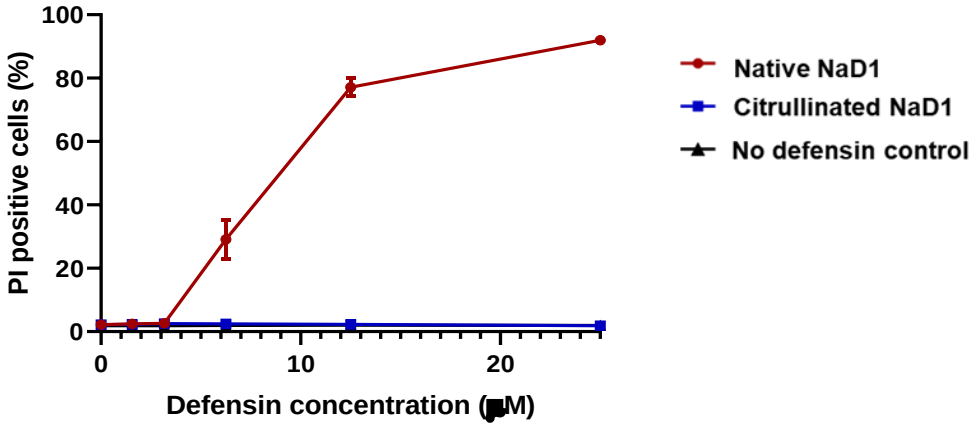

Figure 19. Effect of citrullinated and native NaD1 on the PI uptake of *C. albicans* (ATCC10231)

Percentage PI positive cells tested with various concentrations of native and citrullinated NaD1 following 30 min incubation. No defensin control was included (in black). Data represents mean ± SEM of 3 independent experiments (n=3) performed in triplicate.

To further understand the kinetics and examine the morphological changes a cell undergoes upon treatment with citrullinated NaD1, endpoint and time-course imaging using confocal live laser scanning imaging microscopy (CLSM) was performed. Immobilised *C.albicans* (ATCC10231) cells were treated with either citrullinated NaD1 (25 µM), native NaD1 (25 µM) or a no defensin control in the presence of orange nucleic acid stain PI.

Treatment of *C.albicans* cells with NaD1 over 30 min induced cell permeabilisation which is indicated by the orange PI staining (Figure 20). Treatment with citrullinated NaD1 resulted in no membrane permeabilisation as demonstrated by no PI staining of the cells. No PI staining and membrane permeabilisation was observed in the untreated and no defensins samples.

A time-course imaging of *C.albicans* (ATCC10231) cells treated with native and citrullinated NaD1 were conducted to investigate the kinetics of membrane permeabilisation (Figure 21). Post 02:00 min addition of native NaD1, membrane permeabilisation was detected by weak PI staining. An increase in detection of PI was observed in all cells post 04:00 min addition of NaD1 with all cells being PI positive by 06:00 min. Treatment with citrullinated NaD1 resulted in no membrane permeabilisation over the duration of the time course experiment as demonstrated by no detection of PI staining of cell and this effect remained constant for a period of 00:60 min (Figure 21). Similarly, no membrane permeabilisation was observed in untreated cells and the no defensin control as indicated by no detection of PI staining.

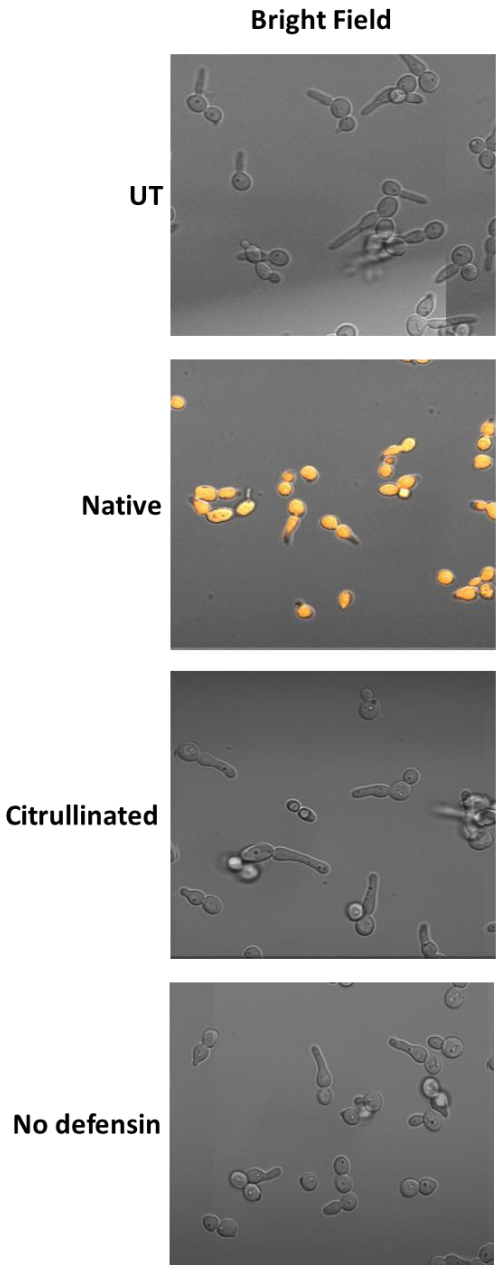

Figure 20. Confocal imaging of *C.albicans* (ATCC10231)

Cells were immobilised onto chamber slides and stained with PI (orange) prior to imaging under Zeiss LSM 800 confocal microscopy in a 37°C/5% C02. Untreated cells, native NaD1 (25 μM), citrullinated NaD1 (25 μM) and no defensins were directly added to cells via capillary while viewing. Images were taken 0-30 min post addition of defensin. Data are representative of three independent experiments.

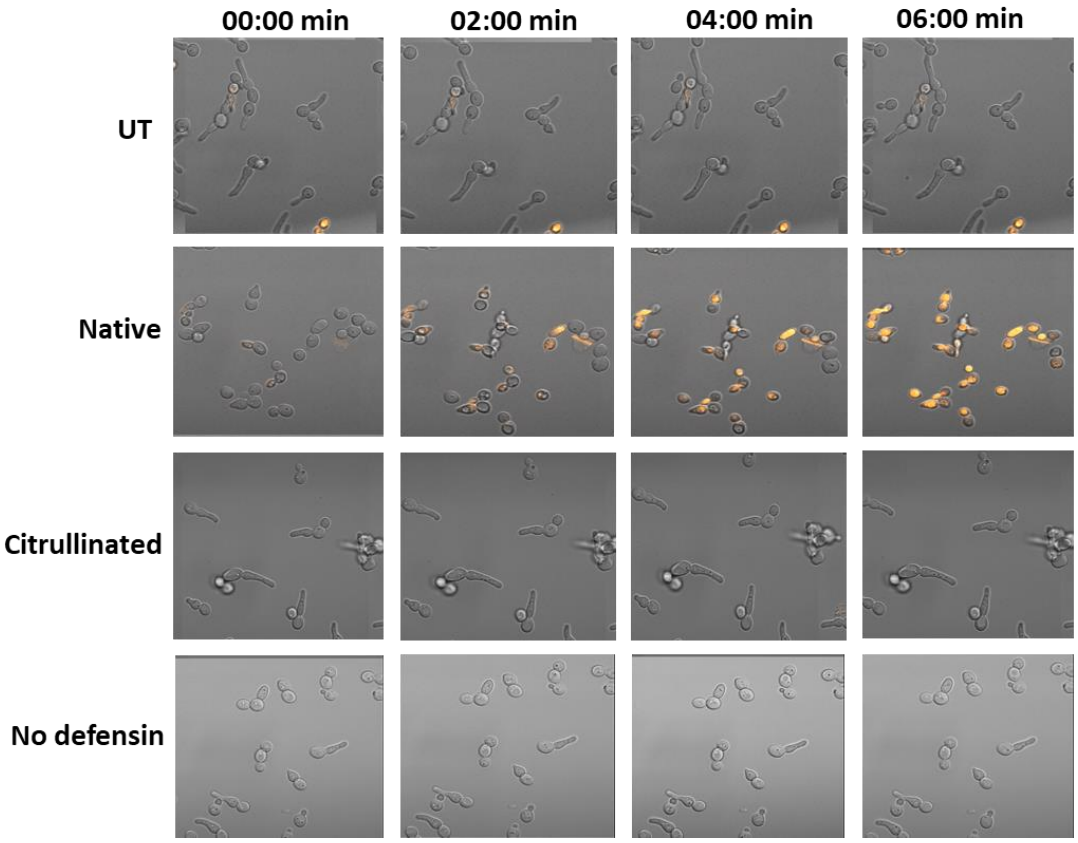

Figure 21. Confocal time course imaging of *C.albicans* (ATCC10231) cells

Cells were immoblised onto chamber slides and stained PI (orange) prior to imaging under Zeiss LSM 800 confocal microscopy in a 37°C/5% C02. Untreated cells, native NaD1 (25 μM), citrullinated NaD1 (25 μM) and no defensins were directly added to cells via capillary while viewing. Images were taken 0-6 min post addition of defensin. Data are representative of three independent experiments.

4.4.3 The effect of citrullinated NaD1 on C. albicans (ATCC90028) growth and membrane permeabilisation

To investigate whether this reduction in anti-fungal activity seen in section *4.4.1* is consistent across different *C. albicans* strains, the effect of citrullinated NaD1 (0–25 µM) on *C. albicans (*ATCC90028) clinical strain following 24 h incubation period was assessed (Figure 22). Native NaD1 (0–25 µM) was used as a positive control. Additionally, a no defensin control was employed used to ensure any effects observed were not due to the reagents present in citrullinated samples.

NaD1 demonstrated a dose-dependent reduction on fungal growth with an IC_{50} of 4.66 µM with growth completely abolished at 25 µM. In contrast, the ability of citrullinated NaD1 to inhibit fungal growth was greatly reduced with an IC_{50} of 166 µM. Additionally, *C. albicans* ATCC90028 clinical strain appears to be more resistant as citrullinated NaD1 demonstrated a reduced activity when compared to the *C. albicans (*ATCC10231) strain (Figure 18). As anticipated, no defensin control exhibited little effect on the fungal growth (Figure 22).

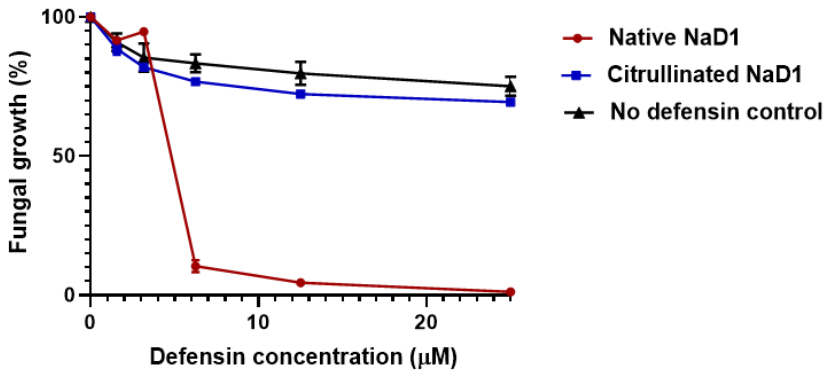

Defensins	IC_{50} (μM)
Native NaD1	4.66
Citrullinated NaD1	166

Figure 22. Effect of citrullinated and native NaD1 on the growth of *C. albicans* (ATCC90028)

Percentage fungal growth of *C. albicans* (ATCC90028) following incubation with native and citrullinated NaD1 (0–25 μM) after 24 h. A no defensin control was included (in black). Data were normalised against an untreated control (assigned 100% growth). IC_{50} values (μM) were calculated and displayed in the adjacent table. Data represents mean ± SEM of 3 independent experiments (n=3) performed in triplicate.

The anti-fungal and PI-permeabilising activity of native and citrullinated NaD1 was further assessed against the ATC90028 clinical strain of *C. albicans*. As above, PI uptake assays were carried out with varying concentrations of citrullinated NaD1 (0–25 μM) on *C. albicans* ATC90028 following 30 min incubation using flow cytometry (Figure 23). Native NaD1 (0–25 μM) and no defensin samples were used as controls.

Native NaD1 demonstrated a dose-dependent effect on PI positivity of *C.albicans* (ATC90028). At concentrations <6 μM, native NaD1 displayed no effect on the membrane permeabilisation, however at higher concentrations PI positivity increased to ~ 70% at 12.5 μM and reached ~ 80% at 25 μM. In contrast, *C.albicans* (ATC90028) was largely unaffected by citrullinated NaD1 even at the highest concentration of 25 μM with almost

negligible PI positivity of cells. Similarly, the no defensin control did not have any effect on the PI positivity of cells.

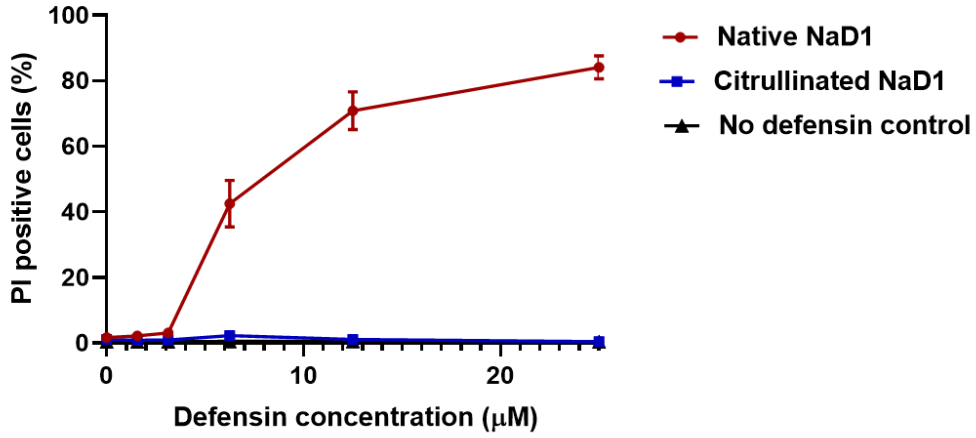

Figure 23. Effect of citrullinated and native NaD1 on the PI uptake of *C. albicans* (ATCC90028)

Percentage PI positive cells of *C. albicans* (ATCC90028) tested with various concentrations of native and citrullinated NaD1 (0–25 µM) following 30 min incubation. No defensin control was included (in black). Data represents mean ± SEM of 3 independent experiments (n=3) performed in triplicate.

4.4.4 Effect of citrullinated NaD1 on mammalian tumour cell viability

In addition to antifungal activity, NaD1 can reduce viability of mammalian tumour cells. To determine if citrullinated NaD1 has any cytotoxic effects on mammalian tumour cells, initially the adherent human tumour cells lines, cervical cancer cells (HeLa) and prostate carcinoma (PC3) cells, were treated with varying concentration of defensins (0–25 µM) and cell viability was assessed after 48 h incubation period using tetrazolium dye-based (MTT) cell viability assays (Figure 24). Native NaD1 (0–25 µM) was used as a control.

As shown in Figure 24, NaD1 reduced HeLa cell viability in a dose-dependent manner with a relatively low IC_{50} value (4.13 µM). In contrast citrullinated NaD1 had no substantial effect on

HeLa cells at lower concentrations (<12.5 µM), as cell viability did not differ from the untreated controls and viability only reduced to ~ 70% at the highest concentration of 25 µM.

Similarly, PC3 viability reduced in a dose-dependent manner when treated with native NaD1 demonstrating a low IC_{50} value (6.06 µM) (Figure 24B). However, citrullinated NaD1 had no significant reduction in the viability of PC3 even at the highest concentration of 25 µM. Interestingly, PC3 cells were apparently more resistant to native and citrullinated NaD1 when compared to HeLa cells illustrated by higher IC_{50} values.

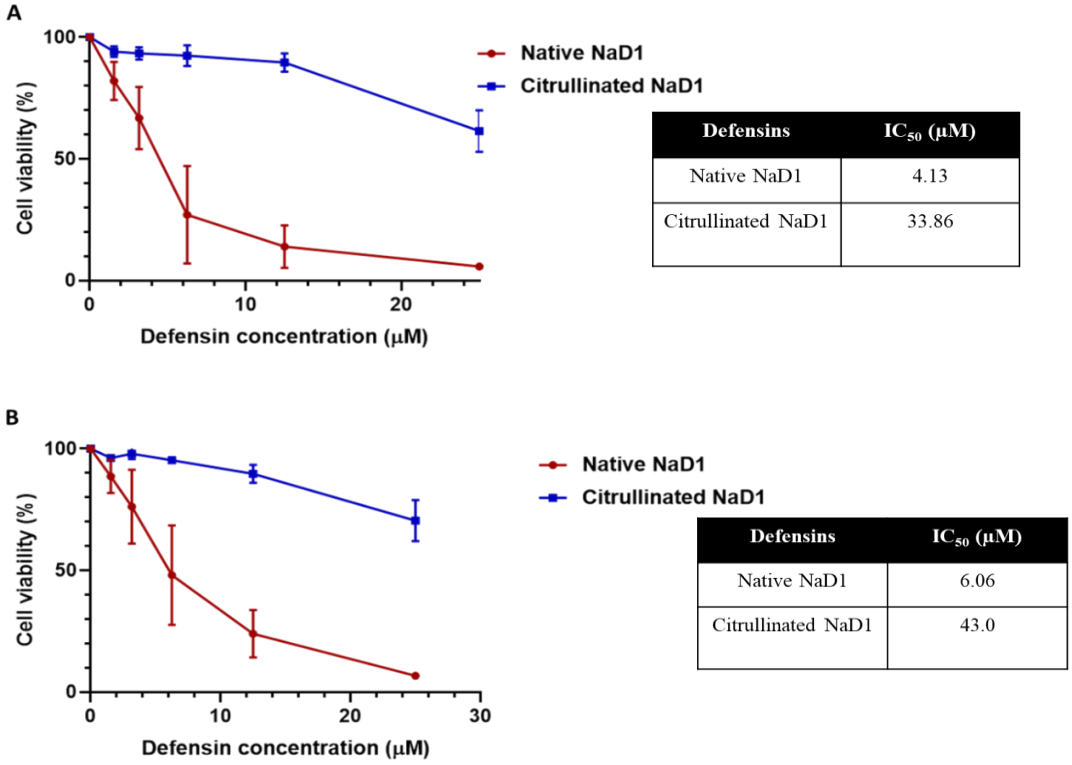

Defensins	IC_{50} (µM)
Native NaD1	4.13
Citrullinated NaD1	33.86

Defensins	IC_{50} (µM)
Native NaD1	6.06
Citrullinated NaD1	43.0

Figure 24. Effect of native and citrullinated NaD1 on HeLa and PC3 cell viability.
(A) HeLa cell and **(B)** PC3 cell viability treated with various concentrations of native and citrullinated NaD1 (0– 25 µM) were assessed using MTT assay. IC_{50} values (µM) were calculated and displayed in the adjacent table. Data represents mean ± SEM of 3 independent experiments (n=3) performed in triplicate. Data were normalised against an untreated control (assigned 100% viability

To further characterise the effect of citrullinated NaD1 on tumour cells, (MTS) cell viability assays were also used to determine whether citrullinated NaD1 (0–25 µM) has any cytotoxic effects against the human suspension tumour cell lines, monocytic lymphoma U937 and monocytic leukemia THP1 cells. Native NaD1 and no defensin control (0–25 µM) were used as controls (Figure 25).

Native NaD1 reduced U937 cell viability in a dose dependent manner with viability abolished at 25 µM. In contrast citrullinated NaD1 had no substantial effect on U937 cell viability even at the highest of 25 µM with viability only reduced to ~ 80% (Figure 25A). The no defensin control exhibited no activity on the cell viability.

Similarly, THP1 cell viability was reduced in a dose-dependent manner when treated with native NaD1 (Figure 25B). However, in contrast to the effects observed with U937 viability, there was no reduction in THP1 cell viability when treated with citrullinated NaD1, with viability increasing to ~ 120% at the highest concentration of 25 µM.

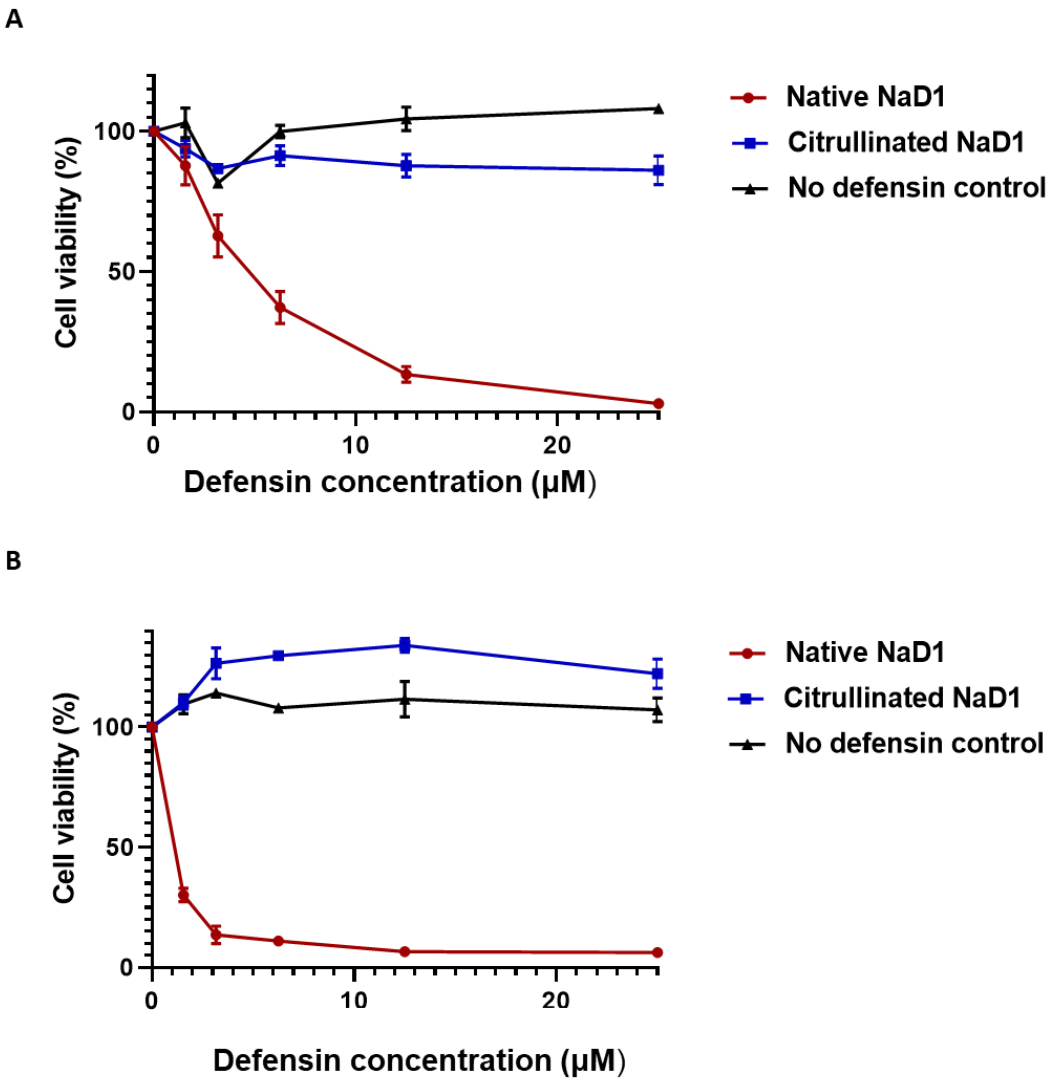

Figure 25. The effect of native and citrullinated NaD1 on U937 and THP1 cell viability **(A)** U937 cell and **(B)** THP1 cell viability treated with various concentrations of native and citrullinated NaD1 (0– 25 μM) were assessed using MTS assay. Data represents mean ± SEM of 3 independent experiments (n=3) performed in triplicate. Data were normalised against an untreated control (assigned 100% viability).

4.4.5 Effect of citrullinated NaD1 on membrane permeabilisation of U937

In addition to fungal cells, defensins are known to also exhibit activity against tumour cells by membrane permeabilisation. To determine the effect of citrullinated NaD1 on membrane permeabilising activity on tumour cells, PI uptake with various concentrations of citrullinated NaD1(0–25 µM) on U937 monocytic lymphoma cells following 30 min incubation was assessed using flow cytometry (Figure 26). Native NaD1 (0–25 µM) and no defensin samples were used as controls.

Native NaD1 displayed a dose-dependent permeabilisation of U937 tumour cells, with ~ 40% PI positivity observed at 25 µM. However, U937 were unaffected by citrullinated NaD1, with almost negligible PI positivity of cells at the highest concentration of 25 µM. Likewise, the no defensin control had no effect on the PI positivity of cells (Figure 26).

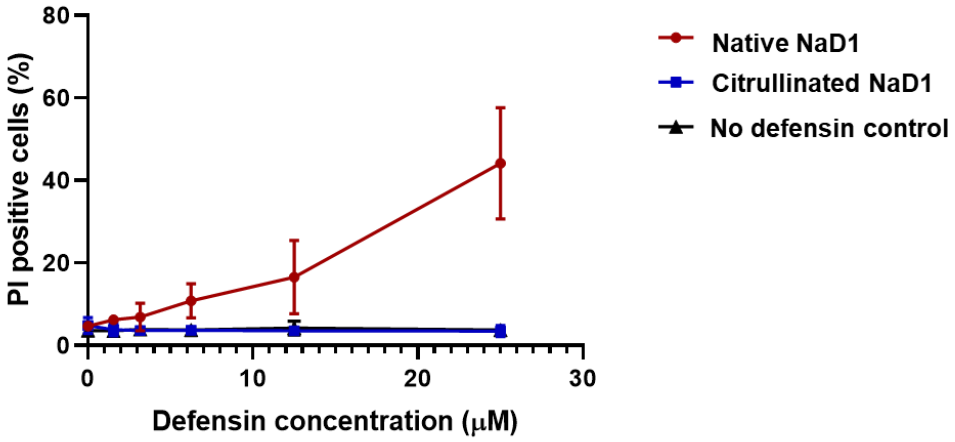

Figure 26. Effect of citrullinated and native NaD1 on the PI uptake of U937 tumour cells. Percentage of PI positive cells tested with various concentrations of native and citrullinated NaD1 following 30 min incubation. No defensin control was included (in black). Data represents mean ± SEM of 3 independent experiments (n=3) performed in triplicate.

Endpoint and time-course imaging using CLSM was performed to further understand and examine the morphological changes U937 cells undergo upon treatment with citrullinated NaD1. Immobilised U937 cells were treated with either citrullinated NaD1 (10 µM), native NaD1 (10 µM) or a no defensin control in the presence of green fluorescent membrane stain PKH67 and orange nucleic acid stain PI.

As shown in Figure 27, treatment of U937 cells with NaD1 over 1 hr induced cell permeabilisation indicated by the orange PI staining and formation of one or more membrane blebs. No PI staining or membrane blebbing occurred in the untreated samples. In contrast citrullinated NaD1 had no effect on membrane permeabilisation as demonstrated by no PI staining of cells. As expected, the no defensin control resulted in no membrane permeabilisation.

A time-course imaging of U937 cells treated with native and citrullinated NaD1 were conducted to investigate the kinetics of membrane permeabilisation (Figure 28). Post 02:00 min of addition of native NaD1, membrane permeabilisation and blebbing was detected by weak PI staining. An increase in detection of PI was observed in all cells post 04:00 min addition of NaD1. No membrane permeabilisation or blebbing was observed in cells treated with citrullinated NaD1 over the duration of the time course experiment as demonstrated by no detection of PI staining of cells. This lack of staining remained constant for a period of 00:60 min (Figure 28). Similarly, no membrane permeabilisation was observed in untreated cells and the no defensin control as indicated by no detection of PI staining.

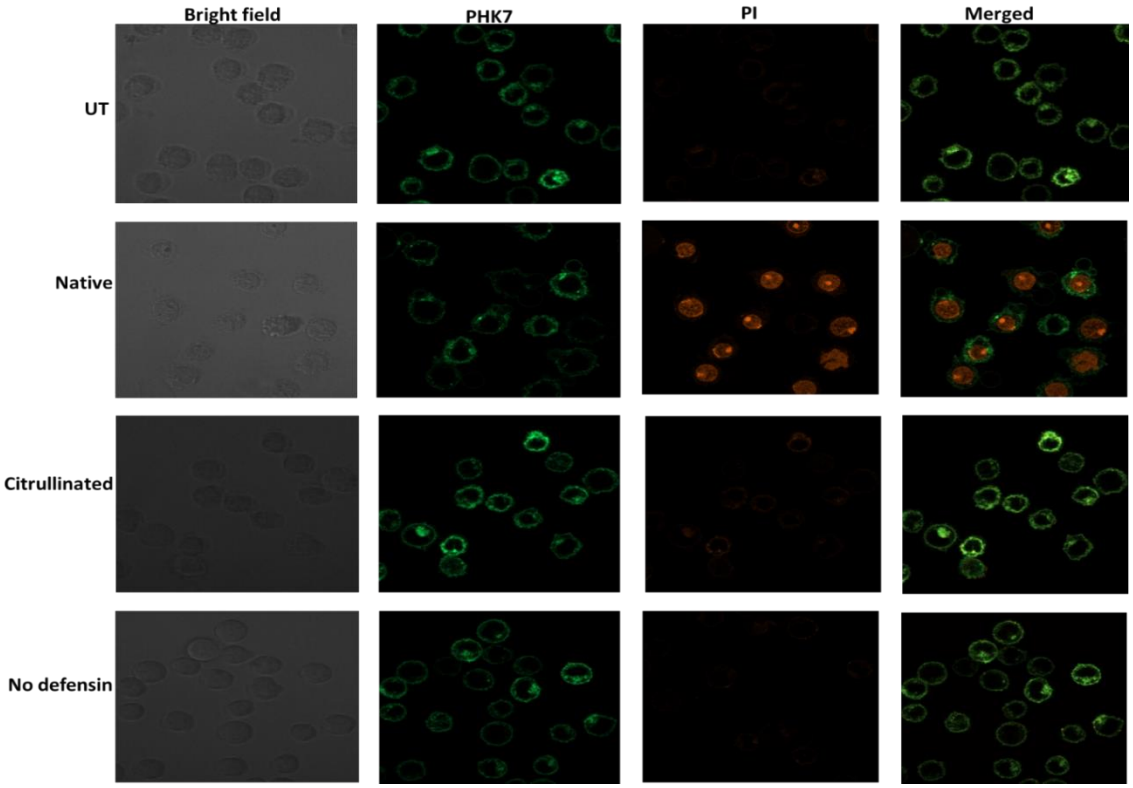

Figure 27. CLSM endpoint imaging of U937 cells

Cells were immobilised onto chambered slides and stained with PKH67 (green) and PI (orange) prior to imaging under Zeiss LSM 800 confocal microscopy in a 37°C/5% $C0_2$. Untreated cells, native NaD1 (10 μM), citrullinated NaD1 (10 μM) and no defensin were directly added to cells via capillary while viewing. Images were taken 0-60 min post addition of defensin. Data are representative of two independent experiments.

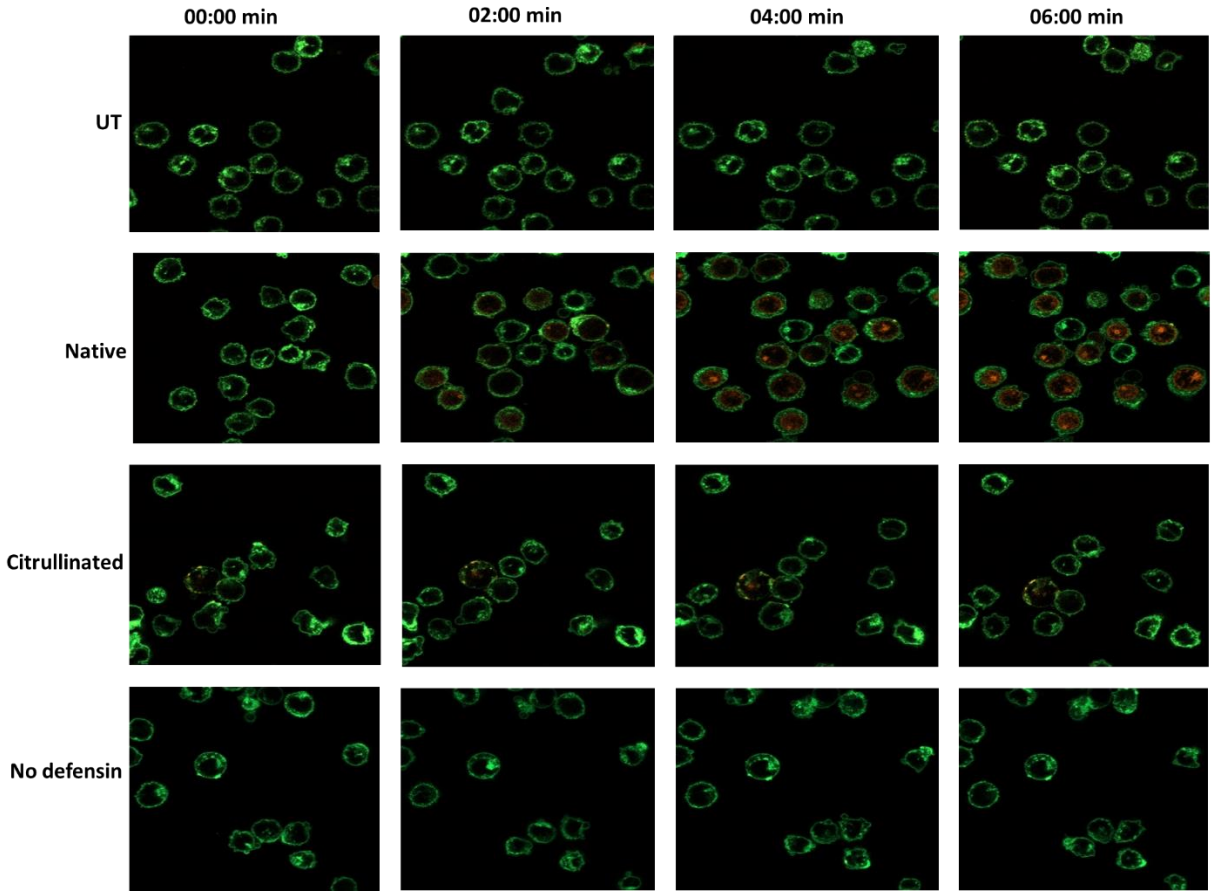

Figure 28. CLSM time course imaging of U937 cells

Cells were immobilised onto chambered slides and stained with PKH67 (green) and PI (orange) prior to imaging under Zeiss LSM 800 confocal microscopy in a 37°C/5% $C0_2$. Untreated cells, native NaD1 (10 μM), citrullinated NaD1 (10 μM) and no defensins were directly added to cells via capillary while viewing. Images were taken 0-6 min post addition of defensin. Data are representative of two independent experiments.

4.5 Recombinant expression and citrullination of NaD1 R40E and NaD1 R39A mutants

To determine whether the observed difference in the activity of native and citrullinated NaD1 was due to citrullination of specific arginine residues, NaD1 mutants R40E and R39A were expressed using the pPIC9 expression system in *P. pastoris*. The defensins were purified using cation exchange column chromatography and concentrated. Yields of 1.2 mg/L and 1.4mg/L were obtained for NaD1 R40E and NaD1 R39A, respectively.

The purity and quality of the expressed defensins were evaluated using SDS-PAGE and immunoblot analysis. Bands at 5.3 kDa were observed for both NaD1 R40E and NaD1 R39A mutants consistent with expected molecular size of NaD1 (Figure 29A). Immunoblot analysis with anti-NaD1, revealed molecular weights similar to that observed with SDS-PAGE (Figure 29B). Despite the successful production and purification of the NaD1 R40E and R39A mutant proteins, the COVID-19 pandemic resulted in a 'lock-out' of the laboratories at LIMS (March-May 2020), and further citrullination experiments involving NaD1 mutant proteins were unable to be performed.

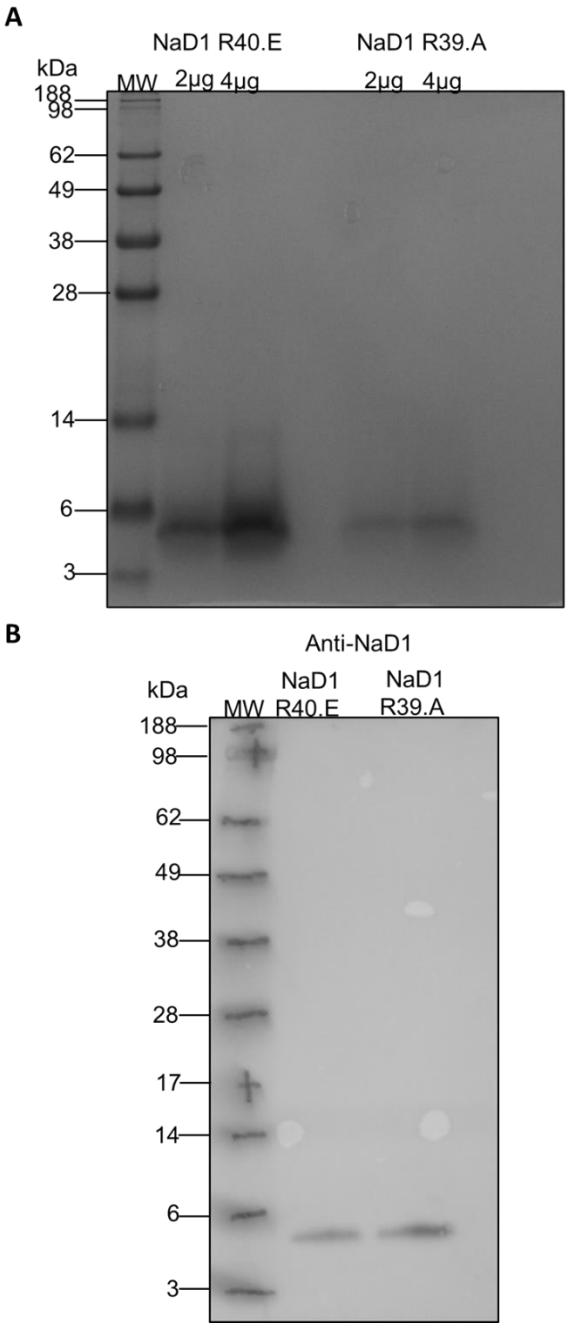

Figure 29. Characterisation of purified NaD1 R40E and NaD1 R39A

(A) SDS-PAGE analysis (2 µg and 4 µg protein/lane) following Coomassie stain of purified NaD1 R40E and NaD1 R39A (**B**) Immunoblot (4 µg protein) of rabbit-anti-NaD1 and HRP conjugated donkey-anti-rabbit antibodies.

Chapter 5
Citrullination and functional analysis of HBD-3

5.1 Introduction

Similar to plant defensins, human defensins such HBD-2 and HBD-3 exhibit membranolytic activity by targeting membrane phospholipids, particularly PIP_2 (Phan et al., 2016; Järvå et al., 2018b). These interactions between the defensins and PIP_2 molecules have been shown to be crucial for the antifungal and anticancer activity of HBD-2 and HBD-3 (Phan et al., 2016; Järvå et al., 2018b). Furthermore, the HBD-2:PIP_2 interaction is mediated by a key arginine residue, R22, while HBD-3:PIP_2 interactions are mediated by a lysine residue (K39) (Table 2). As the plant defensin NaD1 was shown to be citrullinated which affected the antifungal and anticancer activity of the defensin, it was also of interest to determine if human defensins can be citrullinated and if so, whether their functions are impaired. It should be noted that although HBD-3 interacts with PIP_2 primarily through K39 to mediate its membranolytic acitivity, it is a highly positively charged protein containing 5 arginine residues (Figure 8A). Therefore, it was of interest to determine if citrullination would affect the overall charge of HBD-3 leading to a difference in its activity.

5.2 Citrullination of HBD-2 and HBD-3

To determine whether human defensins can be citrullinated, HBD-2 and HBD-3 were treated *in vitro* with the PAD2 (peptidylarginine deaminase 2) enzyme. Citrullination was detected using immunoblot analysis with an anti-citrulline antibody which is able to specifically detect citrulline residues. A band consistent with the molecular weights of HBD-3 at ~ 6 kDa were observed for citrullinated HBD-3 (Figure 30). No detectable band at the expected size of HBD-2, 4.1 kDa, was seen for citrullinated HBD-2 (Figure 30). A band of ~ 5.5-6 kDa was observed for citrullinated LL-37 consistent with the expected molecular weight of LL-37 (Figure 30). No bands were observed for non-citrullinated lanes for HBD-2 and HBD-3 and LL-37.

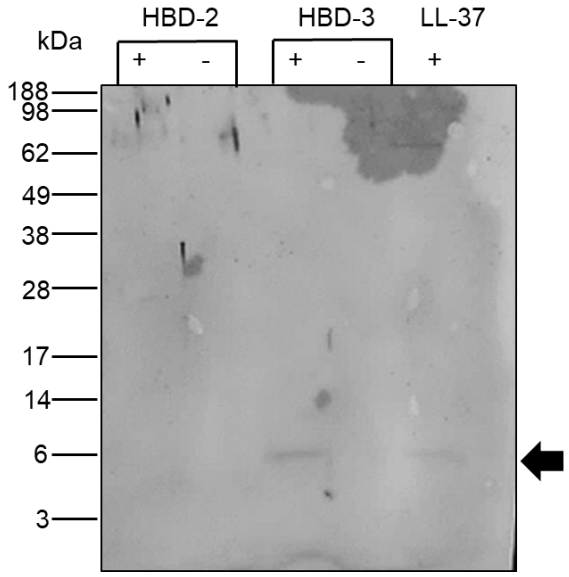

Figure 30. Characterisation of citrullinated HBD-2, HBD-3 and LL-37

Immunoblot of Citrullinated HBD-2 and HBD-3 (10 µg protein) and LL-37 (5 µg protein) probed with anti-citrulline antibody (1:1000 dilution) and detected using HRP conjugated donkey-anti-rabbit antibody. (+ = Citrullinated, - = non-citrullinated). Arrow indicate citrullinated protein bands.

As an increase in 1 Da is observed for every arginine residue that is citrullinated and converted to citrulline, ESI-Q-ToF mass spectrometry was conducted to determine exact mass of citrullinated HBD-2 and HBD-3 in order to confirm if PAD2 was successfully able to citrullinate the human defensins (Figure 31).

No difference in mass was observed for the citrullinated HBD-2 (4325.1) when compared with the native HBD-2 (4325.1) (Figure 31A), consistent with results obtain from immunoblot analysis. Intriguingly, multiple peaks were present for HBD-3 mass spectrometry and with a decrease in 300 Da detected for citrullinated HBD-3 (5031.2) in comparison to native HBD-3 (5341.2) (Figure 31B). These data were inconsistent with immunoblot analysis for citrullinated HBD-3. As HBD-2 does not appear to be citrullinated and HBD-3 appears to be citrullinated on the immunoblot analysis, all subsequent experiments in this chapter were only carried out on HBD-3.

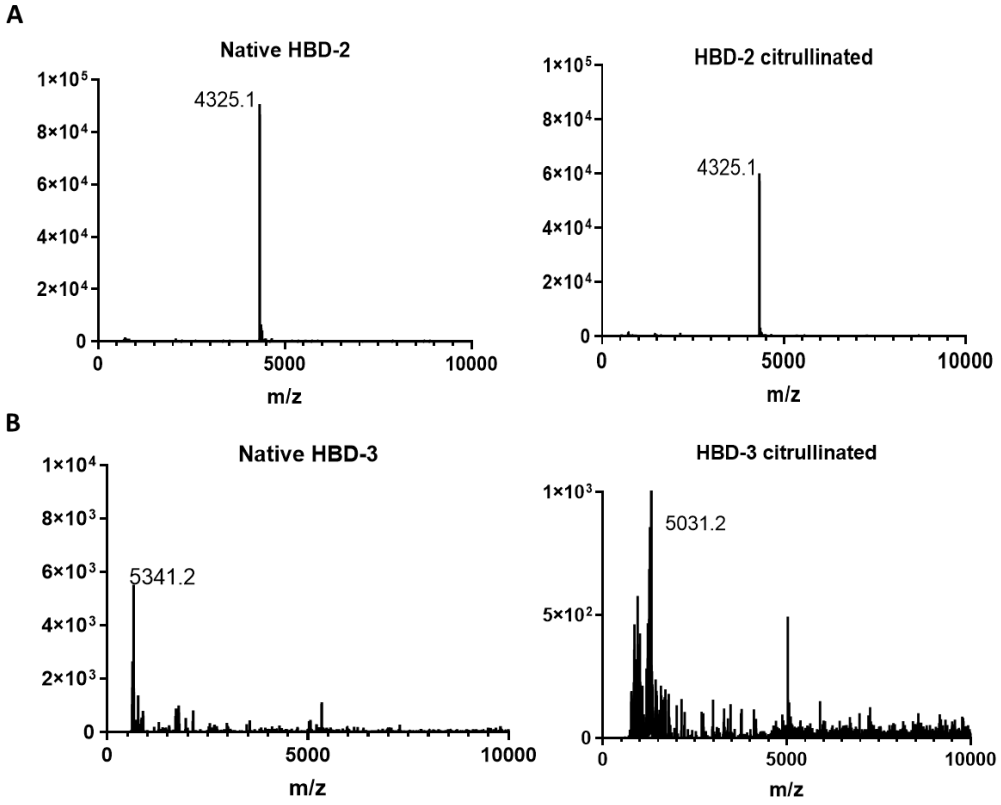

Figure 31. ESI-Q-Tof mass spectrometry analysis of untreated and citrullinated HBD-2 and HBD-3

(A) No increase in mass present between the untreated HBD-2 (4325.1) and citrullinated HBD-2 (4325.1). **(B**) Mass spectrum revealed multiple peaks and a decrease in 300 Da was present for citrullinated HBD-3 (5031.2) in comparison to native HBD-3 (5341.2).

5.3 Functional analysis of citrullinated HBD-3

5.3.1 Effect of citrullinated HBD-3 on fungal growth inhibition

Similar to plant defensins, human defensins including HBD-3 display anti-fungal activity against *C. albicans*. Therefore, to investigate whether citrullinated HBD-3 results in a decrease in activity against *C. albicans*, the effect of citrullinated HBD-3 (0–25 µM) was assessed on *C. albicans* (ATCC10231) following 24 h incubation (Figure 32). Native HBD-3 (0–25 µM) was used as a positive control. Additionally, a no defensin control was employed used to ensure any effects observed were not due to background reagents present in citrullinated samples.

Native HBD-3 displayed a dose-dependent reduction in *C. ablicans* growth with an IC_{50} value of 11.4 µM and growth abolished at 25 µM. Intriguingly, the ability of citrullinated HBD-3 to inhibit fungal growth was reduced ~ 7-fold with an IC_{50} ~ 73 µM. As expected, the no defensin control exhibited a little effect on the fungal growth (Figure 32).

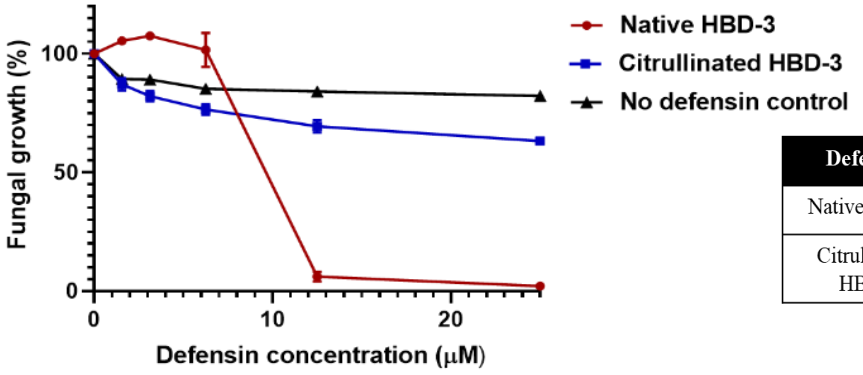

Defensins	IC_{50} (µM)
Native HBD-3	11.4
Citrullinated HBD-3	72.5

Figure 32. Effect of citrullinated and native HBD-3 on the growth of *C. albicans* (ATCC100231)

Percentage fungal growth of *C. albicans* (ATCC10231) following incubation with native and citrullinated HBD-3 (0–25 µM) after 24 h. A no defensin control was included (in black). Data were normalised against an untreated control (assigned 100% growth). IC_{50} values (µM) were calculated and displayed in the adjacent table. Data represents mean ± SEM of 3 independent experiments (n=3) performed in triplicate.

To further determine if the HBD-3 anti-fungal effect would be observed across different *C.albicans* strains, the effect of citrullinated HBD-3 (0–25 µM) was assessed on the *C. albicans* ATCC90028 clinical strain following 24 h incubation (Figure 33). Native HBD-3 and a no defensin control (0–25 µM) were used as controls.

Native HBD-3 displayed a reduction on the fungal growth in a dose-dependent manner with an IC_{50} value of 8.6 µM and growth abolished at 25 µM. ~ 14-fold reduction in fungal growth was seen in citrullinated HBD-3 and *C. albicans* ATCC90028 clinical strain appears to be more resistant as citrullinated HBD-3 demonstrated a reduced activity when compared to the *C. albicans (*ATCC10231) strain (Figure 32). As expected, the no defensin control exhibited little effect on fungal growth (Figure 33).

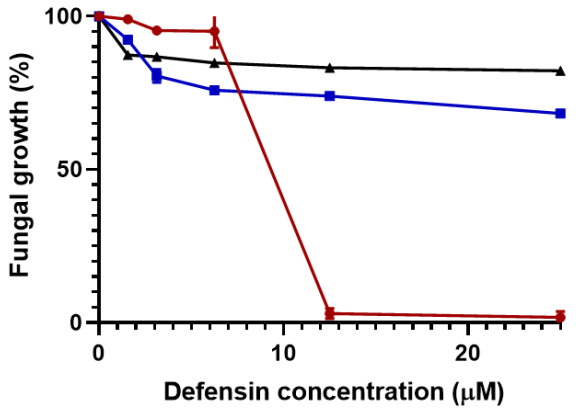

Defensins	IC_{50} (μM)
Native HBD-3	8.6
Citrullinated HBD-3	123

Figure 33. Effect of citrullinated and native HBD-3 on the growth of *C. albicans* (ATCC90028)

Percentage fungal growth of *C. albicans* (ATCC90028) following incubation with native and citrullinated HBD-3 (0–25 μM) after 24 h. A no defensin control was included (in black). Data were normalised against an untreated control (assigned 100% growth). IC_{50} values (μM) were calculated and displayed in the adjacent table. Data represents mean ± SEM of 3 independent experiments (n=3) performed in triplicate.

5.3.2 Effect of citrullinated HBD-3 on membrane permeabilisation

To determine whether citrullinated HBD-3 maintains membrane permeabilising activity, PI uptake with varying concentrations of citrullinated HBD-3 (0–50 μM) on *C. albicans* ATC90028 clinical strain following 30 min incubation was assessed using flow cytometry (Figure 34). Native HBD-3 (0–50 μM) and no defensin samples were used as controls.

Native HBD-3 demonstrated a dose-dependent effect on PI positivity of *C.albicans.* At concentrations <6 μM, native HBD-3 displayed no effect on the on membrane permeabilization, however PI positivity increased to ~ 90% at 50 μM. In contrast, *C.albicans* were largely unaffected by citrullinated HBD-3 even at the highest concentration of 25 μM

with almost negligible PI positivity of cells. Similarly, the no defensin control did not have any effect on the PI positivity of cells (Figure 34).

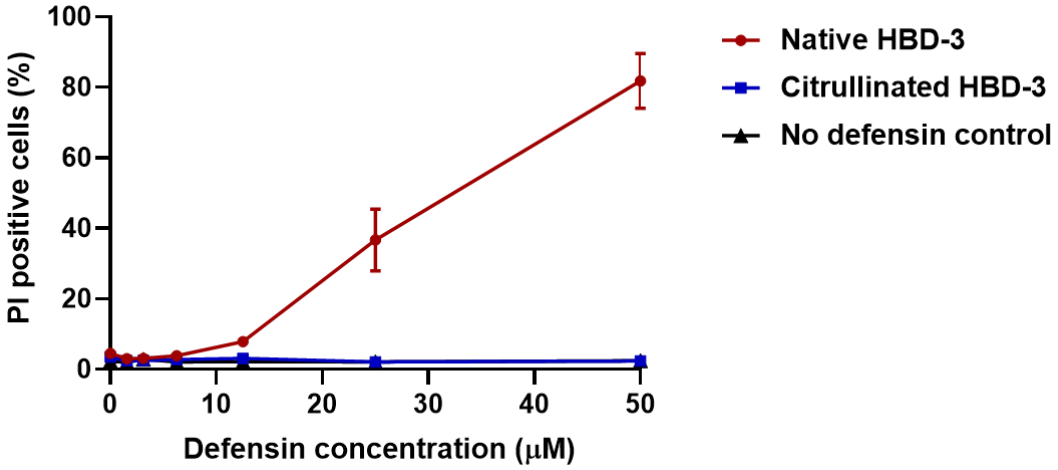

Figure 34. Effect of Citrullinated and native HBD-3 on the PI uptake of *C. albicans* (ATCC10231)

Percentage PI positive cells of *C. albicans* (ATCC10231) tested with various concentrations of native and citrullinated HBD-3 (0–50 μM) following 30 min incubation. No defensin control was included (in black). Data represents mean ± SEM of 3 independent experiments (n=3) performed in triplicate.

To determine whether the HBD-3 anti-fungal activity is consistent across different *C. albicans* strains and whether citrullinated HBD-3 maintains membrane permeabilising activity, PI uptake assays were also carried out on *C.albicans* clinical strain ATCC90028, using varying concentrations of citrullinated HBD-3 (0–50 μM). Following 30 min incubation, PI positivity was assessed using flow cytometry (Figure 35). Native HBD-3 (0–50 μM) and no defensin samples were used as controls.

At concentrations <6 μM, native HBD-3 displayed no effect on the on membrane permeabilisation, however PI positivity increased to ~ 75% at 50 μM. In contrast, *C. albicans*

ATCC90028 was largely unaffected by citrullinated HBD-3 even at the highest concentration of 25 µM with almost negligible PI positivity of cells. Similarly, the no defensin control did not have any effect on the PI positivity of cells (Figure 35).

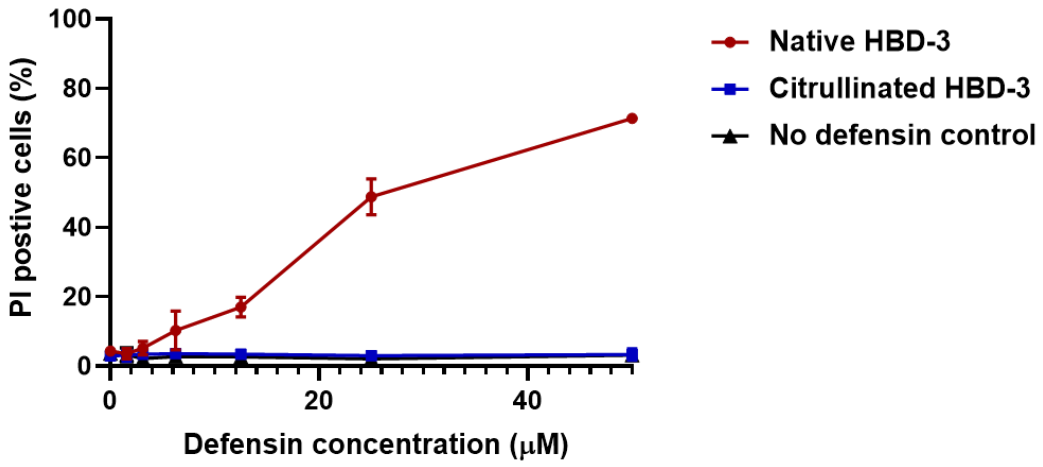

Figure 35. Effect of Citrullinated and native HBD-3 on the PI uptake of *C. albicans* (ATCC90028)

Percentage PI positive cells of *C. albicans* (ATCC90028) tested with various concentrations of native and citrullinated HBD-3 (0–50 µM) following 30 min incubation. No defensin control was included (in black). Data represents mean ± SEM of 3 independent experiments (n=3) performed in triplicate.

5.3.3 Effect of citrullinated HBD-3 on U937 tumour cell permeabilisation

In addition to membrane permeabilisation activity against fungal cells, HBD-3 is known to exhibit activity against tumour cells by membrane permeabilisation. To determine the effect of citrullinated HBD-3 on membrane permeabilising activity on tumour cells, PI uptake with concentrations of citrullinated HBD-3 (0–50 µM) on U937 cells following 30 min incubation was assessed using flow cytometry (Figure 36). Native HBD-3 (0–50 µM) and no defensin samples were used as controls.

Treatment with native HBD-3 displayed a dose-dependent permeabilisation of U937 tumour cells, with ~ 80% PI positivity observed at 50 µM. In contrast, almost negligible PI positivity was observed in U937 cells treated with citrullinated HBD-3 at the highest concentration of 50 µM. Likewise, the no defensin control had no effect on the PI positivity of cells (Figure 36).

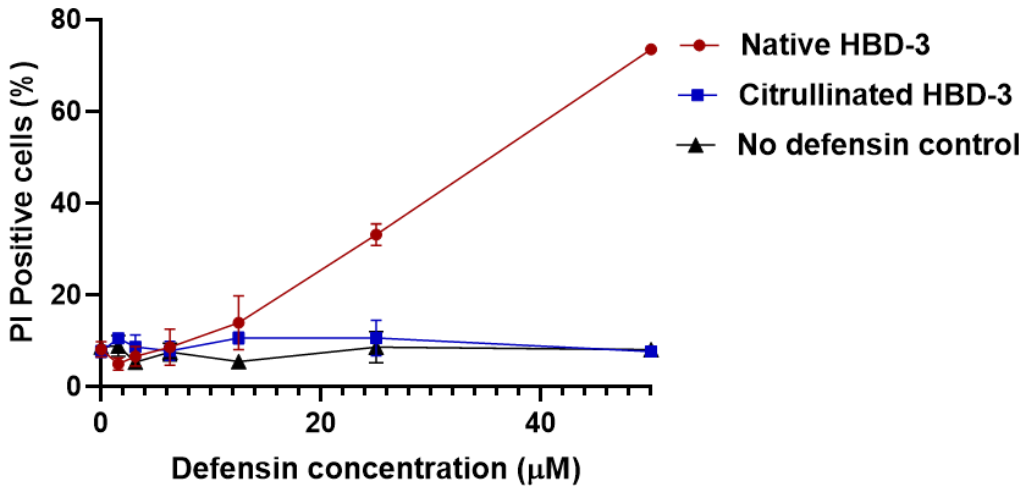

Figure 36. Effect of native and citrullinated HBD-3 on the PI uptake of U937 tumour cells
Percentage of PI positive cells tested with various concentrations of native and citrullinated HBD-3 (0–50 µM) following 30 min incubation. No defensin control was included (in black). Data represents mean ± SEM of 3 independent experiments (n=3) performed in triplicate.

To further examine the kinetics and morphological changes a cells undergoes upon treatment with citrullinated HBD-3, endpoint and time-course imaging using CLSM. Immobilised U937 cells were treated with either citrullinated HBD-3 (50μM), native HBD-3 (50 μM) or a no defensin control in the presence of the nucleic acid stain PI.

Treatment of U937 cells with HBD-3 over 30 min induced cell permeabilisation indicated by the orange PI staining and formation membrane blebs (Figure 37). No PI staining or membrane blebbing occurred in the untreated samples. In contrast citrullinated HBD-3 had no effect on membrane permeabilisation as demonstrated by no PI staining of cells and presence of membrane blebs. As expected, the no defensin control resulted in no membrane permeabilisation.

A time-course imaging of U937 cells treated with native and citrullinated HBD-3 were conducted to investigate the kinetics of membrane permeabilisation (Figure 38). Post 10:00 min of addition of native HBD-3, there was no detection of membrane permeabilisation. However, post 15:min, membrane permeabilisation and blebbing was detected by staining of PI. An increase in PI staining was observed in cells post 30:00 min addition of HBD-3. No membrane permeabilisation or blebbing was observed in cells treated with citrullinated HBD-3 over the duration of the time course experiment as demonstrated by no detection of PI staining of cells. This lack of effect remained constant for a period of 00:30 min (Figure 38). Similarly, no membrane permeabilisation was observed in untreated cells and the no defensin control as indicated by no detection of PI staining.

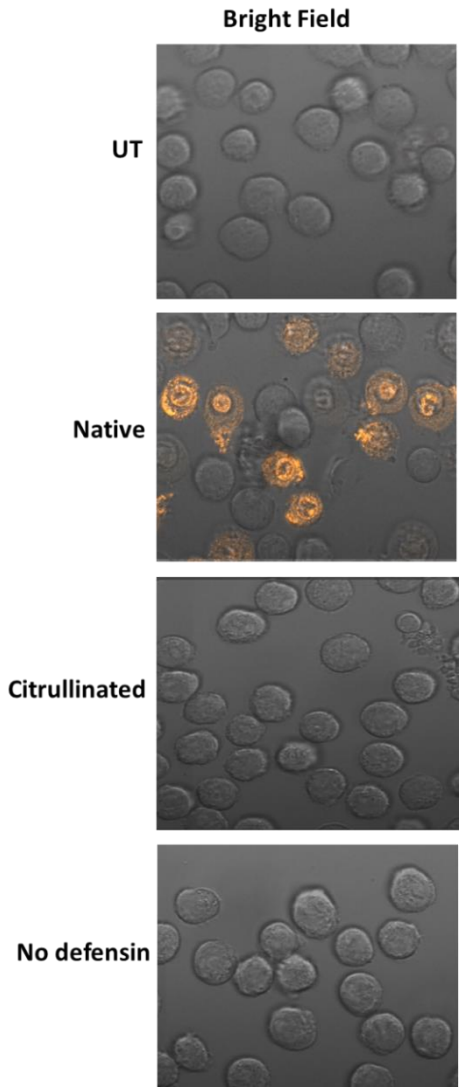

Figure 37. Confocal imaging of U937

Cells were immoblised onto chambered slides and stained with PI (orange) prior to imaging under Zeiss LSM 800 confocal microscopy in a 37°C/5% C02. Untreated cells, native HBD-3 (50 μM), citrullinated HBD-3 (50 μM) and no defensins were directly added to cells via capillary while viewing. Images were taken 0-30 min post addition of defensin. Data are representative fields of view from one independent experiment.

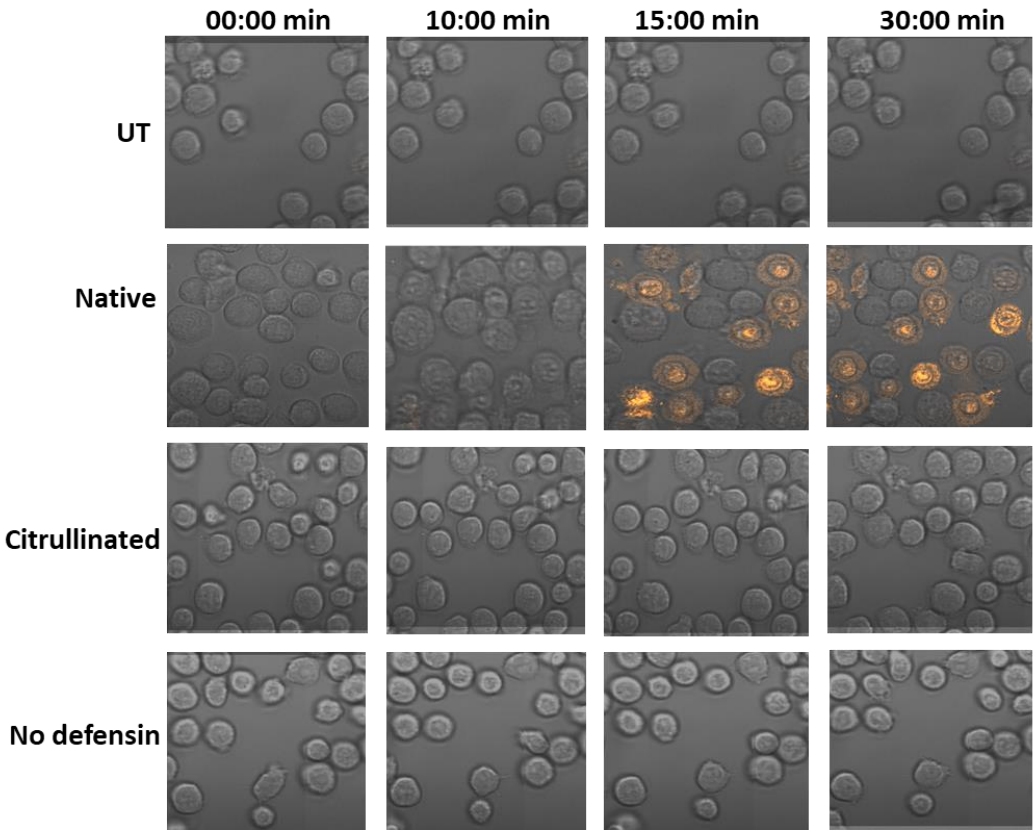

Figure 38. Confocal time course imaging of U937 cells

Cells were immoblised onto chambered slides and stained PI (orange) prior to imaging under Zeiss LSM 800 confocal microscopy in a 37°C/5% C02. Untreated cells, native HBD-3 (50 μM), citrullinated HBD-3 (50 μM) and no defensins were directly added to cells via capillary while viewing. Images were taken 0-6 min post addition of defensin. Data are representative fields of view from one independent experiment.

5.3.4 Effect of citrullinated HBD-3 on cell viability

In addition to anti-fungal activity, human defensins such as HBD-3 can reduce viability of mammalian tumour cells. To determine if citrullinated HBD-3 displays any cytotoxic effects, cervical cancer cells (HeLa) and prostate cancer (PC3) cells were treated with varying concentration of defensins (0–50 μM) and assessed after 48 h incubation period using tetrazolium dye-based (MTT) cell viability assays (Figure 39). Native HBD-3 and no defensin controls (0–50 μM) were used as controls.

As shown in Figure 39A, native HBD-3 reduced HeLa cell viability in a dose-dependent manner with viability nearly abolished at 50 μM. In contrast, citrullinated HBD-3 only reduced HeLa cell viability to ~ 65% at the highest concentration of 50 μM. Native HBD-3 reduced PC3 cell viability to ~ 60% at 50 μM with citrullinated HBD-3 having no effect on the viability at the highest concentration (Figure 39B). The no defensin control little effect on the viability of HeLa and PC3 cells.

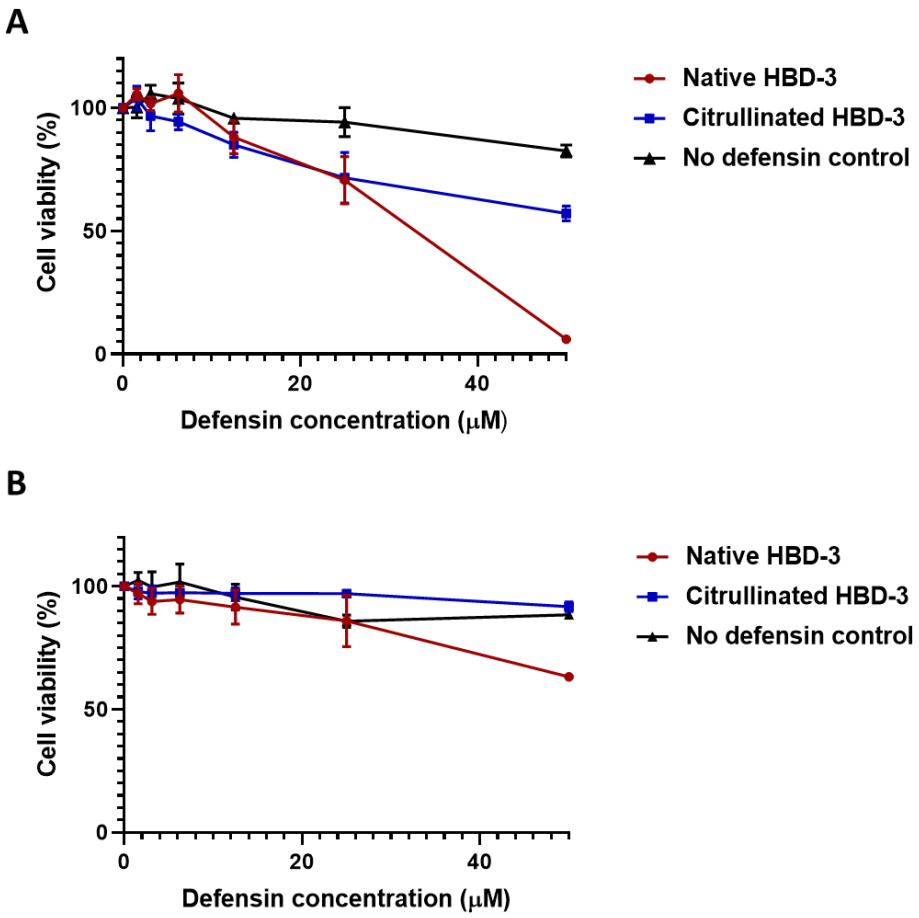

Figure 39. Effect of native and citrullinated HBD-3 on HeLa and PC3 cell viability **(A)** Hela cell and (**B)** PC3 cell viability treated with various concentrations of native and citrullinated HBD-3 (0–50 μM) were assessed using MTT assay. No defensin control was included (in black). Data were normalised against an untreated control (assigned 100% viability). Data represents mean ± SEM of 3 independent experiments (n=3) performed in triplicate.

Chapter 6
Discussion

6.1 Introduction

The innate immune system of eukaryotes is a vital evolutionary component of host defence system and serves as the first line of protection against pathogens. Defensins are a major class of cationic antimicrobial peptides that are produced by plant and animal species and form an integral component of the innate immune system. Defensins are widely known for their antimicrobial and antifungal activities and more recently for their ability to target and lyse mammalian tumour cells (Poon et al., 2014; Baxter et al., 2015; Phan et al., 2016).

Until recently, the mechanism of membranolytic action of defensins was poorly understood. However, studies conducted by the Hulett laboratory (La Trobe University) focusing on plant and human defensins have identified the importance of defensins binding to negatively charged phosphoinositides, particularly PIP_2, in membrane permeabilisation (Poon et al., 2014; Baxter et al., 2015; Phan et al., 2016; Järvå et al., 2018b). The interaction of defensins with PIP_2 was found to be dependent on positively charged residues, particularly arginine, binding to the negatively charged lipid headgroup which ultimately leads to membrane permeabilisation (Poon et al., 2014; Järvå et al., 2018b). Pathogens are equipped with mechanisms to counteract host defences and one such example is the process of citrullination. Citrullination, a post-translational modification, converts positively charged arginine residues into the neutral residue citrulline, a process that can alter protein-protein interactions and even protein function (Koziel et al., 2014; Witalison et al., 2015). Citrullination has been linked with the regulation of innate immunity (Cirioni et al., 2006; Koziel et al., 2014). However, the role of citrullination in regulating plant and mammalian defensins has yet to be investigated. Furthermore, with the increasing interest in defensins as novel therapeutic agents (such as the clinical trials currently underway for NaD1-deriviatives by Hexima Ltd for the topical treatment of onychomycosis

https://hexima.com.au/project_tag/onychomycosis/), it is important that any processes able to inactivate defensins *in vivo* be identified and characterised. Therefore, this project aimed to provide novel insight into citrullination of plant and mammalian defensins and its effect on lipid binding as well as function of defensins.

6.2 Interactions of NaD1, HBD-2 and HBD-3 PI(4,5)P_2

Membranolytic action of defensins is known to be mediated by interaction with membrane phospholipids via key cationic arginine residues. Citrullination converts arginine into neutral citrulline that can change protein function (Gyorgy et al., 2006; Witalison et al., 2015). The reactions catalyzed by PAD enzymes are dependent on the number of arginine residues present and surface exposure of these residues. The citrullination of model defensins NaD1, HBD-2 and HBD-3 were investigated as they contain 4, 2 and 5 exposed arginine residues, respectively (Figure 8). More importantly NaD1 and HBD-2 were chosen as they are known to interact with PIP_2 via Arg40 and Arg22 respectively (Table 2). In this thesis, HBD-3 was initially selected as a negative control as it interacts with PIP_2 via a lysine (Lys39) residue.

6.3 Recombinant defensin expression and characterisation

Pichia pastoris, a eukaryotic methylotrophic yeast was selected as the expression system for this study. Being an eukaryotic expression system, it promotes the correct protein folding and disulphide bond formation of mammalian proteins, which are crucial for defensin function (van der Weerden et al., 2008; Poon et al., 2014; Zhang, 2017). The pPIC9 vector was used for expression of the above mentioned defensins as it allows in frame expression of defensins with α-factor secretion signal, that when cleaved by the Kex2 endoprotease, enables recombinant protein to be secreted into the extracellular medium (Yang et al., 2013). This allowed protein to be purified using cationic exchange column chromatography.

Prior to purification, the pH of defensin preparations were adjusted to 6.0 which was below the isoelectric point of NaD1, HBD-2 and HBD-3 (8.58, 10.5 and 9.16 respectively). This ensured the defensins to be positively charged for purification by cation column chromatography. SDS-PAGE and immunoblot analysis for NaD1, HBD-2 and HBD-3 revealed bands at the expected molecular sizes (5.3 kDa, 4.3 kDa and 5.1 kDa, respectively) confirming the purity and identity of proteins (Figure 9). However, two bands for HBD-2 were observed at approximately 4-4.5 kDa which suggests in addition to the full-length protein, a truncated version may have been purified. To determine if a truncated version of HBD-2 was present in the samples, separation via chromatography or identification by mass spectrometry may be used to further characterise the exact nature of the protein.

CD spectroscopy was used to determine percentage of secondary structures present in the purified defensins. CD spectroscopy measures the absorption of left-handed and right-handed polarised light at a range of wavelengths and estimates the percentage of secondary structures present in the protein by comparing data to known spectra of the previously defined proteins (Sreerama & Woody, 2000). The results confirmed NaD1, HBD-2 and HBD-3 to be correctly folded, as expected based on the known structures of these defensins. Analysis of CD spectrum revealed the characteristic α-helical double minima (222 nm and 208 nm) for NaD1 and β-strand maxima at 195 nm and minima at 208 nm for HBD-2. The CD spectrum for HBD-3 revealed characteristic random coil structure with only 25% β-strand, which was consistent with previous studies of HBD-3 (Boniotto et al., 2003).

6.4 Functional analysis of NaD1, HBD-2 and HBD-3

To confirm the functional activity of recombinantly expressed defensins, growth inhibition, membrane permeability (PI uptake) and cell viability (MTT assays) were performed on a model fungal pathogen (*C. albicans)* and human tumour cell line, HeLa. NaD1 was potent at killing fungal and tumour cells with IC_{50} values of ~ 6 and 3 µM, respectively (Figure 11). Although less potent than NaD1, HBD-3 was also effective in reducing fungal and HeLa cells with IC_{50} values of ~ 7 and 18 µM, respectively. In contrast, HBD-2 was found to be effective in killing *C. albicans* (IC_{50} ~ 9.5 µM), however, failed to reduce viability of HeLa cells (Figure 11). These results are consistent with previously published evidence of NaD1, HBD-2 and HBD-3 activity (Poon et al., 2014; Baxter et al., 2015; Phan et al., 2016; Järvå et al., 2018b), which demonstrates the anti-fungal and anti-cancer of these defensins by targeting membrane phospholipids, particularly PIP_2 and PA, resulting in oligomer formation and membrane permeabilisation (Poon et al., 2014; Kvansakul et al., 2016; Järvå et al., 2018b). It should be noted that in addition to membrane permeabilisation, other mechanisms of cell killing have been reported for defensins. Plant defensin RsAFP2, NaD1 and HsAFP1 have been shown to trigger the release of reactive oxygen species (ROS), induce apoptosis via mitochondrial-dependent mechanisms, and regulate Ca^{2+}/K^{+} efflux in *C. albicans* and pathogenic plant fungi, *Fusarium oxysprum* (De Coninck et al., 2013; van der Weerden & Anderson, 2013). In addition to plant defensins, human defensins have also been shown to mediate cell lysis using various mechanisms. HNP-1, -2, and -3, well characterised α-defensins, have been demonstrated to cause membrane permeabilisation of tumour cells via induction of DNA damage, suppression of DNA synthesis and ion channel formation (Muller et al., 2002; Nishimura et al., 2004).

The ability of HBD-2 to kill *C. albicans* but not HeLa cells is interesting and suggests its mechanism of action is different to that of NaD1 and HBD-3. Previous studies have suggested that the anti-fungal activity of HBD-2 is dependent on its ability to bind PIP_2 and permeabilise the plasma membrane (Järvå et al., 2018b). In contrast to the anti-tumour cell activity of NaD1 and HBD-3, this mechanism does not appear to be conserved for HBD-2 with HeLa cells. There are a few possible explanations, including ineffective uptake of HBD-2 in HeLa cells (as defensins need to be internalised by cells to mediate their lytic activity (Poon et al., 2014; Phan et al., 2016,), attributed to a potential difference in membrane composition or possession of a HBD-2–inactivating mechanism by HeLa cells.

6.5 Citrullination of NaD1, HBD-2, HBD-3 and LL-37

Citrullination is a post-translational modification that has been linked with several diseases including autoimmunity and cancer. In autoimmune disease such as rheumatoid arthritis (RA), autoantibodies target citrullinated proteins that contribute to disease progression, and detection of the presence of such anti-citrulline antibodies are a standard test for RA (Foulquier et al., 2007; Khandpur et al., 2013). In cancer, PAD enzymes are often up-regulated and have been shown to citrullinate a range of proteins, such as components of signaling pathways and the extracellular matrix components, that can promote aspects of tumour progression such as metastasis (Yuzhalin et al., 2018).

Citrullination is also exploited by pathogens to regulate innate immune responses such as antimicrobial activity. For example, citrullination of the antimicrobial peptide LL-37 reduces its antimicrobial activity (Cirioni et al., 2006; Kilsgard et al., 2012; Koziel et al., 2014) . In this thesis, for the first time it was revealed that defensins can be citrullinated. Immunoblot analysis using an anti-citrulline antibody which specifically detect citrulline residues, revealed bands

for NaD1 and HBD-3 at ~ 6 kDa (Figure 12B & Figure 30). However, no bands were observed for HBD-2 suggesting that this defensin is not citrullinated despite containing arginine residues. It should be noted that the anti-citrulline immunoblot analyses also detected bands at approximately 90 kDa and 50 kDa in the LL-37 and NaD1 samples, respectively, suggesting self-citrullination of the PAD2 enzyme. Self-citrullination of PAD4 has been previously reported, however, self-citrullination only affected protein interactions and had no effect on the function of the specificity or function of the enzyme (Andrade et al., 2010; Slack et al., 2011). As there is similarity between PAD2 and PAD4, it is possible that the PAD2 enzyme can undergo self-citrullination that has no effect on its function.

To further confirm citrullination of defensins, ESI-Q-TOF MS analysis was conducted where an increase in 1 Da is observed for every arginine residue that is converted to citrulline. An increase in 3 Da was observed for citrullinated NaD1 (Figure 13 B). NaD1 contains four arginine residues in its primary amino acid sequence (R1, R21, R39 and R40) which are predicted to be exposed, making them accessible for citrullination. Arginine residues that are near the N-terminus and flanked by glutamic acid are less susceptible to citrullination (Tarcsa et al., 1996; Gyorgy et al., 2006; Knuckley et al., 2010; Witalison et al., 2015). Since R1 is located close to the N-terminus and is flanked by glumatic acid, R1 could potentially be the arginine residue that will not be citrullinated in NaD1 (Figure 8). Despite containing two exposed arginine residues (R21 and R22) (Figure 8), HBD-2 does not appear to be citrullinated and these results are consistent with negative result from immunoblot analysis (Figure 30). Indeed, there may be structural explanations for why PAD cannot access all exposed arginine residues in HBD-2 as both the arginine residues are flanked by a proline residue which makes it less susceptible to citrullination (Figure 8). Intriguingly, citrullinated HBD-3 demonstrated

a decrease in 300 Da when compared to uncitrullinated HBD-3 and several molecular species as multiple peaks were observed (Figure 31B). The multiple peaks that appeared on the spectrum suggest that the protein might not be pure or the protein is not stable. In future it would be worth exploring if other PAD enzymes, such as PAD4, influence citrullination of defensins. Furthermore, as citrullination can alter the structure of proteins and lead to changes in function, it would be interesting to use CD spectroscopy to determine any structural changes that may arise from citrullination of the three defensins and if it affects their function**.** It is also important to highlight that in this study all of the citrullination experiments on defensins were done *in vitro*. Although this provides proof of concept that defensins (namely NaD1 and HBD-3 in this instance) can be citrullinated, clearly it is important to determine if defensins are citrullinated *in vivo*. Therefore, future experiments to address this could involve testing mouse and/or patient tissues samples or blood from appropriate settings where citrullination is expected e.g. sites of inflammation or tumours, immunoprecipitating the target defensin and then detecting the presence of any citrulline residues by immunoblotting approaches with an anti-citrulline antibody.

6.6 Interaction of citrullinated NaD1 with cellular lipids

Phosphoinositides, particularly PIP_2, are important components of the plasma membrane in mammalian and fungal cells (Di Paolo & De Camilli, 2006; van Meer et al., 2008). Despite only comprising 0.5-1% of the phospholipids in the mammalian cells, PIP_2 plays a vital role in several membrane regulated processes including ion channel function, signal transduction and cytoskeletal attachment (Meldrum et al., 1991; McLaughlin & Murray, 2005; Phan et al., 2019). While PIP_2 is an important targeted defense against pathogens, there may be mechanisms adopted by pathogens or the body that can directly or indirectly hinder the

effectiveness of PIP_2 function. In defensins such as NaD1 where PIP_2 plays a vital role in host defense, citrullination of NaD1 may prevent defensin:lipid interactions leading to loss of its function. Therefore, the ability of citrullinated NaD1 to bind to membrane phospholipids, particularly PIP_2, and the formation of oligomeric complexes were tested using protein-lipid overlay assays, liposome pulldown assays, chemical (BS^3) crosslinking assays and transmission electron microscopy. Native NaD1 strongly bound to various mono-/bis-/tris-phosphates, including PIP_2, and phosphatidic acid (PA) (Figure 14A & 15). Binding with PIP_2 and PA resulted in the formation of higher order multimeric structures as well long fibril like structures with PIP_2 (Figure 16 & 17A). Citrullinated NaD1 bound with weak relative intensities to various phospholipids including PIP_2 and PA, and was present in the unbound fraction of PC:$PI(4,5)P_2$ (Figure 14B & 15). No higher order multimeric structures were observed for citrullinated NaD1 in the presence of PIP_2 or PA, however, intriguingly flatter elongated structures with PIP_2, were observed in transmission electron microscopy (Figure 16 & 17B).

As mentioned, a number of plant and human defensins are known to mediate membranolytic activity by binding to membrane phospholipids, particularly to PIP_2. NaD1 is known to interact with PIP_2 via arginine residues, particularly R40, and is crucial for NAD1:PIP_2 interactions, oligomerisation and membrane permeabilisation (Poon et al., 2014). Other defensins such as HBD-2, HBD-3 and TPP3 lyse fungal and tumour cells via binding to PIP_2, and HBD-2 specifically interacts with PIP_2 via R22 to mediate cell permeabilisation (Poon et al., 2014; Baxter et al., 2015; Phan et al., 2016; Järvå et al., 2018b). The ability of citrullinated NaD1 to relatively bind to phospholipid, particularly PIP_2 as shown in this study, suggest that other residues in addition to arginine are involved in PIP_2 binding (Figure 14B). NaD1 interacts with

PIP_2 primarily via the characteristic 'KILRR' motif and forms hydrogen bonds with adjacent NaD1 monomers which involves K4, K36, H36, l37 and R40 residues (Poon et al., 2014). While R40 is a crucial residue for PIP_2 interactions and defensin function, mutagenesis studies involving R40 (rNaD1(R40E) indicated some binding to PIP_2 was retained, suggesting that ionic interactions with other residues may still be formed with NaD1 (Poon et al., 2014). This indicates that citrullination of arginine residues do not necessarily inhibit PIP_2 binding as there would be five other hydrogen bond formations which may allow for binding.

Despite citrullinated NaD1 demonstrating some interactions with PIP_2, no higher structures were seen in BS^3 crosslinking assay (Figure 16A). According to (Poon et al., 2014), R40 is crucial for connecting PIP_2 molecules and the formation of oligomeric NaD1:PIP2 structures. NaD1(R40E) mutagenesis studies demonstrated that oligomeric formation was reduced. This is attributed to the fact that loss of interactions with the 4-phoshate moiety results in loss of binding which leads to reduction in oligomerisation which is critically dependent on R40 forming bonds between adjacent PIP_2 molecules (Poon et al., 2014). It should be noted that K4 is involved in the formation of dimers as well as oligomers (Poon et al., 2014). However, mutation of R40 demonstrated a reduction in the formation of oligomers regardless of the presence of K4, which suggests that R40 is a more crucial residue or that both residues are required for the formation of oligomers. This supports the importance of R40 in oligomeric formation and that citrullination of NaD1 (citrullination of R40) may lead to reduced formation of oligomers as it is not able to engage in multiple PIP_2 molecules which play a crucial part of its function. Although some defensins bind to PIP_2, NaD1 and NsD7 have also been shown to bind to PA as well (Kvansakul et al., 2016; Järvå et al., 2018a). NaD1 formed multimeric structures in the presence of PA, while the formation of higher order structures were not seen

for citrullinated NaD1 in the presence of PA (Figure 16B). While R40 is a crucial residue for PIP_2 binding in NaD1, R39 is the crucial residue that is involved in NaD1 binding to PA and the formation of oligomers (Poon et al., 2014; Järvå et al., 2018a). Mutagenesis studies involving NaD1(R39A) revealed its inability to form oligomers with PA, which corresponded to the decreased ability to inhibit growth and kill permeabilise fungal cells, while still maintaining PIP_2 mediated oligomerisation (Järvå et al., 2018a). This indicates the importance of R39 in PA binding and citrullination of R39 may lead to the loss of oligomerisation and prevention of defensin function. Intriguingly, transmission electron microscopy demonstrated the formation of flatter elongated like structures when citrullinated NaD1 was incubated with PIP_2 (Figure 17B). As K4 is involved in the dimerisation of NaD1 molecules and possibly oligomerisation, it is possible that the fibril formation observed might be similar to oligomeric formation. Though the structures appear to be similar to oligomeric formation, further studies are necessary to verify this. The ability to form oligomers is not limited to plant defensins as oligomerisation has been characterised to be an important mechanism of human defensins as well. Human α-defensin 6 and human β-defensin 1 can form nanonet oligomers that have the ability to entangle bacteria and limit bacterial mobility (Chu et al., 2012; Raschig et al., 2017). Despite not knowing the ligands that trigger the formation, the importance of oligomerisation for defensins function is clear. Future structural studies involving citrullinated NaD1 with PIP_2 using X-ray crystallisations to determine citrullinated NaD1:PIP_2 interactions would be worth investigating. As well as more in-depth investigation on the role of citrullinated NaD1 interactions with PA may provide more insightful knowledge to membranolytic permeabilisation.

6.7 Functional analysis of citrullinated NaD1

As defensins, including NaD1, are known to exhibit membranolytic activity by targeting phospholipids, the effect of citrullinated NaD1 on lipid binding may have functional consequences for the functional ability of the defensin. The anti-fungal activity of citrullinated NaD1 was examined using *C. albicans* (ATCC10231) growth inhibition assays (Figure 18) . Native NaD1 inhibited the growth of fungal cells in a dose-dependent manner, abolishing fungal growth at 12.5 µM. In contrast, citrullinated NaD1 had a greatly reduced ability to inhibit fungal growth. The highly conserved β2-β3 loop (residues 38-42 for TPP3 and 36-40 for NaD1) motif among class II solanaceous defensins have been identified as crucial for PIP_2 binding and defects in PIP_2 binding can lead to the impairment of defensin function (Poon et al., 2014; Baxter et al., 2015). Mutagenesis studies of NaD1(NaD1 (R40E)) resulted in a significant reduction of fungal growth as a result of the inability to bind to PIP_2 and form oligomeric structures (Poon et al., 2014). Similarly, mutagenesis studies on NaD1(R39A) and residues of TPP3 involved in PIP_2 and PA binding and oligomerisation have revealed a reduction in fungal growth (Baxter et al., 2015). NaD1 (R39A) mutation was effective in abolishing fungal growth at higher concentrations due to its ability to bind to PIP_2 via the R40 residue (Järvå et al., 2018a). However, citrullinated NaD1 displayed no substainal effect on the fungal growth as both arginine residues involved in PIP_2 and PA binding may be citrullintated which accounts for the reduction in antifungal activity. This suggests that citrullination of arginine residues, particularly R40 and R39A, of NaD1 can modify the anti-fungal activity of this defensin. This reduction in antifungal activity against *C. albicans* (10231) was also observed on a different *C. albicans* clinical strain (ATCC90028). (Figure 22). However, this strain appears to be more resistant as both native and citrullinated NaD1 demonstrated reduced

activity at the highest concentration. The lipid composition in the plasma membrane between *C. albicans* vary between strains as the total ratio of PA and PIP_2 (40:1 to 6:1) composition is different and it may therefore account for the difference in activity observed for native and citrullinated NaD1 (Badrane et al., 2008; Singh et al., 2010). Apart from NaD1 and TPP3 β2-β3 loop, a closely resembling β2-β3 loop (RGFRRR) of plant defensin MtDef4 has been shown to be crucial for fungal cell entry which is mediated by PA binding and mutations of the loop result in impaired MtDef4 function (Sagaram et al., 2013). Additionally, mutations in the regions equivalent to KILRR loop of NaD1, crucial in lipid binding, have been implicated to be important for antifungal activity of other plant defensins. Mutations in RsAFP2 and MsDef1have been demonstrated to affect the antifungal activity (De Samblanx et al., 1997; Sagaram et al., 2013). Collectively, these studies indicate the importance of lipid binding on anti-fungal activity and where mutations or modifications such as citrullination of key arginine residues may result in impaired activity. Future investigation with higher defensin concentrations and fungal inhibition assays on wide range of fungal strains known to be affected by NaD1 including *Fusarium oxysporum*, *Fusarium graminearum* and *Saccharomyces cerevisiae*, should be carried out to further confirm effects of citrullination on the anti-fungal activity of defensins. Additionally, as plant defensins are also known to exhibit other mechanisms of antifungal activity in addition to membrane permeabilisation, such as production of ROS and promoting apoptosis (section 6.4), further studies would be necessary to confirm that reduction of fungal activity seen in growth inhibition is accredited to citrullination alone or other mechanisms.

Many defensins have the ability to permeabilise plasma membrane of fungal cells. Therefore, PI uptake assays were conducted to determine whether citrullinated NaD1 had any effect on membranolytic activity. Native NaD1 demonstrated a dose-dependent permeabilisation of *C. albicans*, with ~100 % permeabilisation for fungal cells at 25 μM (Figure 19). In contrast, citrullinated NaD1 had negligible effect on PI uptake of fungal cells. As with the fungal growth inhibition assays, PI uptake was investigated on different *C. albicans* strains (ATCC90028). A dose-dependent permeabilisation of *C. albicans* was shown with native NaD1 reaching 80% PI positivity, while citrullinated NaD1 demonstrated negligible PI positivity (Figure 23). This is further supported by the CLS microscopy on *C. albicans* (ATCC 10231), whereby PI uptake was observed in cells treated with NaD1 and no PI uptake was seen in cells treated with citrullinated NaD1 over the time course of 30 min (Figure 20 & 21). Taken together, these data support the notion that lipid composition of the fungal cell membrane may affect the activity of defensins.

In addition to permeabilising fungal cells, NaD1 is known to permeabilise tumour cells. Therefore, PI uptake of U937 cells with native and citrullinated NaD1 was investigated. Native NaD1 demonstrated a dose-dependent permeabilisation of U937 cells, with ~ 40% permeabilisation for U937 at 25 μM (Figure 26). In contrast, citrullinated NaD1 had no effect on PI uptake of fungal and tumour cells. This is further supported by end-point and time course CLS microscopy where PI uptake and membrane blebbing was not observed in cells treated with citrullinated NaD1 over the time course of 60 min (Figure 27 & 28). However, it should be noted that the negligible effect seen with citrullinated NaD1 on PI uptake by fungal and tumour cells may be a result of the shorter incubation time period (30 min), in contrast to effect that was seen on growth inhibition of fungal cells which involved a longer incubation period

(24 h) (Figure 18 & 22). Therefore, it would be interesting to further investigate incubation times of citrullinated defensin on fungal and tumour activity.

The cytotoxic effect of citrullinated NaD1 on the cell viability of the human tumour adherent cell lines HeLa and PC3 and suspension cell lines U937 and THP1 was assessed using MTT and MTS assays, respectively. HeLa and PC3 cell viability were reduced in a dose-dependent manner when treated with native NaD1. No significant reduction in viability was observed for HeLa and PC3 cells treated with citrullinated NaD1, with viability only reducing to 65 % and 80%, respectively, at the highest concentration tested of 25 µM (Figure 24). Similarly, U937 and THP1 cell viability was reduced in a dose-dependent manner when treated with native NaD1. Upon treatment with citrullinated NaD1 there was no substantial reduction in U937 cell viability with viability only reaching 85% (Figure 25A). However, interestingly there was an increase in THPI cell viability when treated with citrullinated NaD1(Figure 25B). Despite the difference in overall lipid composition of fungal and mammalian cells (mammalian cells contain higher levels of zwitterionic phospholipids whereas fungal cells contain more anionic phospholipids), PIP_2 plays an important role in both species (Di Paolo & De Camilli, 2006; van Meer et al., 2008). Similar inhibition of activity was observed in fungal and tumour cells upon treatment with citrullinated NaD1, which further supports the crucial role played by PIP_2 and suggests the blocking of a conserved mechanism of action by defensin citrullination. Similar to fungal growth inhibition (Figure 18 & 22), there was some reduction in HeLa and PC3 tumour cell viability upon incubation with citrullinated NaD1 for a longer duration (>24 h), indicating that some anti-fungal and anti-tumour cell activity is retained and exposure time may be an important factor. It is possible that the higher cell viability of THP1 cells may be result from citrullinated NaD1 having increased enzymatic activity without having an effect

on cell viability or citrullinated NaD1 may affect different cell lines in different ways. In addition, CAPs have demonstrated selective tumour killing using various mechanisms such as necrotic membrane disruption, induction of DNA damage and suppression of DNA synthesis (Lichtenstein et al., 1988; Muller et al., 2002). Therefore, it would be interesting to determine that reduction of cell viability seen in MTT assays is accredited to citrullination alone or other mechanisms.

6.8 Recombinant expression and citrullination of NaD1 R40E and NaD1 R39A mutants

As only three of the four arginine residues of NaD1 appear to be citrullinated (section 4.5), two arginine mutants of NaD1 (NaD1 R40E and NaD1 R39A) were generated to investigate if either of these residues are citrullinated. The NaD1 mutants were expressed and purified, with immunoblot analysis revealing bands at the expected molecular weights. The successful expression and purification of these NaD1 arginine mutants now enables future studies to confirm citrullination of these residues, and if so, additional functional studies to determine the role of these citrullinated arginine residues in regulating PIP_2 binding and cell killing.

6.9 Functional analysis of citrullinated HBD-3

HBD-3, a class of trans defensins, is inducibly expressed and secreted by epithelial cells, non-epithelial cells, neutrophils and monocytes (Harder et al., 2001; Harder et al., 2004; Sørensen et al., 2006). Of the known β-defensins, HBD-3 is possibly the most potent antimicrobial defensin exhibiting a broad range of anti-bacterial, anti-fungal and anti-viral activities (Harder et al., 2001; Quiñones-Mateu et al., 2003; Feng et al., 2005). HBD-3 is also a chemoattractive, that stimulates the production of chemokine expression as well as activates antigen presenting cells, contributing widely to both innate and adaptive immunity (Ferris et

al., 2013; Petrov et al., 2013). Recently it was demonstrated that HBD-3 binds to phosphoinositides, particularly PIP_2, and this is crucial for the anti-tumour activity (Phan et al., 2016). Despite NaD1 and HBD-3 sharing a relatively low sequence identity, HBD-3 shares a conserved β2- β3 loop motif with NaD1 and interactions of HBD-3 with PIP_2 is mediated by a lysine 39 (K39) residue (equivalent to R40 of NaD1) (Phan et al., 2016). As citrullination is involved in the conversion of arginine residues to citrulline, HBD-3 appears to be citrullinated as it contains 5 arginine residues in its sequence (Figure 8A & 30). Further, the overall high net positive charge (+11) of HBD-3 is related to its anti-microbial activity (Hoover et al., 2003; Klüver et al., 2005). Therefore, it is interesting to determine if citrullination of the arginine residues may affect the overall charge of HBD-3 which in turn may affect the anti-fungal and ant-cancer activity of HBD-3.

The anti-fungal activity of citrullinated HBD-3 was assessed using fungal growth inhibition assay and membrane permeabilisation PI uptake assay on *C.albicans* clinical strains (ATCC 10231 & 90028). Native HBD-3 reduced fungal growth in a dose-dependent manner for both strains. Interestingly citrullinated HBD-3 resulted in a reduction of anti-fungal activity against both strains with ~ 65% and 75% respectively (Figure 32 & 33). PI uptake assay revealed a dose dependent effect on the PI positivity of *C.albicans* when treated with native HBD-3 with almost negligible permeabilisation when treated with citrullinated HBD-3 even at the highest concentration (Figure 34 & 35). Despite not interacting with PIP_2 for its function, citrullinated HBD-3 displays an effect on the anti-fungal activity of the defensins. HBD-3 has a net charge of +11 and it has been speculated that its anti-microbial activity is related to this high net positive charge (Hoover et al., 2003; Klüver et al., 2005). Recently it has been speculated that HBD-3 activity is initiated by the accumulation of HBD-3 at the surface of a cell by

electrostatic interactions which eventually leads to internalisation of HBD-3. Once internalised, HBD-3 can bind to PIP_2 in the inner plasma membrane causing membrane permeabilisation (Phan et al., 2016). Therfore, it is possible that citrullination of the arginne residues may decrease the net charge of the protein and lead to a decrease in the electrostatic interaction between the postively charged defensin and the negatively charged lipid. This decrease may affect binding of HBD-3 to PIP_2 and ultimately reduce the activity of the defensin. Additionally it is also possible that the electrostatic attraction may aid in the stability of defensin-lipid interactions and a decrease in attraction will lead to an decline in the anti-microbial activity. Indeed, this may be account for the reduction in anti-fungal activity of citrullinated HBD-3. However, some activity is retained as HBD-3 is still able to bind to PIP_2 via the K39 residue once it enters the plasma membrane. It should be noted that citrullination might hinder the internalisation process of HBD-3. The PI uptake assay on fungal cells demonstrated almost negligable PI postivity when treated with citrullinated HBD-3, similar to that of citrullinated NaD1. This may provide further support that the cell exposure time plays an important factor in the action of citrullinated HBD-3 as this may perhaps slow internalisation process.

In addition to anti-fungal acitivity, HBD-3 is known to exhibit cytolytic activity against tumour cells via membrane permeablisation. The cytolytic activity of citrullinated HBD-3 was tested using PI uptake assays on U937 cells. While native HBD-3 displayed an increase in PI postivity of U937 dose-dependently, citrullinated NaD1 result in ~ 10% positivity at the highest concentration of 50 μM (Figure 36). This is further supported by end-point and time course CLS microscopy where PI uptake and membrane blebbing was not observed in cells treated with citrullinated HBD-3 over the time course of 30min (Figure 37 & 38). MTT cell viability

demonstrated a dose-dependent reduction of HeLa and PC3 when treated with native HBD-3 (Figure 39). Upon treatment with citrullinated HBD-3, HeLa cell viability was reduced to ~ 55% while there was no reduction in the viability of PC3 cells (Figure 38). It should be noted that native HBD-3 reduced PC3 cell viability to only ~ 65% at the highest concentration, therefore, it may account for the no change in cell viability with citrullinated HBD-3. As previously mentioned, the reduction in charge leading to a decrease in electrostatic attraction may account for the reduction in anti-cancer activity seen. The two residues that have been found to be important for HBD-3 binding to PIP_2 are K32 and K39. Mutagenesis studies involving HBD-3 (K32A) and HBD-3 (K39A), revealed some binding of HBD-3 to PIP_2 with HBD-3 (K32A) and significant loss of binding to PIP_2 with HBD-3 (K39A) (Phan et al., 2016). This is further supported by cell viability and membrane permeabilisation assays which demonstrated impaired impaired cytolytic activity by HBD-3 mutants (Phan et al., 2016). It should be noted that for both mutants, interaction with PA was substantially retained with subsequent HBD-3 activity. However, the specificity of HBD-3 to other membrane lipids and the formation of oligomers, as described for plant defensins, are yet to be determined. Therefore further studies needed to determine the importance of olgiomerisation for HBD-3 function and if citrullination of HBD-3 may affect its function in terms of lipid binding.

As with fungal and bacterial cells, certain CAPs have bee shown to selectively exhibit anti-tumour activity by various mechansims. Melittin, an α-helical CAP, and Bovine lactoferrrin are known to lytic tumor cells by forming barrel-stave pores or nectrotic membrane permeabilsation repectively (Sui et al., 1994; Mader, 2005). HNP-1, -2, and -3, have been demonstrated to cause membrane permeabilisation of tumour cells via induction of DNA damage, suppression of DNA synthesis and ion channel formation (Muller et al., 2002;

Nishimura et al., 2004). However, some defensins, such as HNP1 and HBD-3, also contain cytolytic activity against primary cells lines albeit at higher concentrations to tumour cells (Phan et al., 2016). Therefore, in future studies, the effect of citrullinated defensins on primary cell lines should be investigated to determine if there is selective anti-tumour activity.

Concluding remarks

Defensins play a vital role in the host defence system against invading pathogens through membranolytic action by binding to membrane phospholipids. However, post-translational modifications such as protein citrullination by pathogens can render aspects of the immune system ineffective. In summary, this study has identified for the first time, through immunoblot and mass spectrometry that defensins, particularly NaD1 and HBD-3, can be citrullinated by PAD enzymes. It was suggested that the interaction of citrullinated NaD1 and HBD-3 have reduced capacity to bind PIP_2, an important target membrane phospholipid for the lytic activity of these defensins. Furthermore, functional analysis of citrullinated NaD1 and HBD-3 on fungal and tumour cell lines revealed a significant reduction in defensin activity indicating a potential important role of citrullination in regulating defensin function. Overall, this study has established a preliminary understanding of defensin citrullination and highlights potential issues for the use of defensins as anticancer and antimicrobial therapeutic agents

Appendix

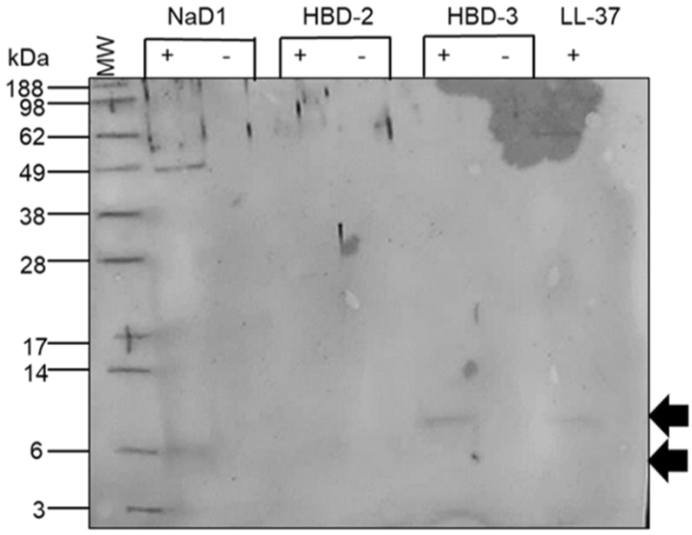

Figure 1. Characterisation of citrullinated NaD1, HBD-2, HBD-3 and LL-37

Citrullinated NaD1, HBD-2 and HBD-3 (10 µg protein) probed with anti-citrulline antibody (1:1000 dilution) and detected using HRP conjugated donkey-anti-rabbit antibody. (+ = Citrullinated, - = non-citrullinated).

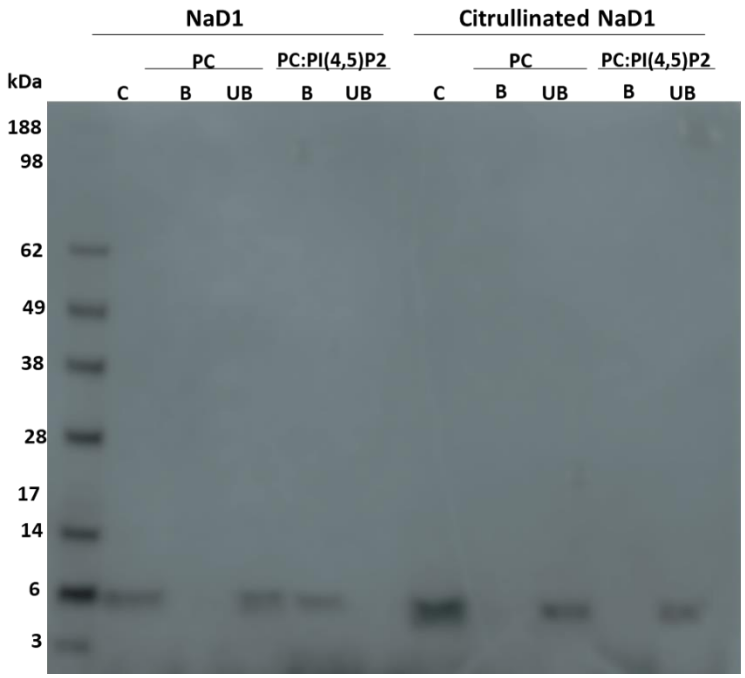

Figure 2. Binding of native and citrullinated NaD1 to PI(4,5)P_2

Liposome pull down assay of liposomes containing PC only or PC:PI(4,5)P2 were incubated with 1 ug of native and citrullinated NaD1, before centrifugation of bound (pellet) and unbound (supernatant) to separate fractions followed by SDS-PAGE and comassie blue staining

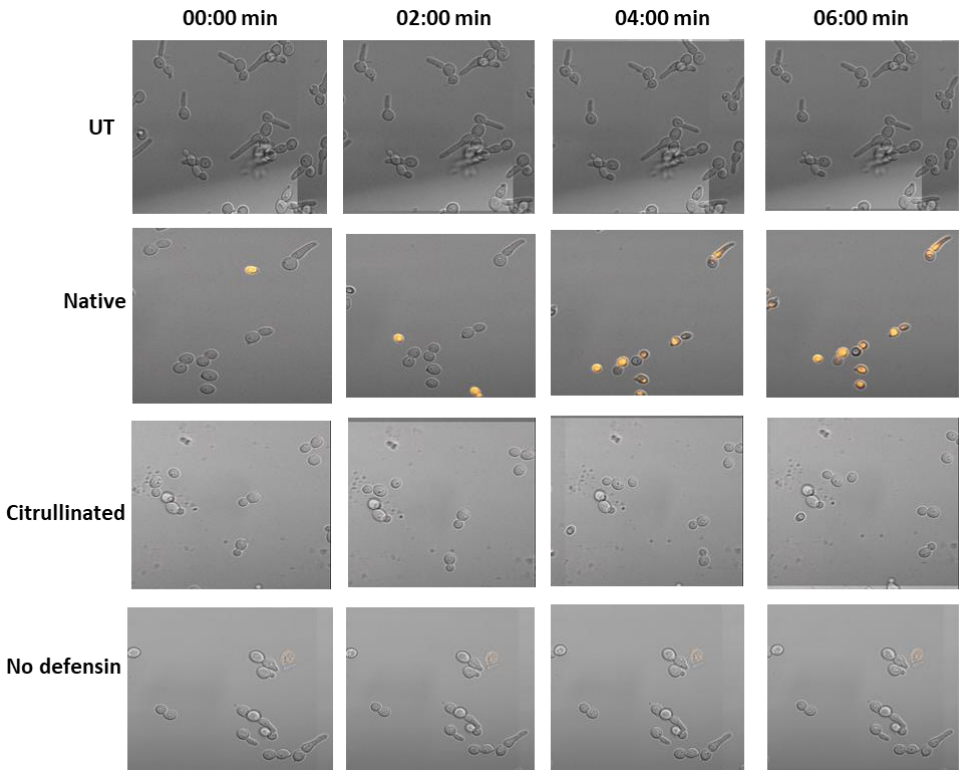

Figure 3. Confocal time course imaging of C.albicans (ATCC10231) cells

Cells were immoblised onto chamberslide and stained PI (orange) prior to imaging under Zeiss LSM 800 confocal microscopy in a 37°C/5% C02. Untreated cells, native NaD1 (25 μM), citrullinated NaD1 (25 μM) and no defensins were directly added to cells via capillary while viewing. Images were taken 0-6 min post addition of defensin. Data are representative of three independent experiment

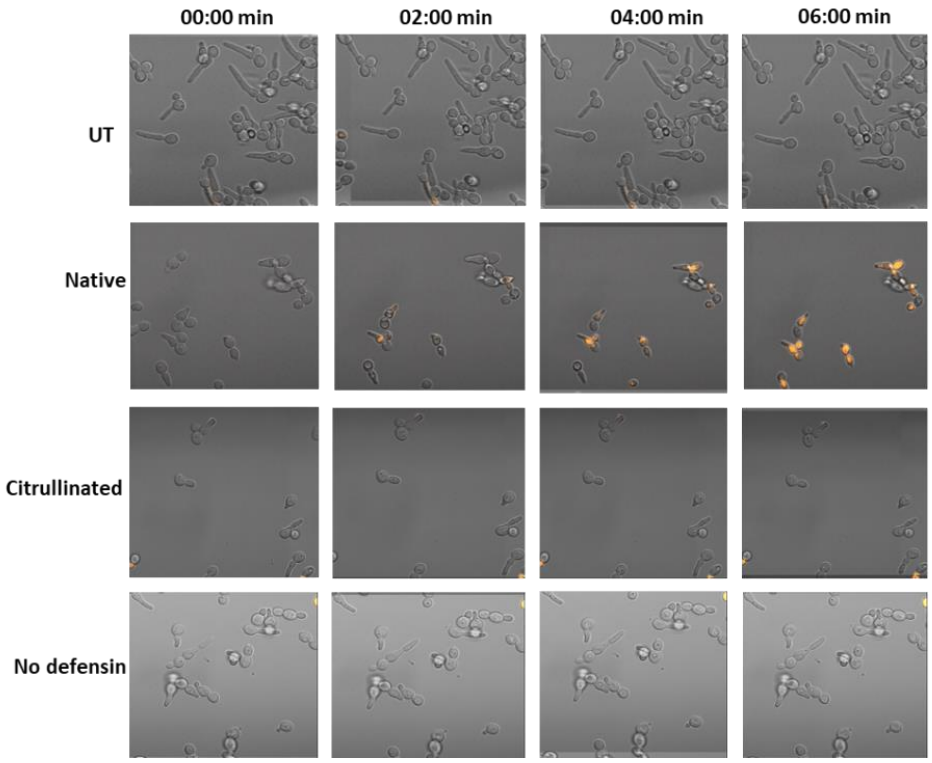

Figure 4. Confocal time course imaging of C.albicans (ATCC10231) cells

Cells were immoblised onto chamberslide and stained PI (orange) prior to imaging under Zeiss LSM 800 confocal microscopy in a 37°C/5% C02. Untreated cells, native NaD1 (25 μM), citrullinated NaD1 (25 μM) and no defensins were directly added to cells via capillary while viewing. Images were taken 0-6 min post addition of defensin. Data are representative of three independent experiment

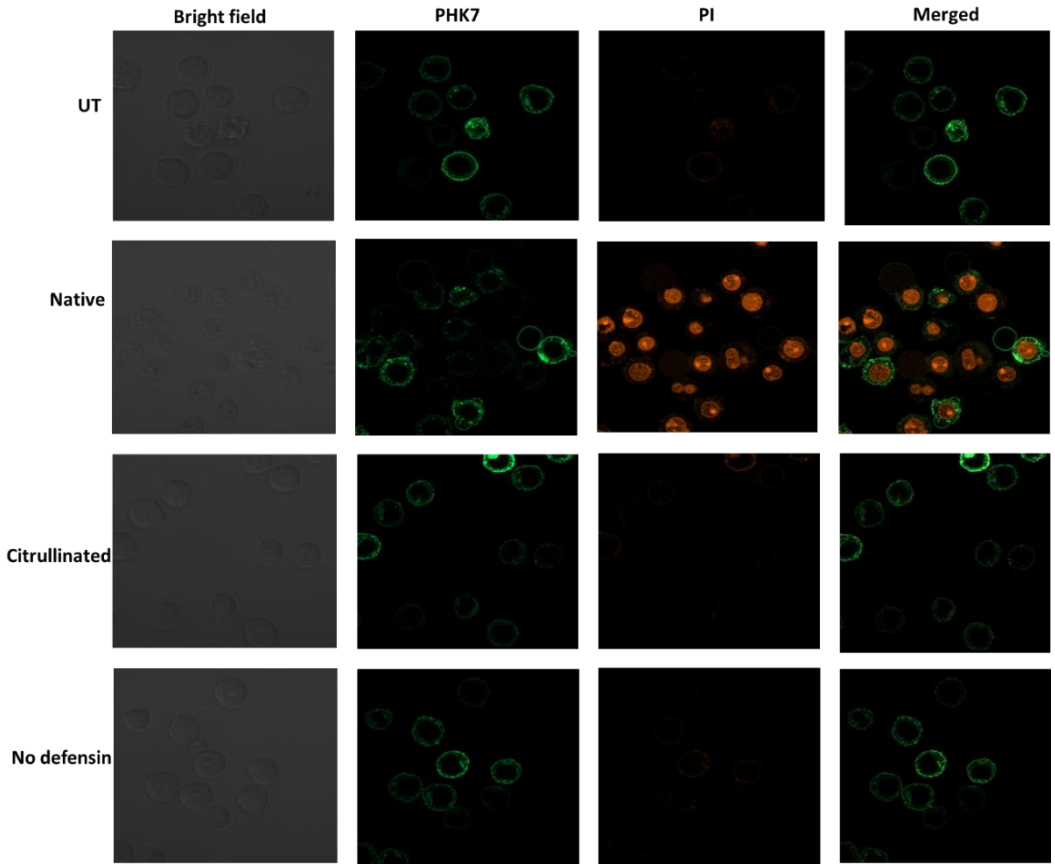

Figure 5. CLSM endpoint imaging of U937 cells

Cells were immoblised onto chambered slide and stained with PKH67 (green) and PI (orange) prior to imaging under Zeiss LSM 800 confocal microscopy in a 37°C/5% $C0_2$. Untreated cells, native NaD1 (10 μM), citrullinated NaD1 (10 μM) and no defensins were directly added to cells via capillary while viewing. Images were taken 0-60 min post addition of defensin.

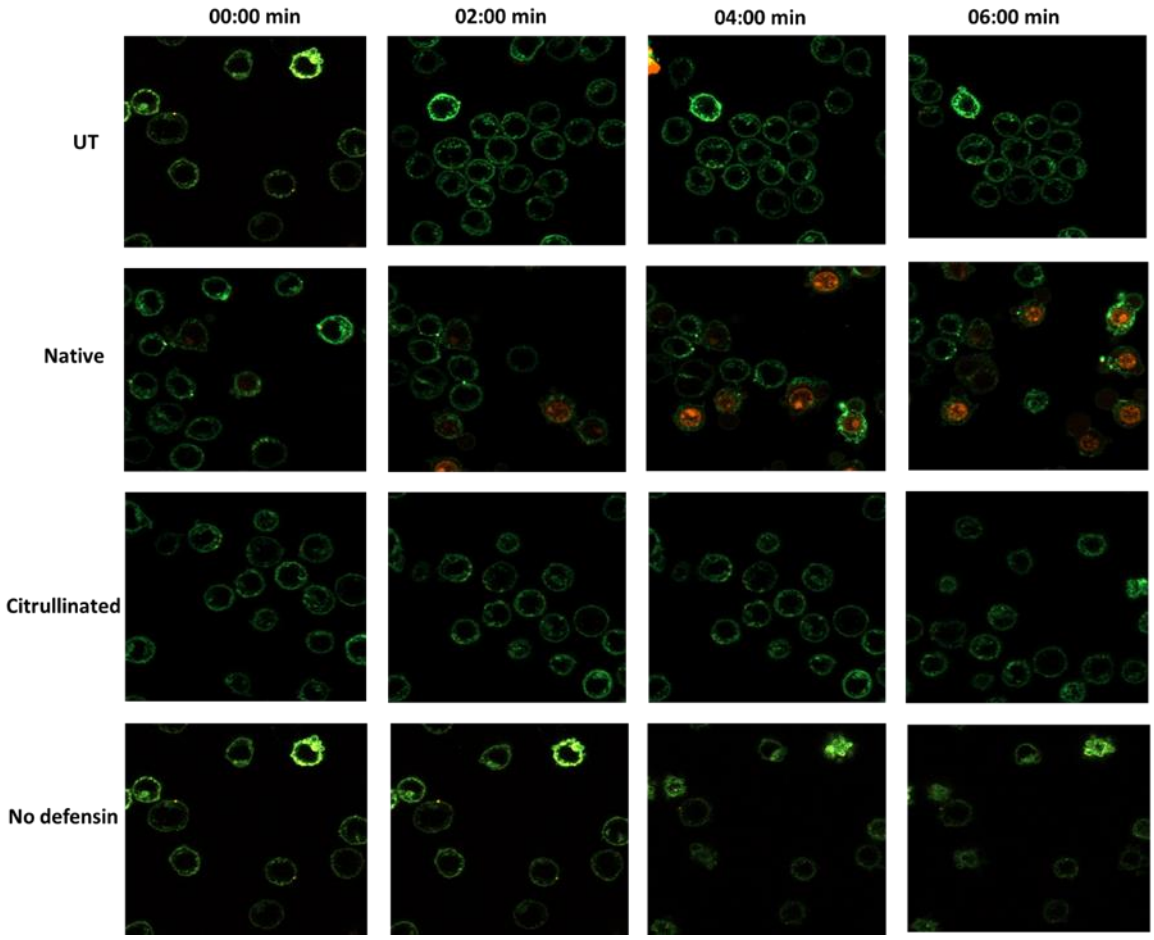

Figure 6. CLSM time course imaging of U937 cells

Cells were immoblised onto chambered slide and stained with PKH67 (green) and PI (orange) prior to imaging under Zeiss LSM 800 confocal microscopy in a 37°C/5% C02. Untreated cells, native NaD1 (10 μM), citrullinated NaD1 (10 μM) and no defensins were directly added to cells via capillary while viewing. Images were taken 0-6 min post addition of defensins.

List of References

Alghamdi M, Alasmari D, Assiri A, Mattar E, Aljaddawi AA, Alattas SG, Redwan EM (2019) An Overview of the Intrinsic Role of Citrullination in Autoimmune Disorders. *J Immunol Res* **2019**: 1-39

Andrade F, Darrah E, Gucek M, Cole RN, Rosen A, Zhu X (2010) Autocitrullination of human peptidyl arginine deiminase type 4 regulates protein citrullination during cell activation. *Arthritis and rheumatism* **62:** 1630-1640

Arita K, Shimizu T, Hashimoto H, Hidaka Y, Yamada M, Sato M (2006) Structural basis for histone N-terminal recognition by human peptidylarginine deiminase 4. *Proceedings of the National Academy of Sciences* **103**: 5291

Bachmann MF, Kopf M (2001) On the role of the innate immunity in autoimmune disease. *The Journal of experimental medicine* **193**: F47-F50

Badrane H, Nguyen MH, Cheng S, Kumar V, Derendorf H, Iczkowski KA, Clancy CJ (2008) The Candida albicans phosphatase Inp51p interacts with the EH domain protein Irs4p, regulates phosphatidylinositol-4,5-bisphosphate levels and influences hyphal formation, the cell integrity pathway and virulence. *Microbiology* **154**: 3296-3308

Bastian A, Schäfer H (2001) Human α-defensin 1 (HNP-1) inhibits adenoviral infection in vitro. *Regulatory Peptide*s **101**: 157-161

Baxter AA, Lay FT, Poon IKH, Kvansakul M, Hulett MD (2017) Tumor cell membrane-targeting cationic antimicrobial peptides: novel insights into mechanisms of action and therapeutic prospects. C*ellular and molecular life science*s *: CMLS* **74**: 3809-3825

Baxter AA, Richter V, Lay FT, Poon IKH, Adda CG, Veneer PK, Phan TK, Bleackley MR, Anderson MA, Kvansakul M, Hulett MD (2015) The Tomato Defensin TPP3 Binds Phosphatidylinositol (4,5)-Bisphosphate via a Conserved Dimeric Cationic Grip Conformation To Mediate Cell Lysis. *Molecular and Cellular Biology* **35**: 1964

Bicker KL, Thompson PR (2013) The protein arginine deiminases: Structure, function, inhibition, and disease. *Biopolymers* **99**: 155-163

Blachère NE, Parveen S, Frank MO, Dill BD, Molina H, Orange DE (2017) High-Titer Rheumatoid Arthritis Antibodies Preferentially Bind Fibrinogen Citrullinated by Peptidylarginine Deiminase 4. *Arthritis Rheumatol* **69**: 986-995

Boniotto M, Antcheva N, Zelezetsky I, Tossi A, Palumbo V, Verga Falzacappa MV, Sgubin S, Braida L, Amoroso A, Crovella S (2003) A study of host defence peptide beta-defensin 3 in primates. *The Biochemical journal* **374**: 707-14

Brentville VA, Vankemmelbeke M, Metheringham RL, Durrant LG (2020) Post-translational modifications such as citrullination are excellent targets for cancer therapy. *Seminars in Immunology* **47**: 101393

Brinkmann V (2004) Neutrophil Extracellular Traps Kill Bacteria. Science 303: 1532-1535

Brogden KA (2005) Antimicrobial peptides: pore formers or metabolic inhibitors in bacteria? *Nature reviews Microbiology* **3**: 238-50

Cantarino N, Musulen E, Valero V, Peinado MA, Perucho M, Moreno V, Forcales SV, Douet J, Buschbeck M (2016) Downregulation of the Deiminase PADI2 Is an Early Event in Colorectal Carcinogenesis and Indicates Poor Prognosis. *Molecular cancer research : MCR* **14**: 841-8

Chang X, Han J (2006) Expression of peptidylarginine deiminase type 4 (PAD4) in various tumors. *Molecular carcinogenesis* **45**: 183-96

Chang X, Han J, Pang L, Zhao Y, Yang Y, Shen Z (2009) Increased PADI4 expression in blood and tissues of patients with malignant tumors. *BMC cancer* **9**: 40

Chang X, Yamada R, Suzuki A, Sawada T, Yoshino S, Tokuhiro S, Yamamoto K (2005) Localization of peptidylarginine deiminase 4 (PADI4) and citrullinated protein in synovial tissue of rheumatoid arthritis. *Rheumatology (Oxford)* **44**: 40-50

Christophorou MA, Castelo-Branco G, Halley-Stott RP, Oliveira CS, Loos R, Radzisheuskaya A, Mowen KA, Bertone P, Silva JCR, Zernicka-Goetz M, Nielsen ML, Gurdon JB, Kouzarides T (2014) Citrullination regulates pluripotency and histone H1 binding to chromatin. *Nature* **507**: 104-108

Chu H, Pazgier M, Jung G, Nuccio S-P, Castillo PA, De Jong MF, Winter MG, Winter SE, Wehkamp J, Shen B (2012) Human α-defensin 6 promotes mucosal innate immunity through self-assembled peptide nanonets. *Science* **337**: 477-481

Cirioni O, Giacometti A, Ghiselli R, Bergnach C, Orlando F, Silvestri C, Mocchegiani F, Licci A, Skerlavaj B, Rocchi M, Saba V, Zanetti M, Scalise G (2006a) LL-37 protects rats against lethal sepsis caused by gram-negative bacteria. *Antimicrob Agents Chemother* **50**: 1672-9

Claushuis TAM, van der Donk LEH, Luitse AL, van Veen HA, van der Wel NN, van Vught LA, Roelofs JJTH, de Boer OJ, Lankelma JM, Boon L, de Vos AF, van 't Veer C, van der Poll T (2018) Role of Peptidylarginine Deiminase 4 in Neutrophil Extracellular Trap Formation and Host Defense during Klebsiella pneumoniae– Induced Pneumonia-Derived Sepsis. *Journal of immunology (Baltimore, Md : 1950)* **201**: 1241-1252

Crona DJ, Milowsky MI, Whang YE (2015) Androgen receptor targeting drugs in castration-resistant prostate cancer and mechanisms of resistance. Clin Pharmacol Ther **98**: 582-589

Cutrona KJ, Kaufman BA, Figueroa DM, Elmore DE (2015) Role of arginine and lysine in the antimicrobial mechanism of histone-derived antimicrobial peptides. *FEBS Lett* **589**: 3915-3920

de Bont CM, Boelens WC, Pruijn GJM (2018) NETosis, complement, and coagulation: a triangular relationship. *Cell Mol Immunol* **16**: 19-27

De Coninck B, Cammue BPA, Thevissen K (2013) Modes of antifungal action and in planta functions of plant defensins and defensin-like peptides. *Fungal Biology Reviews* **26**: 109-120

de Rycke L, Nicholas AP, Cantaert T, Kruithof E, Echols JD, Vandekerckhove B, Veys EM, de Keyser F, Baeten D (2005) Synovial intracellular citrullinated proteins colocalizing with peptidyl arginine deiminase as pathophysiologically relevant antigenic determinants of rheumatoid arthritis-specific humoral autoimmunity. *Arthritis and rheumatism* **52**: 2323-2330

De Samblanx GW, Goderis IJ, Thevissen K, Raemaekers R, Fant F, Borremans F, Acland DP, Osborn RW, Patel S, Broekaert WF (1997) Mutational analysis of a plant defensin from radish (Raphanus sativus L.) reveals two adjacent sites important for antifungal activity. *J Biol Chem* **272**: 1171-9

Denning N-L, Aziz M, Gurien SD, Wang P (2019) DAMPs and NETs in Sepsis. *Front Immunol* **10**: 2536-2536

Devlin EJ, Denson LA, Whitford HS (2017) Cancer Treatment Side Effects: A Meta-analysis of the Relationship Between Response Expectancies and Experience. *Journal of pain and symptom management* **54**: 245-258.e2

Dhar SK, St. Clair DK (2009) Nucleophosmin Blocks Mitochondrial Localization of p53 and Apoptosis. *J Biol Chem* **284**: 16409-16418

Di Paolo G, De Camilli P (2006) Phosphoinositides in cell regulation and membrane dynamics. *Nature* **443**: 651-7

Dürr UHN, Sudheendra US, Ramamoorthy A (2006) LL-37, the only human member of the cathelicidin family of antimicrobial peptides. *Biochimica et biophysica acta Biomembranes* **1758**: 1408-1425

Feng Z, Jiang B, Chandra J, Ghannoum M, Nelson S, Weinberg A (2005) Human Beta-defensins: Differential Activity against Candidal Species and Regulation by Candida albicans. *J Dent Res* **84**: 445-450

Ferris LK, Mburu YK, Mathers AR, Fluharty ER, Larregina AT, Ferris RL, Falo LD (2013) Human Beta-Defensin 3 Induces Maturation of Human Langerhans Cell–Like Dendritic Cells: An Antimicrobial Peptide that Functions as an Endogenous Adjuvant. *J Invest Dermatol* **133**: 460-468

Goulas T, Mizgalska D, Garcia-Ferrer I, Kantyka T, Guevara T, Szmigielski B, Sroka A, Millán C, Usón I, Veillard F, Potempa B, Mydel P, Solà M, Potempa J, Gomis-Rüth FX (2015) Structure and mechanism of a bacterial host-protein citrullinating virulence factor, Porphyromonas gingivalis peptidylarginine deiminase. *Sci Rep* **5**: 11969-11969

Guo Q, Fast W (2011) Citrullination of Inhibitor of Growth 4 (ING4) by Peptidylarginine Deminase 4 (PAD4) Disrupts the Interaction between ING4 and p53. *J Biol Chem* **286**: 17069-17078

Gyorgy B, Toth E, Tarcsa E, Falus A, Buzas EI (2006) Citrullination: a posttranslational modification in health and disease. *Th*e international journal of biochemistry & cell biology **38**: 1662-77

Hajishengallis G (2014) Periodontitis: from microbial immune subversion to systemic inflammation. *Nat Rev Immunol* **15**: 30-44

Hanahan D, Weinberg RA (2011) Hallmarks of cancer: the next generation. Cell 144: 646-74

Hancock RE, Diamond G (2000) The role of cationic antimicrobial peptides in innate host defences. *Trends in microbiology* **8**: 402-10

Hancock RE, Sahl HG (2006) Antimicrobial and host-defense peptides as new anti-infective therapeutic strategies. *Nature biotechnology* **24**: 1551-7

Harder J, Bartels J, Christophers E, Schröder J-M (2001) Isolation and characterization of human β-defensin-3, a novel human inducible peptide antibiotic. *Journal of Biological Chemistry* **276**: 5707-5713

Harder J, Meyer-Hoffert U, Wehkamp K, Schwichtenberg L, Schröder J-M (2004) Differential gene induction of human β-defensins (hBD-1,-2,-3, and-4) in keratinocytes is inhibited by retinoic acid. *Journal of Investigative Dermatology* **123**: 522-529

Heather P, Mike D, Mark BH, Anthony JK, Christine CW (2012) Requirements for NADPH oxidase and myeloperoxidase in neutrophil extracellular trap formation differ depending on the stimulus. *J Leukoc Biol* **92**: 841-849

Hongjie Y, Pingxin L, Bryan JV, Suting Z, Paul RT, Pugh BF, Yanming W (2008) Histone Arg Modifications and p53 Regulate the Expression of OKL38, a Mediator of Apoptosis. *J Biol Chem* **283**: 20060-20068

Hoover DM, Wu Z, Tucker K, Lu W, Lubkowski J (2003) Antimicrobial characterization of human β-defensin 3 derivatives. *Antimicrobial agents and chemotherapy* 47: 2804-2809

Hsu P-C, Liao Y-F, Lin C-L, Lin W-H, Liu G-Y, Hung H-C (2014) Vimentin Is Involved in Peptidylarginine Deiminase 2-Induced Apoptosis of Activated Jurkat Cells. *Molecules and cells* **37**: 426-434

Inagaki M, Takahara H, Nishi Y, Sugawara K, Sato C (1989) Ca2+-dependent deimination-induced disassembly of intermediate filaments involves specific modification of the amino-terminal head domain. *J Biol Chem* **264**: 18119-18127

Järvå M, Lay FT, Phan TK, Humble C, Poon IKH, Bleackley MR, Anderson MA, Hulett MD, Kvansakul M (2018a) X-ray structure of a carpet-like antimicrobial defensin–phospholipid membrane disruption complex. *Nature Communications* **9**: 1962

Järvå M, Phan TK, Lay FT, Caria S, Kvansakul M, Hulett MD (2018b) Human β-defensin 2 kills Candida albicans through phosphatidylinositol 4,5-bisphosphate-mediated membrane permeabilization. *Science advances* **4**: eaat0979-eaat0979

Khandpur R, Carmona-Rivera C, Vivekanandan-Giri A, Gizinski A, Yalavarthi S, Knight JS, Friday S, Li S, Patel RM, Subramanian V, Thompson P, Chen P, Fox DA, Pennathur S, Kaplan MJ (2013) NETs are a source of citrullinated autoantigens and stimulate inflammatory responses in rheumatoid arthritis. *Science translational medicine* **5**: 178ra40

Kilsgard O, Andersson P, Malmsten M, Nordin SL, Linge HM, Eliasson M, Sorenson E, Erjefalt JS, Bylund J, Olin AI, Sorensen OE, Egesten A (2012) Peptidylarginine deiminases present in the airways during tobacco smoking and inflammation can citrullinate the host defense peptide LL-37, resulting in altered activities. *American journal of respiratory cell and molecular biology* **46**: 240-8

Klüver E, Schulz-Maronde S, Scheid S, Meyer B, Forssmann W-G, Adermann K (2005) Structure−Activity Relation of Human β-Defensin 3: Influence of Disulfide Bonds and Cysteine Substitution on Antimicrobial Activity and Cytotoxicity. *Biochemistry* **44**: 9804-9816

Knuckley B, Causey CP, Jones JE, Bhatia M, Dreyton CJ, Osborne TC, Takahara H, Thompson PR (2010) Substrate specificity and kinetic studies of PADs 1, 3, and 4 identify potent and selective inhibitors of protein arginine deiminase 3. *Biochemistry* **49**: 4852-63

Konig MF, Andrade F (2016) A Critical Reappraisal of Neutrophil Extracellular Traps and NETosis Mimics Based on Differential Requirements for Protein Citrullination. *Front Immunol* **7**: 461-461

Koziel J, Bryzek D, Sroka A, Maresz K, Glowczyk I, Bielecka E, Kantyka T, Pyrc K, Svoboda P, Pohl J, Potempa J (2014) Citrullination alters immunomodulatory function of LL-37 essential for prevention of endotoxin-induced sepsis. *Journal of immunology (Baltimore, Md : 1950)* **192**: 5363-72

Kvansakul M, Lay FT, Adda CG, Veneer PK, Baxter AA, Phan TK, Poon IK, Hulett MD (2016) Binding of phosphatidic acid by NsD7 mediates the formation of helical defensin-lipid oligomeric assemblies and membrane permeabilization. *Proc Natl Acad Sci U S A* **113**: 11202-11207

Lacerda AF, Vasconcelos EAR, Pelegrini PB, Grossi de Sa MF (2014) Antifungal defensins and their role in plant defense. *Front Microbiol* **5**: 116-116

Lange S, Gallagher M, Kholia S, Kosgodage US, Hristova M, Hardy J, Inal JM (2017) Peptidylarginine Deiminases-Roles in Cancer and Neurodegeneration and Possible Avenues for Therapeutic Intervention via Modulation of Exosome and Microvesicle (EMV) Release? *International journal of molecular sciences* **18**

Lay FT, Anderson MA (2005) Defensins--components of the innate immune system in plants. *Current protein & peptide science* **6**: 85-101

Lay FT, Brugliera F, Anderson MA (2003) Isolation and properties of floral defensins from ornamental tobacco and petunia. *Plant Physiol* **131**: 1283-93

Lay FT, Mills GD, Poon IKH, Cowieson NP, Kirby N, Baxter AA, van der Weerden NL, Dogovski C, Perugini MA, Anderson MA, Kvansakul M, Hulett MD (2012) Dimerization of plant defensin NaD1 enhances its antifungal activity. *J Biol Chem* **287**: 19961-19972

Lay FT, Poon S, McKenna JA, Connelly AA, Barbeta BL, McGinness BS, Fox JL, Daly NL, Craik DJ, Heath RL, Anderson MA (2014) The C-terminal propeptide of a plant defensin confers cytoprotective and subcellular targeting functions. *BMC plant biology* **14**: 41-41

Lee YH, Coonrod SA, Kraus WL, Jelinek MA, Stallcup MR (2005) Regulation of coactivator complex assembly and function by protein arginine methylation and demethylimination. *Proc Natl Acad Sci U S A* **102**: 3611-3616

Lewis HD, Liddle J, Coote JE, Atkinson SJ, Barker MD, Bax BD, Bicker KL, Bingham RP, Campbell M, Chen YH, Chung C-w, Craggs PD, Davis RP, Eberhard D, Joberty G, Lind KE, Locke K, Maller C, Martinod K, Patten C et al. (2015) Inhibition of PAD4 activity is sufficient to disrupt mouse and human NET formation. *Nat Chem Biol* **11**: 189-191

Li P, Wang D, Yao H, Doret P, Hao G, Shen Q, Qiu H, Zhang X, Wang Y, Chen G (2010) Coordination of PAD4 and HDAC2 in the regulation of p53-target gene expression. *Oncogene* **29**: 3153-3162

Li P, Yao H, Zhang Z, Li M, Luo Y, Thompson PR, Gilmour DS, Wang Y (2008) Regulation of p53 Target Gene Expression by Peptidylarginine Deiminase 4. Mol Cell Biol **28**: 4745-4758

Lichtenstein AK, Ganz T, Nguyen TM, Selsted ME, Lehrer RI (1988) Mechanism of target cytolysis by peptide defensins. Target cell metabolic activities, possibly involving endocytosis, are crucial for expression of cytotoxicity. *Journal of immunology (Baltimore, Md : 1950)* **140**: 2686-94

Lupyan D, Mezei M, Logothetis DE, Osman R (2010) A molecular dynamics investigation of lipid bilayer perturbation by PIP2. *Biophys J* **98**: 240-247

Mader JS (2005) Bovine lactoferricin selectively induces apoptosis in human leukemia and carcinoma cell lines. *Mol Cancer Ther* **4**: 612-624

Mader JS, Ewen C, Hancock RE, Bleackley RC (2011) The human cathelicidin, LL-37, induces granzyme-mediated apoptosis in regulatory T cells. *Journal of immunotherapy (Hagerstown, Md : 1997)* **34**: 229-35

Majsnerowska M, Noens EEE, Lolkema JS (2018) Arginine and Citrulline Catabolic Pathways Encoded by the arc Gene Cluster of Lactobacillus brevis ATCC 367. J*ournal of bacteriology* **200**

Mangat P, Wegner N, Venables PJ, Potempa J (2010) Bacterial and human peptidylarginine deiminases: targets for inhibiting the autoimmune response in rheumatoid arthritis? *Arthritis Res Ther* **12**: 209-209

Masson-Bessière C, Sebbag M, Girbal-Neuhauser E, Nogueira L, Vincent C, Senshu T, Serre G (2001) The Major Synovial Targets of the Rheumatoid Arthritis-Specific Antifilaggrin Autoantibodies Are Deiminated Forms of the α- and β-Chains of Fibrin. *Journal of immunology (Baltimore, Md : 1950)* **166**: 4177-4184

McElwee JL, Mohanan S, Griffith OL, Breuer HC, Anguish LJ, Cherrington BD, Palmer AM, Howe LR, Subramanian V, Causey CP, Thompson PR, Gray JW, Coonrod SA (2012) Identification of PADI2 as a potential breast cancer biomarker and therapeutic target. *BMC cancer* **12**: 500-500

McElwee JL, Mohanan S, Horibata S, Sams KL, Anguish LJ, McLean D, Cvita I, Wakshlag JJ, Coonrod SA (2014) PAD2 Overexpression in Transgenic Mice Promotes Spontaneous Skin Neoplasia. *Cancer Res* **74**: 6306-6317

McGraw WT, Potempa J, Farley D, Travis J (1999) Purification, characterization, and sequence analysis of a potential virulence factor from Porphyromonas gingivalis, peptidylarginine deiminase. *Infection and immunity* **67**: 3248-56

McLaughlin S, Murray D (2005) Plasma membrane phosphoinositide organization by protein electrostatics. *Nature* **438**: 605-611

Meldrum E, Parker PJ, Carozzi A (1991) The PtdIns-PLC superfamily and signal transduction. *BBA - Molecular Cell Research* **1092**: 49-71

Mesa MA, Vasquez G (2013) NETosis. *Autoimmune diseases* **2013**

Metzler KD, Fuchs TA, Nauseef WM, Reumaux D, Roesler J, Schulze I, Wahn V, Papayannopoulos V, Zychlinsky A (2011) Myeloperoxidase is required for neutrophil extracellular trap formation: implications for innate immunity. *Blood* **117**: 953-959

Mizoguchi M, Manabe M, Kawamura Y, Kondo Y, Ishidoh K, Kominami E, Watanabe K, Asaga H, Senshu T, Ogawa H (1998) Deimination of 70-kD Nuclear Protein During Epidermal Apoptotic Events In Vitro. *J Histochem Cytochem* **46**: 1303-1309

Muller CA, Markovic-Lipkovski J, Klatt T, Gamper J, Schwarz G, Beck H, Deeg M, Kalbacher H, Widmann S, Wessels JT, Becker V, Muller GA, Flad T (2002) Human alpha-defensins HNPs-1, -2, and -3 in renal cell carcinoma: influences on tumor cell proliferation. *The American journal of pathology* **160**: 1311-24

Neeli I, Radic M (2013) Opposition between PKC isoforms regulates histone deimination and neutrophil extracellular chromatin release. *Front Immunol* **4**: 38-38

Nishimura M, Abiko Y, Kurashige Y, Takeshima M, Yamazaki M, Kusano K, Saitoh M, Nakashima K, Inoue T, Kaku T (2004) Effect of defensin peptides on eukaryotic cells: primary epithelial cells, fibroblasts and squamous cell carcinoma cell lines. *Journal of dermatological science* **36**: 87-95

Papayannopoulos V, Metzler KD, Hakkim A, Zychlinsky A (2010) Neutrophil elastase and myeloperoxidase regulate the formation of neutrophil extracellular traps. *J Cell Biol* **191**: 677-691

Peschel A, Sahl H-G (2006) The co-evolution of host cationic antimicrobial peptides and microbial resistance. *Nature Reviews Microbiology* **4**: 529

Petrov V, Funderburg N, Weinberg A, Sieg S (2013) Human β defensin-3 induces chemokines from monocytes and macrophages: diminished activity in cells from HIV-infected persons. *Immunology* **140**: 413-420

Phan TK, Lay FT, Poon IK, Hinds MG, Kvansakul M, Hulett MD (2016) Human beta-defensin 3 contains an oncolytic motif that binds PI(4,5)P2 to mediate tumour cell permeabilisation. *Oncotarget* **7**: 2054-69

Phan TK, Williams SA, Bindra GK, Lay FT, Poon IKH, Hulett MD (2019) Phosphoinositides: multipurpose cellular lipids with emerging roles in cell death. *Cell death and differentiation* **26**: 781-793

Pilsczek FH, Salina D, Poon KKH, Fahey C, Yipp BG, Sibley CD, Robbins SM, Green FHY, Surette MG, Sugai M, Bowden MG, Hussain M, Zhang K, Kubes P (2010) A Novel Mechanism of Rapid Nuclear Neutrophil Extracellular Trap Formation in Response to Staphylococcus aureus. *Journal of immunology (Baltimore, Md : 1950)* **185**: 7413-7425

Poon IK, Baxter AA, Lay FT, Mills GD, Adda CG, Payne JA, Phan TK, Ryan GF, White JA, Veneer PK, van der Weerden NL, Anderson MA, Kvansakul M, Hulett MD (2014)

Phosphoinositide-mediated oligomerization of a defensin induces cell lysis. *eLife* **3***:* e01808-e01808

Potempa M, Potempa J (2012) Protease-dependent mechanisms of complement evasion by bacterial pathogens. *Biol Chem* **393**: 873-888

Pyrc K, Milewska A, Kantyka T, Sroka A, Maresz K, Kozieł J, Nguyen K-A, Enghild JJ, Knudsen AD, Potempa J (2013) Inactivation of Epidermal Growth Factor by Porphyromonas gingivalis as a Potential Mechanism for Periodontal Tissue Damage. *Infection and immunity* **81**: 55-64

Quiñones-Mateu ME, Lederman MM, Feng Z, Chakraborty B, Weber J, Rangel HR, Marotta ML, Mirza M, Jiang B, Kiser P, Medvik K, Sieg SF, Weinberg A (2003) Human epithelial β-defensins 2 and 3 inhibit HIV-1 replication. *AIDS* **17**: F39-F48

Quirke A-M, Lugli EB, Wegner N, Hamilton BC, Charles P, Chowdhury M, Ytterberg AJ, Zubarev RA, Potempa J, Culshaw S, Guo Y, Fisher BA, Thiele G, Mikuls TR, Venables PJW (2014) Heightened immune response to autocitrullinated Porphyromonas gingivalis peptidylarginine deiminase: a potential mechanism for breaching immunologic tolerance in rheumatoid arthritis. *Ann Rheum Dis* **73**: 263-269

Raschig J, Mailänder-Sánchez D, Berscheid A, Berger J, Strömstedt AA, Courth LF, Malek NP, Brötz-Oesterhelt H, Wehkamp J (2017) Ubiquitously expressed Human Beta Defensin 1 (hBD1) forms bacteria-entrapping nets in a redox dependent mode of action. *PLoS Pathog* **13**: e1006261-e1006261

Riedl S, Zweytick D, Lohner K (2011) Membrane-active host defense peptides--challenges and perspectives for the development of novel anticancer drugs. *Chemistry and physics of lipids* **164**: 766-81

Rogers GE, Harding HW, Llewellyn-Smith IJ (1977) The origin of citrulline-containing proteins in the hair follicle and the chemical nature of trichohyalin, an intracellular precursor. *Biochimica et biophysica acta* **495**: 159-75

Romero V, Fert-Bober J, Nigrovic PA, Darrah E, Haque UJ, Lee DM, Van Eyk J, Rosen A, Andrade F (2013) Immune-mediated pore-forming pathways induce cellular hypercitrullination and generate citrullinated autoantigens in rheumatoid arthritis. *Science translational medicine* **5**: 209ra150-209ra150

Sagaram US, El-Mounadi K, Buchko GW, Berg HR, Kaur J, Pandurangi RS, Smith TJ, Shah DM (2013) Structural and Functional Studies of a Phosphatidic Acid-Binding Antifungal Plant Defensin MtDef4: Identification of an RGFRRR Motif Governing Fungal Cell Entry. *PLoS One* **8**: e82485-e82485

Schibli DJ, Hunter HN, Aseyev V, Starner TD, Wiencek JM, McCray PB, Vogel HJ (2002). The solution structures of the human β-defensins lead to a better understanding of the potent bactericidal activity of HBD3 against Staphylococcus aureus. *Journal of Biological Chemistry*, **277**(10), 8279-8289.

Selsted ME, Ouellette AJ (2005) Mammalian defensins in the antimicrobial immune response. *Nature immunology* **6**: 551-7

Senshu T, Akiyama K, Kan S, Asaga H, Ishigami A, Manabe M (1995) Detection of Deiminated Proteins in Rat Skin: Probing with a Monospecific Antibody After Modification of Citrulline Residues. *J Invest Dermatol* **105**: 163-169

Senshu T, Kan S, Ogawa H, Manabe M, Asaga H (1996) Preferential Deimination of Keratin K1 and Filaggrin during the Terminal Differentiation of Human Epidermis. *Biochem Biophys Res Commun* **225**: 712-719

Shafee TM, Lay FT, Hulett MD, Anderson MA (2016) The Defensins Consist of Two Independent, Convergent Protein Superfamilies. *Molecular biology and evolution* **33**: 2345-56

Shafee TM, Lay FT, Phan TK, Anderson MA, Hulett MD (2017) Convergent evolution of defensin sequence, structure and function. *Cellular and molecular life sciences : CMLS* **74**: 663-682

Sharma P, Lioutas A, Fernandez-Fuentes N, Quilez J, Carbonell-Caballero J, Wright RHG, Di Vona C, Le Dily F, Schüller R, Eick D, Oliva B, Beato M (2019) Arginine Citrullination at the C-Terminal Domain Controls RNA Polymerase II Transcription. *Mol Cell* **73**: 84-96.e7

Singh A, Prasad T, Kapoor K, Mandal A, Roth M, Welti R, Prasad R (2010) Phospholipidome of Candida: Each Species of Candida Has Distinctive Phospholipid Molecular Species. *OMICS* **14**: 665-677

Slack JL, Jones LE, Bhatia MM, Thompson PR (2011) Autodeimination of Protein Arginine Deiminase 4 Alters Protein–Protein Interactions but Not Activity. Biochemistry 50: 3997-4010

Slade DJ, Subramanian V, Thompson PR (2014) Pluripotency: citrullination unravels stem cells. *Nat Chem Biol* **10**: 327

Sørensen OE, Thapa DR, Roupé KM, Valore EV, Sjöbring U, Roberts AA, Schmidtchen A, Ganz T (2006) Injury-induced innate immune response in human skin mediated by transactivation of the epidermal growth factor receptor. *J Clin Invest* **116**: 1878-1885

Sreerama N, Woody RW (2000) Estimation of Protein Secondary Structure from Circular Dichroism Spectra: Comparison of CONTIN, SELCON, and CDSSTR Methods with an Expanded Reference Set. *Anal Biochem* **287**: 252-260

Stobernack T, du Teil Espina M, Mulder LM, Palma Medina LM, Piebenga DR, Gabarrini G, Zhao X, Janssen KMJ, Hulzebos J, Brouwer E, Sura T, Becher D, van Winkelhoff AJ, Götz F, Otto A, Westra J, van Dijl JM (2018) A Secreted Bacterial Peptidylarginine Deiminase Can Neutralize Human Innate Immune Defenses. *mBio* **9**: e01704-18

Sui SF, Wu H, Guo Y, Chen KS (1994) Conformational changes of melittin upon insertion into phospholipid monolayer and vesicle. *J Biochem* **116**: 482-487

Tang YQ, Yuan J, Osapay G, Osapay K, Tran D, Miller CJ, Ouellette AJ, Selsted ME (1999) A cyclic antimicrobial peptide produced in primate leukocytes by the ligation of two truncated alpha-defensins. *Science* **286**: 498-502

Tanikawa C, Espinosa M, Suzuki A, Masuda K, Yamamoto K, Tsuchiya E, Ueda K, Daigo Y, Nakamura Y, Matsuda K (2012) Regulation of histone modification and chromatin structure by the p53–PADI4 pathway. *Nat Commun* **3**: 676-676

Tarcsa E, Marekov LN, Mei G, Melino G, Lee SC, Steinert PM (1996) Protein unfolding by peptidylarginine deiminase. Substrate specificity and structural relationships of the natural substrates trichohyalin and filaggrin. *J Biol Chem* **271**: 30709-30716

Tilvawala R, Nguyen SH, Maurais AJ, Nemmara VV, Nagar M, Salinger AJ, Nagpal S, Weerapana E, Thompson PR (2018) The Rheumatoid Arthritis-Associated Citrullinome. *Cell chemical biology* **25**: 691-704.e6

Trouw LA, Haisma EM, Levarht EWN, van der Woude D, Ioan-Facsinay A, Daha MR, Huizinga TWJ, Toes RE (2009) Anti-cyclic citrullinated peptide antibodies from rheumatoid arthritis patients activate complement via both the classical and alternative pathways. *Arthritis and rheumatism* **60**: 1923-1931

Turvey SE, Broide DH (2010) Innate immunity. *Journal of Allergy and Clinical Immunology* **125**: S24-S32

van der Weerden NL, Anderson MA (2013) Plant defensins: Common fold, multiple functions. *Fungal Biology Reviews* **26**: 121-131

van der Weerden NL, Lay FT, Anderson MA (2008) The plant defensin, NaD1, enters the cytoplasm of Fusarium oxysporum hyphae. *J Biol Chem* **283**: 14445-52

van Meer G, Voelker DR, Feigenson GW (2008) Membrane lipids: where they are and how they behave. *Nat Rev Mol Cell Biol* **9**: 112-124

Vossenaar ER, Zendman AJ, van Venrooij WJ, Pruijn GJ (2003) PAD, a growing family of citrullinating enzymes: genes, features and involvement in disease. *BioEssays : news and reviews in molecular, cellular and developmental biology* **25**: 1106-18

Wang F, Chen FF, Gao WB, Wang HY, Zhao NW, Xu M, Gao DY, Yu W, Yan XL, Zhao JN, Li XJ (2016) Identification of citrullinated peptides in the synovial fluid of patients with rheumatoid arthritis using LC-MALDI-TOF/TOF. *Clinical rheumatology* **35**: 2185-94

Wang L, Song G, Zhang X, Feng T, Pan J, Chen W, Yang M, Bai X, Pang Y, Yu J, Han J, Han B (2017) PADI2-Mediated Citrullination Promotes Prostate Cancer Progression. *Cancer Res* **77**: 5755-5768

Wang Y, Li M, Stadler S, Correll S, Li P, Wang D, Hayama R, Leonelli L, Han H, Grigoryev SA, Allis CD, Coonrod SA (2009) Histone hypercitrullination mediates chromatin decondensation and neutrophil extracellular trap formation. *J Cell Biol* **184**: 205-213

Witalison EE, Thompson PR, Hofseth LJ (2015) Protein Arginine Deiminases and Associated Citrullination: Physiological Functions and Diseases Associated with Dysregulation. *Current drug targets* **16**: 700-10

Yang D, Biragyn A, Kwak LW, Oppenheim JJ (2002) Mammalian defensins in immunity: more than just microbicidal. *Trends in Immunology* **23**: 291-296

Yang S, Kuang Y, Li H, Liu Y, Hui X, Li P, Jiang Z, Zhou Y, Wang Y, Xu A, Li S, Liu P, Wu D (2013) Enhanced production of recombinant secretory proteins in Pichia pastoris by optimizing Kex2 P1' site. *PLoS One* **8**: e75347

Yin LM, Edwards MA, Li J, Yip CM, Deber CM (2012) Roles of hydrophobicity and charge distribution of cationic antimicrobial peptides in peptide-membrane interactions. *J Biol Chem* **287**: 7738-45

Yuzhalin AE (2019) Citrullination in Cancer. *Cancer Res* **79**: 1274-1284

Yuzhalin AE, Gordon-Weeks AN, Tognoli ML, Jones K, Markelc B, Konietzny R, Fischer R, Muth A, O'Neill E, Thompson PR, Venables PJ, Kessler BM, Lim SY, Muschel RJ (2018) Colorectal cancer liver metastatic growth depends on PAD4-driven citrullination of the extracellular matrix. *Nat Commun* **9**: 4783

Zhang L (2017) Different dynamics and pathway of disulfide bonds reduction of two human defensins, a molecular dynamics simulation study. *Proteins* **85**: 665-681

Zheng L, Nagar M, Maurais AJ, Slade DJ, Parelkar SS, Coonrod SA, Weerapana E, Thompson PR (2019) Calcium Regulates the Nuclear Localization of Protein Arginine Deiminase 2. *Biochemistry* **58**: 3042-3056